Project Title:

QUalifying and Implementing a user-centric designed and EfficienT electric vehicle

Project Acronym: QUIET

GA: 769826

Topic: Electric vehicle user-centric design for optimized energy efficiency

Topic identifier: GV-05-2017

Type of action: RIA Research and Innovation action

Deliverable No.	QUIET D4.1	
Deliverable Title	System and components for more efficient heating (infrared), cooling (propane based AC-System and thermal management (PCM techniques)	
Scheduled Deliverable Date	2019-07	
Actual (granted) Deliverable Date	2019-08	
Deliverable Type	Report	
Dissemination level	Public	
Written by	Daniel Habenbacher (ATT) Esther Kiseritzky (RUBITHERM) Harald Grantner (AVL) Gerald Zotter (AVL) Daniel Biernatzki (VEN)	2019-08-28 2019-08-15 2019-08-30 2019-09-05 2019-08-29
Checked by	Jürgen Roither (AIT) Hansjörg Kapeller (AIT)	2019-08-26 2019-09-06
Approved by	WP Leader (AVL) Coordinator (AIT) Quality Coordinator (HRE-G)	2019-09-06 2019-09-06 2019-09-06
Status	Version 1.4	2019-09-06

This project has received funding from the European Union's Horizon 2020 research and innovation programme under grant agreement No. 769826. The content of this publication is the sole responsibility of the Consortium partners listed herein and does not necessarily represent the view of the European Commission or its services.

Publishable Executive Summary

The objectives of QUIET are to reduce the energy needed for cooling and heating the cabin of an electric vehicle under different driving conditions, by at least 30 % compared to the Honda baseline 2017 and a weight reduction of about 20 % of vehicle components (e.g. doors, windshields, seats, heating and air conditioning) is also addressed. These efforts will finally lead to a minimum of 25 % driving range increase under both hot (+40 °C) and cold (-10 °C) weather conditions.

This is achieved by exploiting the synergies of a technology portfolio in the areas of:

- user centric design with enhanced passenger comfort and safety
- light weight materials with enhanced thermal insulation properties
- and optimized vehicle energy management

The developed technologies will be integrated and qualified in a Honda B-segment electric vehicle validator.

Among these, a novel refrigerant for cooling, combined with an energy-saving heat pump operation for heating, advanced thermal storages based on phase change materials and powerfilms for infrared radiative heating of the cabin was developed and will be investigated. This new concept promises a smart and efficient energy supply of the all related powertrain components and the cabin, a fast mode change between heating and cooling with the use of low amounts of refrigerant. All the here mentioned components, which are used in this smart concept are part of work package WP4, the actual status and development parameters are described in the present report D4.1.

Detailed analysis and assessment of the present status of the donator vehicle (Honda FIT EV) and derivation of reasonable options for re-design of the vehicle thermal management system (VTMS) was done as first step. Extensive test incl. data analysis and assessment were done for the entire vehicle, the passenger compartment and single components like particular heat exchangers, HVAC blower, AC compressor, etc. Additionally, development, layout, design and first simulations of a new HVAC / vehicle thermal management system incl. heat pump, and the choice of suitable components were done. An investigation of the donator vehicle geometrical situation, for later integration of the new VTMS system was performed as well.

Based on the geometrical investigation / packaging assessment, the status evaluation of the donator vehicle and on the results of the system simulation, the AC circuit and the coolant circuits incl. all heat exchangers, valves, hoses etc. were designed, specified and parts were ordered for build-up at the AC system testbed.

Special developed components are necessary for an efficient usage of the alternative refrigerant, which allows to heat up the cabin via an energy-efficient heat pump also for really cold conditions. In the present reporting period a special compressor and a special electronic expansion valve (EXV) were developed for that refrigerant and tested as single components to derive data for later usage of these parts in mobile AC system and to enable the entire VTMS calibration. Therefore, both parts went through a detailed component testing phase. They will be used for testbed measurements in late summer 2019 to proof their ability to improve the overall system efficiency with alternative refrigerant. For the used refrigerant, a special safety / security concept, which is required, were developed. This safety / security concept includes a new and a safe way for the passenger and the environment in case of a security alert.

For improving the passenger comfort by still saving energy, radiation heating surfaces will finally be implemented in the vehicle. The geometrical situation inside the passenger compartment was investigated to

This project has received funding from the European Union's Horizon 2020 research and innovation programme under grant agreement No. 769826. The content of this publication is the sole responsibility of the Consortium partners listed herein and does not necessarily represent the view of the European Commission or its services.

identify possible position of radiation heating elements. At the beginning of the current investigations a coupled 3D-1D simulation of passenger comfort and an efficiency calculation for usage of the powerfilms / radiation heating elements were done. The results are presented here as well. The radiation heating elements and their application to particular parts of the vehicle interior are shown as well.

For storage of heat / energy by means of phase change materials (PCM), and later usage of this heat for e.g. defrosting of the vehicle front end condenser a thermal storage tank is planned for the vehicle set-up. Within the reporting period evaluation of the different implementations of PCM and start first tests with PCM-aluminium foam composites were done. The results look promising and are presented in this report. Although new aluminium foam composites are currently in purchasing for further improvement of the energy storage charging and discharging.

This project has received funding from the European Union's Horizon 2020 research and innovation programme under grant agreement No. 769826. The content of this publication is the sole responsibility of the Consortium partners listed herein and does not necessarily represent the view of the European Commission or its services.

Table of Contents

This project has received funding from the European Union's Horizon 2020 research and innovation programme under grant agreement No. 769826. The content of this publication is the sole responsibility of the Consortium partners listed herein and does not necessarily represent the view of the European Commission or its services.

This project has received funding from the European Union's Horizon 2020 research and innovation programme under grant agreement No. 769826. The content of this publication is the sole responsibility of the Consortium partners listed herein and does not necessarily represent the view of the European Commission or its services.

This project has received funding from the European Union's Horizon 2020 research and innovation programme under grant agreement No. 769826. The content of this publication is the sole responsibility of the Consortium partners listed herein and does not necessarily represent the view of the European Commission or its services.

List of Figures

This project has received funding from the European Union's Horizon 2020 research and innovation programme under grant agreement No. 769826. The content of this publication is the sole responsibility of the Consortium partners listed herein and does not necessarily represent the view of the European Commission or its services.

This project has received funding from the European Union's Horizon 2020 research and innovation programme under grant agreement No. 769826. The content of this publication is the sole responsibility of the Consortium partners listed herein and does not necessarily represent the view of the European Commission or its services.

List of Tables

This project has received funding from the European Union's Horizon 2020 research and innovation programme under grant agreement No. 769826. The content of this publication is the sole responsibility of the Consortium partners listed herein and does not necessarily represent the view of the European Commission or its services.

Abbreviations and Nomenclature

Table 1: List of Abbreviations and Nomenclature.

Symbol or Shortname	Description
EV	Electric Vehicle
WP	Work Package
HVAC	Heating, Ventilation and Air Conditioning
WLTP	World Harmonized Light Vehicle Test Procedure
PI	Polyimid
ECU	Electric Control Unit
GUI	Graphical User Interface
RHS	Radiant Heating System
HTC	Heat transfer coefficient
MET	Metabolic equivalent of task
PMV	Predicted mean vote Index
MAC	Mobile Air Condition
PRV	Pressure Relief Valve
VTMS	Vehicle Thermal Management System
COP	Coefficient of Performance
EER	Energy Efficiency Ratio

This project has received funding from the European Union's Horizon 2020 research and innovation programme under grant agreement No. 769826. The content of this publication is the sole responsibility of the Consortium partners listed herein and does not necessarily represent the view of the European Commission or its services.

1. Introduction

The objectives of the QUIET project are to reduce the energy needed for cooling and heating the cabin of an electric vehicle under different driving conditions, by at least 30 % compared to the Honda baseline 2017 and a weight reduction of about 20 % of vehicle components (e.g. doors, windshields, seats, heating and air conditioning) is also addressed. These efforts will finally lead to a minimum of 25 % driving range increase under both hot (+40 °C) and cold (-10 °C) weather conditions.

This is achieved by exploiting the synergies of a technology portfolio in the areas of:

- user centric design with enhanced passenger comfort and safety
- light weight materials with enhanced thermal insulation properties
- and optimized vehicle energy management

The developed technologies will be integrated and qualified in a Honda B-segment electric vehicle validator.

Among these, a novel refrigerant for cooling, combined with an energy-saving heat pump operation for heating, advanced thermal storages based on phase change materials and powerfilms for infrared radiative heating of the cabin will be investigated. All the here mentioned components are part of work package WP4, the actual status and development parameters are described in the present deliverable report D4.1.

Detailed analysis and assessment of the present status of the donator vehicle (Honda FIT EV) and derivation of reasonable options for re-design of the vehicle thermal management system (VTMS) was done as first step. Extensive test incl. data analysis and assessment were done for the entire vehicle, the passenger compartment and single components like particular heat exchangers, HVAC blower, AC compressor, etc. Additionally, development, layout, design and first simulations of a new HVAC / vehicle thermal management system incl. heat pump, and the choice of suitable components were done. An investigation of the donator vehicle geometrical situation, for later integration of the new VTMS system was performed as well.
Based on the geometrical investigation / packaging assessment, the status evaluation of the donator vehicle and on the results of the system layout, the AC circuit and the coolant circuits incl. all heat exchangers, valves, hoses etc. were designed and parts were procured for build-up at the AC system testbed.

Special adapted components are necessary for an efficient usage of R290 as refrigerant. In the present reporting period a special compressor and a special electronic expansion valve (EXV) were developed and tested as single components to derive data for later usage of these parts in the AC circuit and to enable AC system calibration. Both parts went through a detailed component testing phase. They will be used for testbed measurements in late summer / autumn 2019 to proof their ability to improve overall system efficiency with refrigerant R290.
For the used refrigerant R290 (Propane), even in small portions, a special safety / security concept is required. This safety / security concept, incl. a new shut-off valve (PRV) and a safe way for Propane dumping in case of a security alert were developed.

For improving the passenger comfort by still saving energy, radiation heating surfaces will finally be implemented in the vehicle. The geometrical situation inside the passenger compartment was investigated to identify possible position of radiation heating elements. At the beginning of the current investigations a coupled 3D-1D simulation of passenger comfort and an efficiency calculation for usage of the powerfilms / radiation heating elements were done. The results are presented here as well. The radiation heating elements and their application to particular parts of the vehicle interior are shown as well.

This project has received funding from the European Union's Horizon 2020 research and innovation programme under grant agreement No. 769826. The content of this publication is the sole responsibility of the Consortium partners listed herein and does not necessarily represent the view of the European Commission or its services.

For storage of heat / energy by means of phase change materials (PCM), and later usage of this heat for e.g. defrosting of the vehicle front end condenser a thermal storage tank is planned for the vehicle set-up. Within the reporting period evaluation of the different implementations of PCM and start first tests with PCM-aluminium foam composites were done. The results look promising and are presented in this report. Although new aluminium foam composites are currently in purchasing for improvement of the energy storage charging and discharging.

1.1. Description of the deliverable -- Goals

The deliverable deals with the innovative system and components for compressor and valve (EXV & SRV), for Propane (R290) based AC-System, for infrared heating elements & for advanced PCM thermal storage modules. It is associated with task: T4.4. This report describes the layout and development of those components and gives further information regarding their properties. Finally, information regarding testbed build-up and actual measurement schedule is given.

This project has received funding from the European Union's Horizon 2020 research and innovation programme under grant agreement No. 769826. The content of this publication is the sole responsibility of the Consortium partners listed herein and does not necessarily represent the view of the European Commission or its services.

2. Powerfilms for infrared radiative and convective heating (ATT)

The ATT related part in this project is the development of an energy saving interior heating concept. Here, radiative heating elements should be placed inside the vehicle on suitable interior parts to obtain the same level of comfort while convective heating power is reduced.

Tasks:

- Comfort simulation
- Definition of suitable interior parts that can be heated
- Design of heating elements
- Production of heating elements and control unit
- Integration and optimization of ECU parameters

2.1. Comfort Simulation

Due to the fact, that ATT did not receive suitable and not enough data for simulating the desired vehicle, another, comparable vehicle was chosen. Therefore, all parameters and graphs of chapter 2.1 (Comfort Simulation) as well as chapter 2.2 (Efficiency Simulation), are not referring to the donator vehicle. All calculated and simulated values can be taken as an indicator for the desired vehicle.

2.1.1. General Information

For the comfort simulation the following simulation tools were used:

- OpenFOAM
- TheseusFE [1], [2]

A tailor-made workflow for comfort simulation was elaborated and specific interfaces were programmed Therefore, it was possible to interconnect the simulation tools. The simulation workflow for the comfort simulation is displayed in Figure 1.

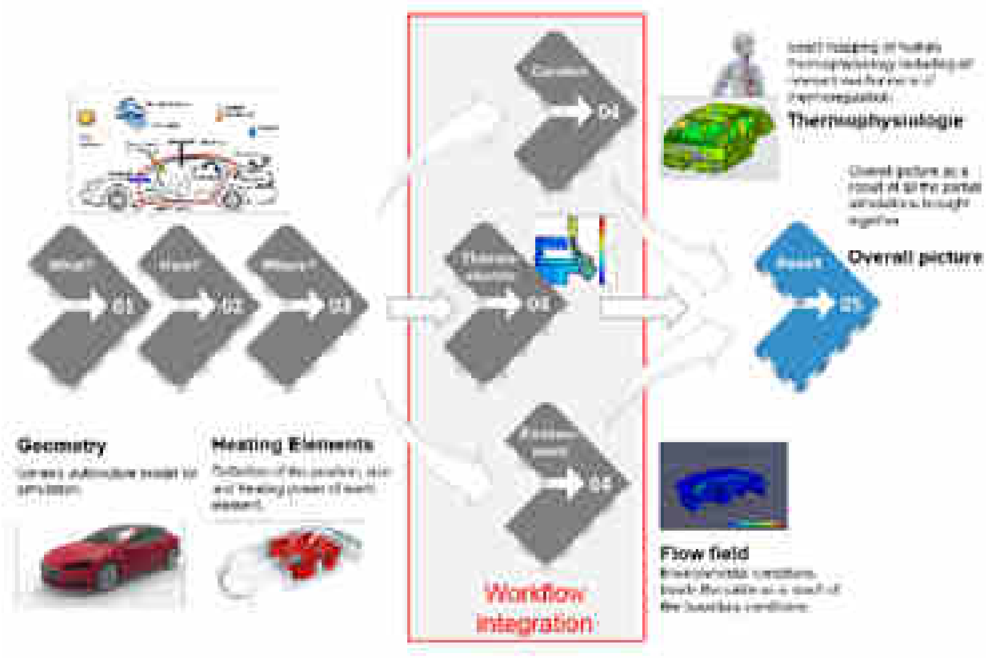

Figure 1: Simulation workflow for comfort simulation

This project has received funding from the European Union's Horizon 2020 research and innovation programme under grant agreement No. 769826. The content of this publication is the sole responsibility of the Consortium partners listed herein and does not necessarily represent the view of the European Commission or its services.

2.1.2. Simulation Model

2.1.2.1. Car model

For the simulation the most suited surfaces were selected. In Table 2 the material parameters can be seen. Following parts were chosen to be heated in the simulation model:

- Door Cover upper (both sides)
- Door Cover lower (both sides)
- Armrest door (both sides)
- Sunvisor (both sides)
- Armrest
- Footwell Driver
- Footwell Passenger

Table 2: Material parameters for the thermal simulation model [3]

Material	λ [W/mK]	cp [J/kgK]	P [kg/m³]
Glas Foam	0,033	1100	910
Decor (hd)	0,15	960	1380
ESG Glass	0,9	800	2535
Wood wool	0,15	1300	600
PU-foam II	0,033	1100	1100
Fleece + board	0,04	1200	60
Blank sheet	46	460	7860
Rubber hair	0,026	1005	30
PU-foam (ld)	0,033	1100	70
Fabric	0,07	1300	430
PVC (ld)	0,15	960	1100
PU-foam (ld II)	0,035	1140	66
PU + EPDM	0,16	1420	1000
Carpet	0,07	1300	167
PU-foam (hd)	0,033	1100	700
PU-foam (md)	0,033	1100	175
EPDM	0,16	1420	1600
Greenglass-G90	0,9	800	2563
PVB	0,2	1200	1100
PUR film	0,033	100	40

This project has received funding from the European Union's Horizon 2020 research and innovation programme under grant agreement No. 769826. The content of this publication is the sole responsibility of the Consortium partners listed herein and does not necessarily represent the view of the European Commission or its services.

Fleece	0,04	1200	58
Bitumen	0,16	1420	1500
PVC + PE-foam	0,033	1100	140
Air	0,027	1000	1,3
Synthetic rubber	0,06	2300	1500
Hard rubber	0,16	1420	1150
PU-foam + fleece	0,035	1140	66
Fibregl. + Poly. + Fabric	0,07	1300	910
Aluminium	238	945	2700
Polypropylen PP-T20	0,22	1700	1050
Leather	0,135	1490	850

2.1.2.2. Thermal Manikin

The Thermal Manikin is a thermal model representing a human body. A virtual thermal manikin model FIALA-FE is implemented in TheseusFE. With this model not only the human thermophysical mechanisms can be simulated but also the human thermal comfort can be evaluated. The model includes the following body parts (in brackets are the number of different areas of the body part):

- Head (2)
- Face (1)
- Neck (2)
- Shoulder left / right (1)
- Thorax (8)
- Abdomen (4)
- Arms left / right (6)
- Hands left / right (2)
- Legs left / right (6)
- Feet left / right (2)

The thermal manikin is displayed in Figure 2 with the different mentioned areas. For all these areas it is possible to simulate the specific comfort.

This project has received funding from the European Union's Horizon 2020 research and innovation programme under grant agreement No. 769826. The content of this publication is the sole responsibility of the Consortium partners listed herein and does not necessarily represent the view of the European Commission or its services.

Figure 2: Manikin with the coloured body areas

Further it is necessary to specify an activity level. The metabolic equivalent of task (MET) is the objective measure of the ratio of the rate at which a person expends energy, relative to the mass of that person, while performing some specific physical activity compared to a reference, set by convention at 3.5 ml of oxygen per kilogram per minute, which is roughly equivalent to the energy expended when sitting quietly.

The following parameters were applied:

- Activity level: 1.2
- Radiation model: active
- Thermal regulation: active
- Clothing: Winter (see Table 3)

Table 3: Clothing values for winter [4]

ensemble			fabric				global parameters					
		description	description	thickness of fabric (mm)	intrinsic fabric insulation (m²K/W)	evaporative resistance of fabric (m²Pa/W)	Icl (clo)		Recl (m²Pa/W)		fcl	
							serial	measur.	serial	measur.	serial	measur.
1.	Men's Business Suit & Winter Jacket	briefs t-shirt calf length dress socks long sleeve shirt, shirt collar trousers, straight, long, fitted waist outdoor jacket, warm hard-soled street shoes	jersey single knit, 100% cotton jersey single knit, 100% cotton rib knit, 75% hi-bulk orlon acrylic, 25% stretch nylon broadcloth, plain weave, 65% polyester, 35% cotton pinwale corduroy, 75% cotton, 25% polyester tweed plain weave, 50% wool, 50% polyester / lining, plain weave, 100% polyester - vinyl	1.270 1.270 3.383 0.533 1.580 1.727 / 0.102 - 2.700	0.036 0.006 0.086 0.025 0.041 0.049 / 0.008 -	4.0 4.0 3.3 3.4 6.6 6.5 / 1.8 - 7.9	1.33	-	29.0	-	1.26	-

This project has received funding from the European Union's Horizon 2020 research and innovation programme under grant agreement No. 769826. The content of this publication is the sole responsibility of the Consortium partners listed herein and does not necessarily represent the view of the European Commission or its services.

For the activity level the value of 1.2 was chosen, because driving a car is in general not exhausting. Typical values can be seen in Table 4.

Table 4: Different activities and their corresponding MET [5]

Activity level	Definition	Descriptive measure
Sedentary	≤1.5 METs	Activities that usually involve sitting or reclining and that have little additional movement
Light	1.6–2.9 METs	An activity that does not cause a noticeable change in breathing heart rate (eg. walking slowly, cooking a meal)
Moderate	3.0–5.9 METs	An activity that is able to be conducted whilst maintaining a conversation uninterrupted (walking at 3–4.5 mph, vacuuming, mowing lawn)
Vigorous	≥6.0 METs	An activity in which a conversation generally cannot be maintained uninterrupted (walking at ≥5.0 mph, jogging, cycling at ≥10 mph or uphill)

This project has received funding from the European Union's Horizon 2020 research and innovation programme under grant agreement No. 769826. The content of this publication is the sole responsibility of the Consortium partners listed herein and does not necessarily represent the view of the European Commission or its services.

2.1.2.3. Boundary Conditions

Since the dynamic simulation of the flow field is expensive in time and resources, the simulation was adapted so that there was just one static flow field. This would lead to a much too high heating power in the start phase. To eliminate these problems, the inlet temperatures were adapted in a way that the heating powers are the same as the measured ones.

The inlet temperatures for the simulation and the measured ones are displayed in Figure 3.

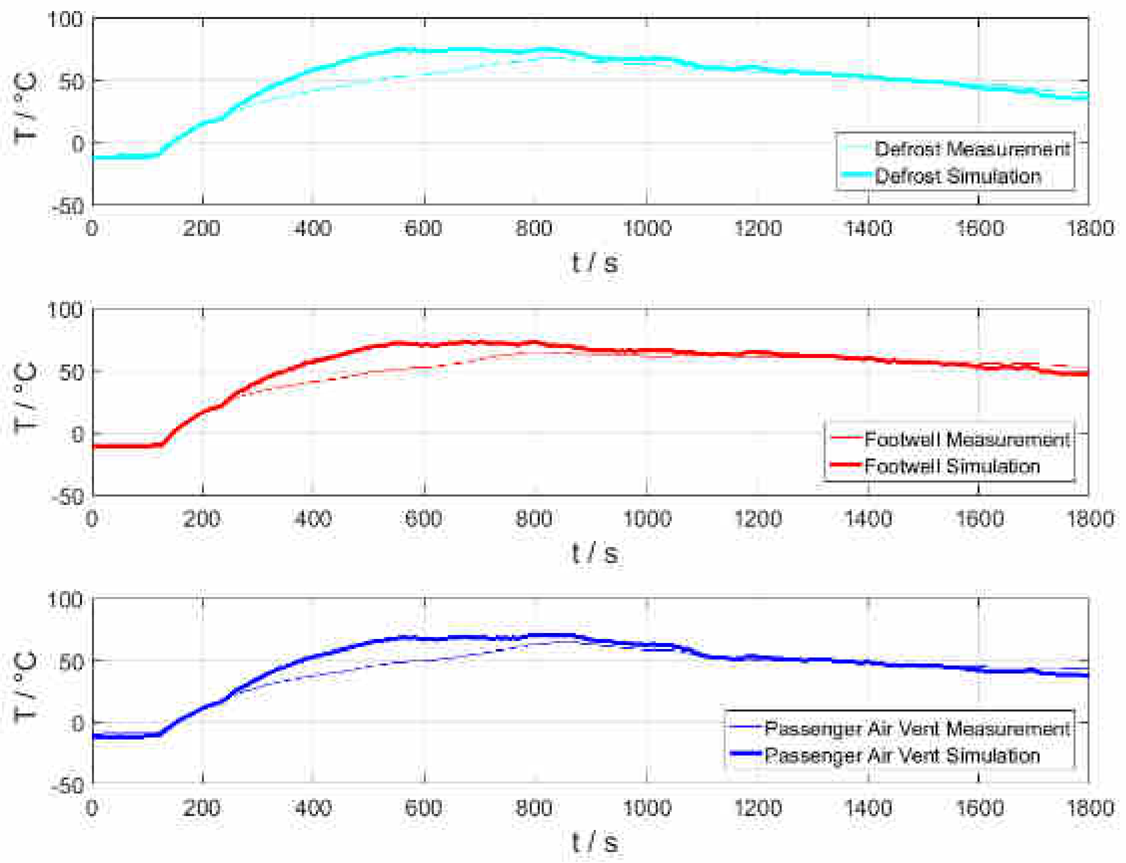

Figure 3: Measured and simulated air temperatures

In addition, the following parameters were used:

- Ambient Temperature of -12,5°C
- Starting Temperature of -12,5°C

This project has received funding from the European Union's Horizon 2020 research and innovation programme under grant agreement No. 769826. The content of this publication is the sole responsibility of the Consortium partners listed herein and does not necessarily represent the view of the European Commission or its services.

In Table 5 the mass flows are listed for the two simulations. Baseline is the simulation without heating elements, the second simulation is done with a reduced mass flow and with activated radiant heating elements.

Table 5: Mass flows of the different inlets [6]

	Baseline m_p = 320 kg/h	With radiant heating elements m_p = 240 kg/h
Inlet	Percental volume flow	Percental volume flow
Defrost	28	37
Middle Inlets front & rear	0	0
Side inlets front	18	16
Footwell front	30	26
Footwell rear	24	21

The total airflow of the defrost stays the same for the baseline and the system with the RHS. This is since the defrost function cannot be adopted by the RHS. The total mass flow is reduced with the RHS because the overall power stays the same, the difference in air vent power is shifted to the RHS.

The simulation was done with these two settings and the results were compared. The evaluation of the data is done in chapter 2.2.

The heating elements have constant heating power up to 60°C and are reduced to no power at 70°C. This will simulate the controller of the heating elements.

2.1.3. Data analysis and assessment

Most of the data was received directly from the simulation, such as comfort against time or power consumption. This data is shown in chapter 2.2. Other data which required further calculations are mentioned in chapter 2.2.3, with the mathematical equations for the operation.

2.1.3.1. PMV- Index

The first simulated value is the PMV-Index [7] for both, driver and passenger with and without radiant heating system. The PMV, i.e. Predicted mean vote Index, is a global Index referring to the whole body. Following numbers describe the PMV – Index:

- +3 hot
- +2 warm
- +1 slightly warm
- 0 neutral
- -1 slightly cool
- -2 cool
- -3 cold

This project has received funding from the European Union's Horizon 2020 research and innovation programme under grant agreement No. 769826. The content of this publication is the sole responsibility of the Consortium partners listed herein and does not necessarily represent the view of the European Commission or its services.

The PMV target value is 0 which means enjoyable. The graph for the PMV Index is depicted in Figure 4. The simulation with the Powerfilm reaches the target value faster than the one without heating elements.

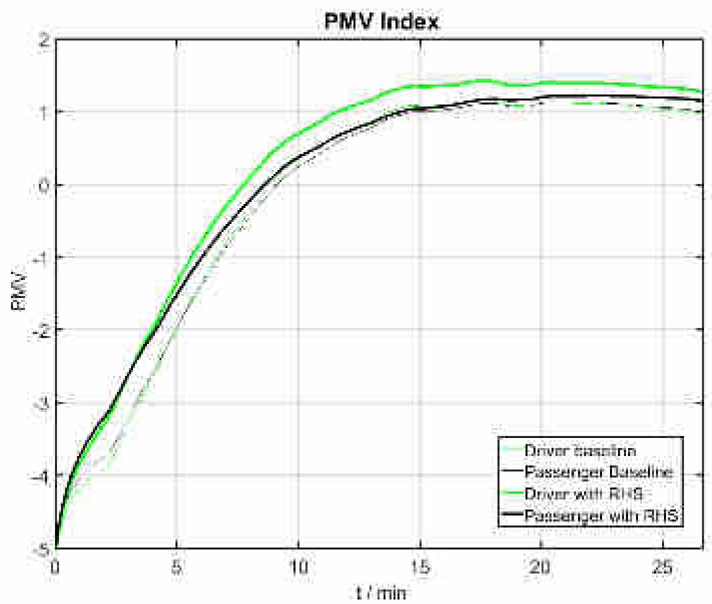

Figure 4: PMV Index for driver and passenger with and without heating elements

2.1.3.2. Local Comfort Index

The Local Comfort Index [7] is like the PMV a global index. The target value is 3, which means neutral. In Figure 5 the ISO Local Comfort is displayed. The simulation with the radiant heating system reaches the neutral level faster than the one without.

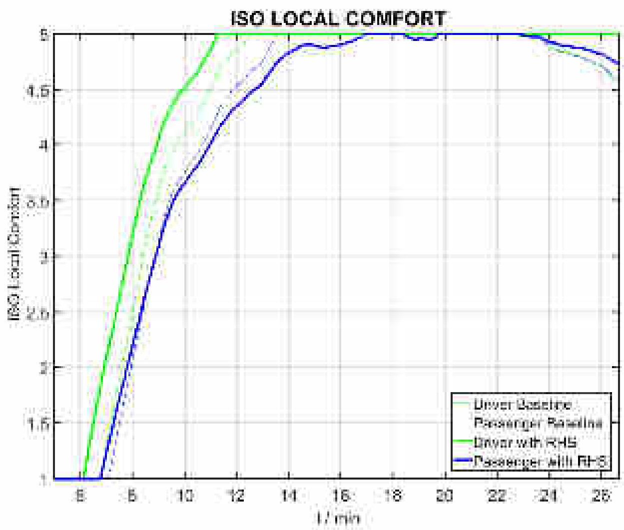

Figure 5: ISO Local Comfort for driver and passenger with and without heating elements

This project has received funding from the European Union's Horizon 2020 research and innovation programme under grant agreement No. 769826. The content of this publication is the sole responsibility of the Consortium partners listed herein and does not necessarily represent the view of the European Commission or its services.

2.1.3.3. Zhang Thermal Sensation Index

Zhang's local thermal comfort prediction is based on a huge number of human climate chamber tests at the University of Berkley, California. Based on regression analysis Hui Zhang developed in [8] a powerful mathematical framework for the prediction of the local thermal sensation and comfort.

In Figure 6 the Zhang Thermal Sensation Index is displayed. The target value is 0. There cannot be seen any bigger differences between the versions.

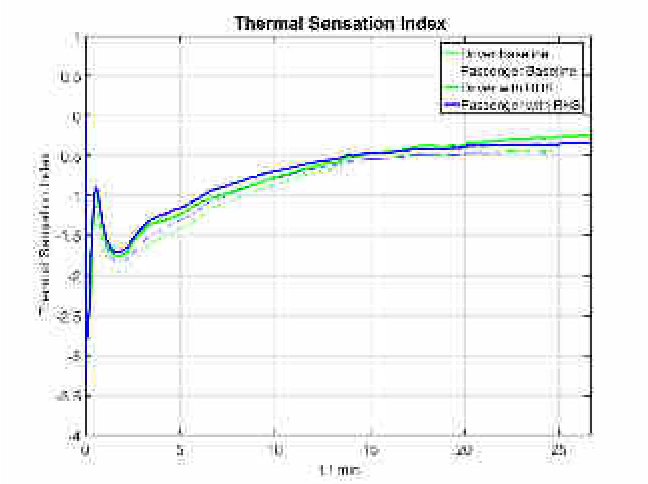

Figure 6: Thermal Sensation Index for driver and passenger with and without heating elements

2.1.3.4. Heating Power

In Figure 7 the power output of the heating elements is displayed. The heating power stays constant in the beginning and gets reduced after a specific time until the steady state is reached.

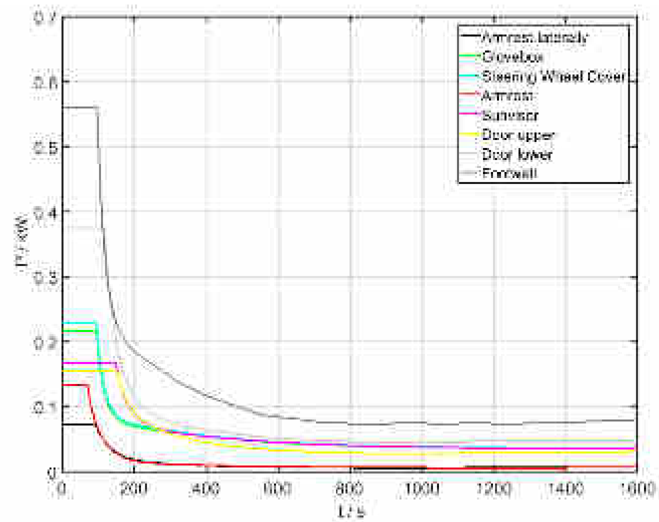

Figure 7: Heating Power for the heating elements

This project has received funding from the European Union's Horizon 2020 research and innovation programme under grant agreement No. 769826. The content of this publication is the sole responsibility of the Consortium partners listed herein and does not necessarily represent the view of the European Commission or its services.

In Figure 8 the power entry of the convective heating system can be seen for the baseline and the combined heating system.

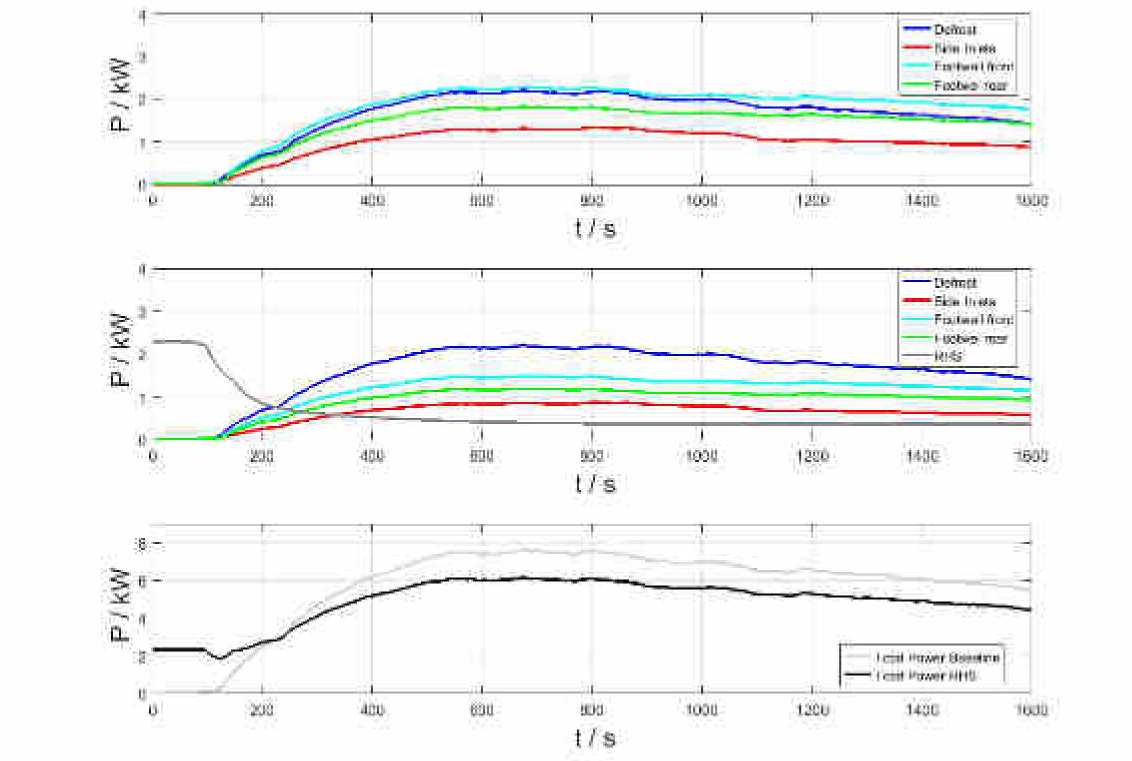

Figure 8: Heating Power Output of baseline, Radiant Heating System (RHS), and total power comparison

2.1.3.5. Energy consumption

In Figure 9 the energy consumption of the baseline and the RHS is displayed. After 10 minutes the RHS has an energetical advantage. The energy calculation is given in (1)

( ) = ( ) (1)

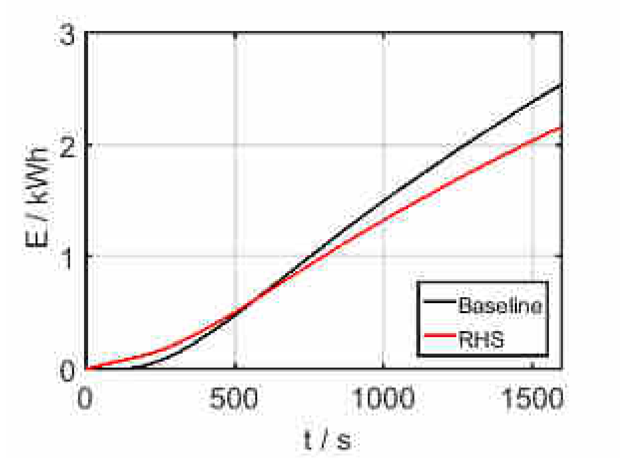

Figure 9: Power consumption over time

This project has received funding from the European Union's Horizon 2020 research and innovation programme under grant agreement No. 769826. The content of this publication is the sole responsibility of the Consortium partners listed herein and does not necessarily represent the view of the European Commission or its services.

2.1.3.6. Heating system efficiency

For the efficiency calculation the inlet energy as well as the outlet energy are considered, since these quantities are time dependent also the efficiency is time dependent. Especially in the first 10 minutes the gap in efficiency is big, after this time the gap stays constant, the efficiency of the RHS is always better than the conventional heating system. The time dependent efficiencies can be seen in Figure 10, the calculation of the efficiency is given in (2).

$$= \frac{-}{\quad\quad} \qquad (2)$$

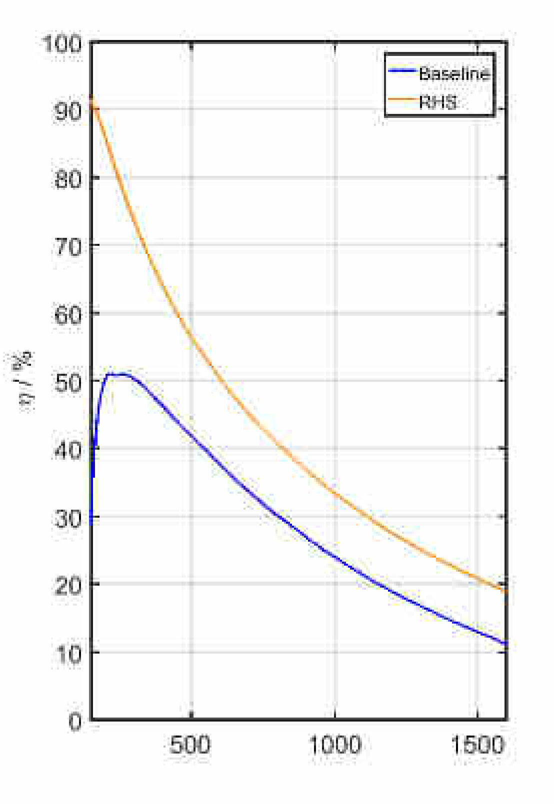

Figure 10: Efficiency over time

2.2. Efficiency Simulation

2.2.1. General information

This simulation aims to calculate the efficiency of heating elements placed on either the surface facing to the passenger (called A-side), or the opposite surface (called B-side). In addition, different thicknesses of insulation were taken into consideration.

2.2.2. Simulation Modell

In Figure 11 the simulation model is displayed. Here the heater position is on the A-side (shown in pink). When the heater is placed on the B-side, the heater is positioned between the 3 mm ABS and the insulation.

This project has received funding from the European Union's Horizon 2020 research and innovation programme under grant agreement No. 769826. The content of this publication is the sole responsibility of the Consortium partners listed herein and does not necessarily represent the view of the European Commission or its services.

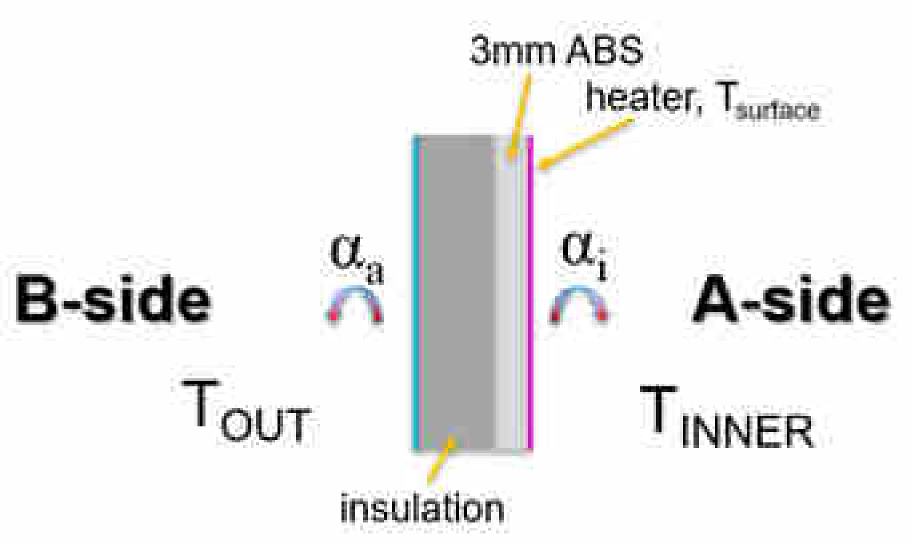

Figure 11: Efficiency calculation model

The model parameters are given in Table 6.

Table 6: Modell parameter for the efficiency calculation [3]

Parameter	Value
Thickness ABS	3 mm
Heat Capacity ABS	1400 J / kgK
Heat Capacity Foam	1500 J / kgK
Heat Conductivity ABS	0,17 W / mK
Heat Conductivity ABS	0,035 W / mK
Density ABS	1040 kg / m³
Density Foam	17 kg / m³
Emissivity outer	0,92
Emissivity inner	0,92
Outer temperature	0°C
Inner temperature	20°C
HTC outer	2,5 W / m²K
HTC inner	5 W / m²K

This project has received funding from the European Union's Horizon 2020 research and innovation programme under grant agreement No. 769826. The content of this publication is the sole responsibility of the Consortium partners listed herein and does not necessarily represent the view of the European Commission or its services.

2.2.3. Simulation Results

The temperature profiles of different insulation thicknesses are given in Figure 12. The colors of the lines refer to the simulated temperatures: Yellow: 80 °C; Green: 60 °C; Blue: 40 °C

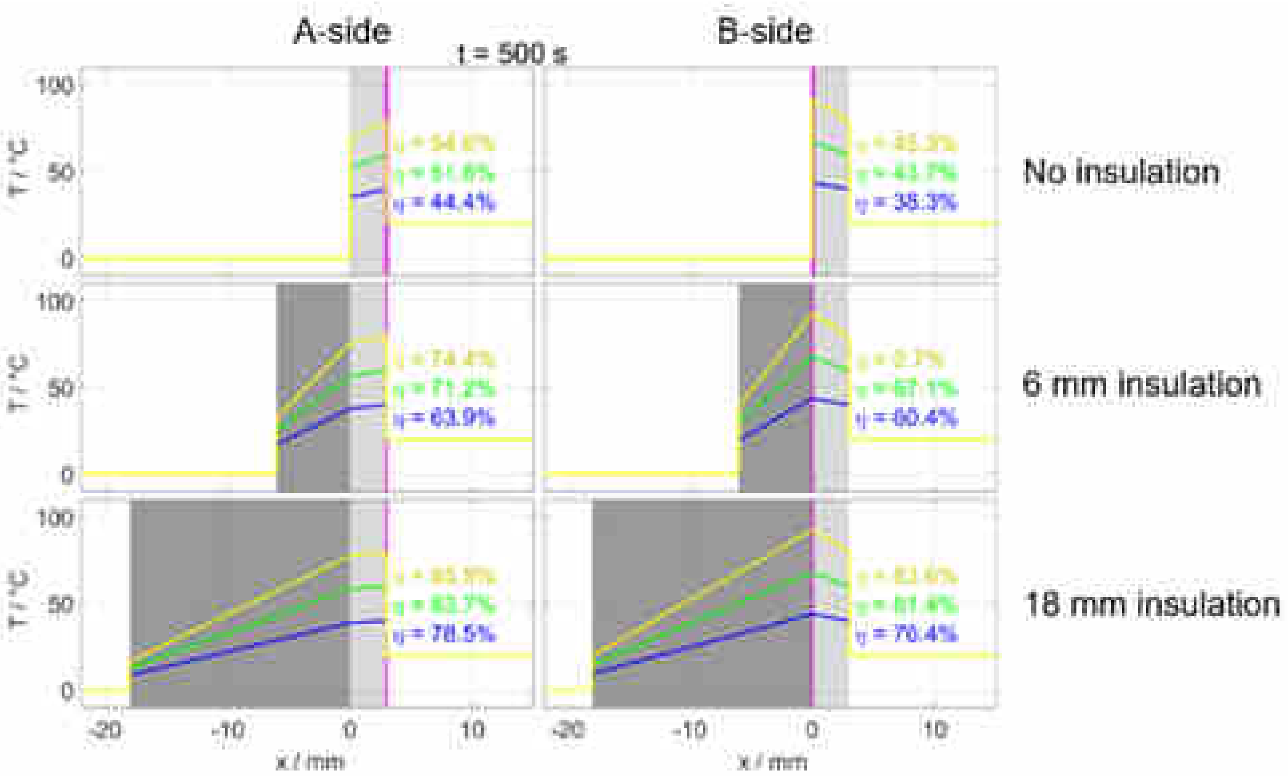

Figure 12: Temperature profiles of different insulation thicknesses (the colours of the lines refer to the simulated temperatures: Yellow: 80°C; Green: 60°C; Blue: 40°C)

The total efficiency depends on the outer temperature. The efficiency profiles for different set-ups are given in Figure 13.

This project has received funding from the European Union's Horizon 2020 research and innovation programme under grant agreement No. 769826. The content of this publication is the sole responsibility of the Consortium partners listed herein and does not necessarily represent the view of the European Commission or its services.

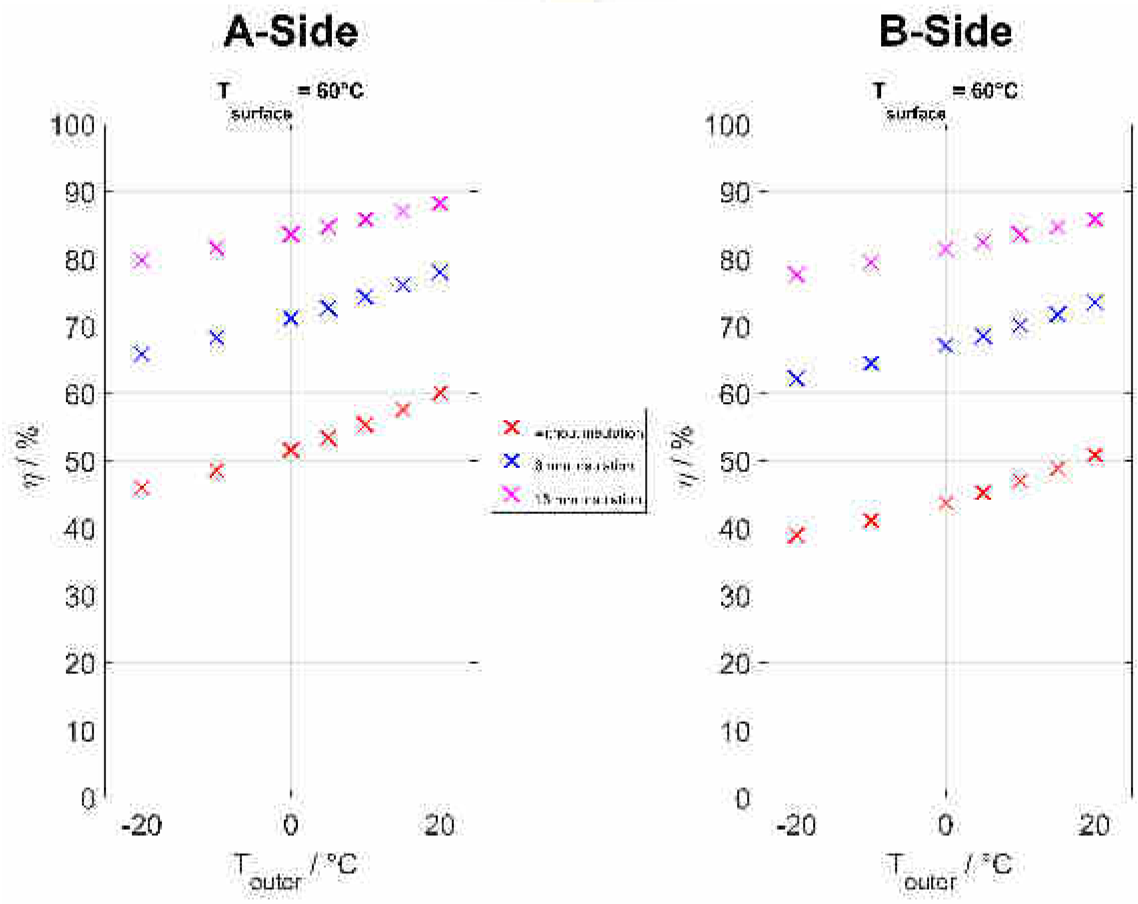

Figure 13: Efficiency graphs (left: A-Side, right: B-Side) for different set-ups for a heater temperature of 60°C and an inner temperature of 20°C

2.3. Technical design of Powerfilms

Different interior components have been sent to ATT. Following parts around the front passengers of the car have been identified as suitable parts where heating elements can be applied:

- 2 heating elements at each door (8)
- 2 sunvisors (2)
- Footwell driver (1)
- Footwell passenger (1)
- Roof (4, above each passenger)

In total, 16 heating foils are going to be applied inside the car.

This project has received funding from the European Union's Horizon 2020 research and innovation programme under grant agreement No. 769826. The content of this publication is the sole responsibility of the Consortium partners listed herein and does not necessarily represent the view of the European Commission or its services.

2.3.1. Electronic Control Unit (ECU)

For powering and control of the Radiant Heating System (RHS) an Electronic Control Unit (ECU, Figure 14) for custom-made control of the heating foils has been developed by ATT. In addition, a Graphical User Interface (GUI) allows an on-line monitoring of all relevant telemetry data of the heating foils, such as the (mean) temperature, voltage and power consumption of each foil. Each of the 16 heaters can be accessed separately and controlled individually. The electronics of the control unit autonomously adjusts the power unit to provide the power per area [W/m²], defined by the user in the GUI.

The ECU itself gets the power directly from the supply voltage of the car. Since the ECU and the heating foils are designed for a power of 48 V, a DC/DC converter (400 V to 48 V) is interposed.

Here, the control of the heating foils is not given via the GUI. The customer controls the ECU through its own software via the CAN interface. The necessary CAN IDs and the structure of the data frames will be provided by ATT. The correct control of the control unit is ensured by the customer via the CAN communication. However, the control unit is protected against the entry of incorrect data that would endanger the operational safety.

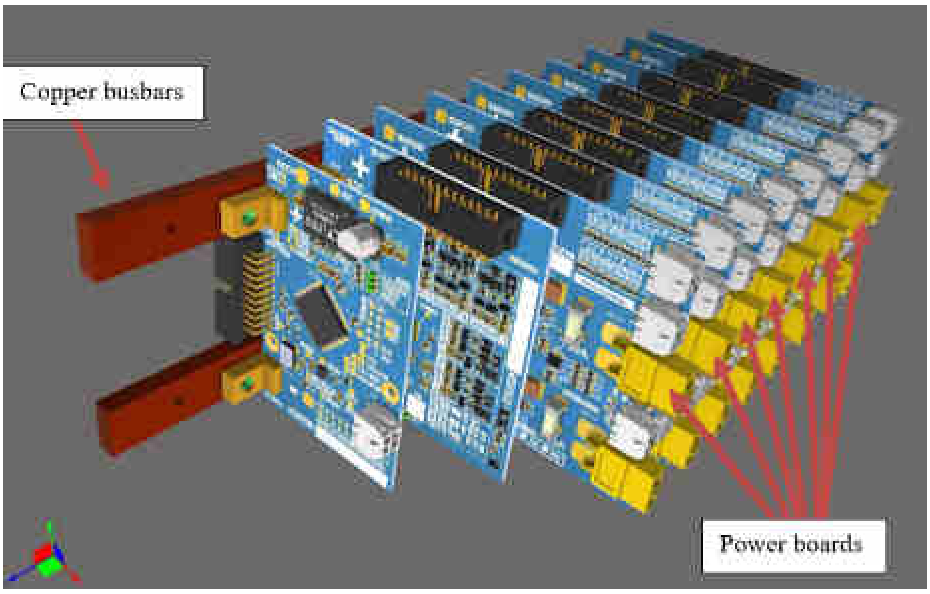

Figure 14: ECU Assembly

The ECU 's firmware complies with the following functionalities:

- Control of the heating foils
  - Power control
- Current draw and voltage level
- CAN communication
- Read-out of calibration values

This project has received funding from the European Union's Horizon 2020 research and innovation programme under grant agreement No. 769826. The content of this publication is the sole responsibility of the Consortium partners listed herein and does not necessarily represent the view of the European Commission or its services.

2.3.2. Positions, design and simulation of infrared heating foils

The ATT design process is shown hereinafter at the example of the sunvisor.

At first, the contour of the heating foil is selected from the CAD data (shown in Figure 15). The surface is checked in the CAD program with a specific tool, to avoid excessive distortions when unwinding the areas from 3D to 2D data. If the distortion reaches a value above ~2 %, small cuts around the contour must be made. These cuts allow higher flexibility of the heating foil.

Figure 15: CAD data of the sunvisor with selected geometry for the heating foil (left), contacting tab on the back side of an interior part (right)

For subsequent connection to the ECU, a contacting tab is attached to the geometry of the heating foil. This tab can be placed at any position around of the foil. The tab is (if possible) inserted through the component on the back, which is shown in Figure 15 on the right side. After the geometry with the contacting tab is finished, the contour of the foil is cut from any material by a laser to place it on the physical part of the car (Figure 16) to detect any deviations of the geometry from the interior part.

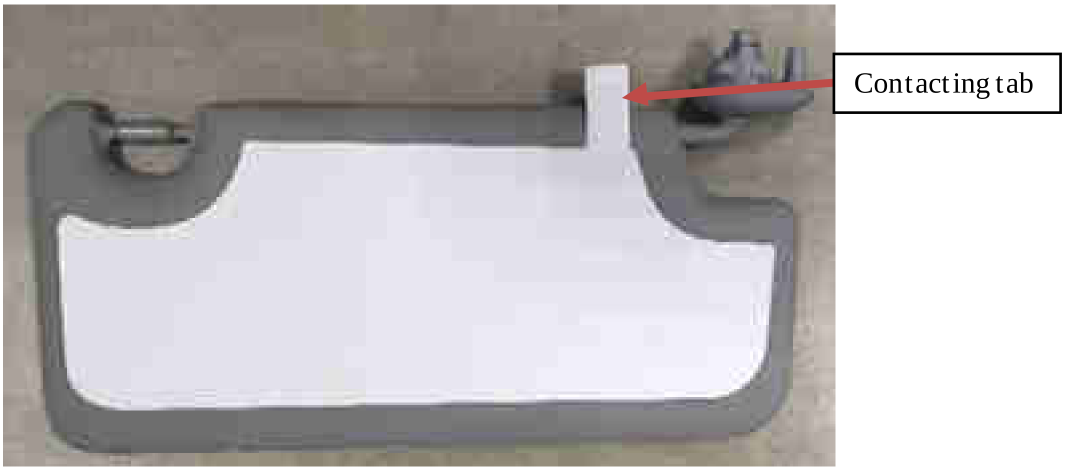

Figure 16: Geometry of the heating foil of the sunvisor with contacting tab, cut by a laser

This project has received funding from the European Union's Horizon 2020 research and innovation programme under grant agreement No. 769826. The content of this publication is the sole responsibility of the Consortium partners listed herein and does not necessarily represent the view of the European Commission or its services.

Here, the heating power for the foils is assumed with a value of about 1500 W / m². This heating power can be adjusted through the distance between the electrodes and the mixture of the used carbon ink. The electrodes are split into 2 types of electrodes:

- Main electrodes
- Side electrodes

The main electrodes are those on the outside regions of the contour. The width of the electrodes can be easily calculated if the voltage and the parameters of the copper are known. The side electrodes are the electrodes inside the geometry. The distance between these electrodes is the main parameter of the power density. For the assumed heating power of 1500 W / m² and the used carbon ink, a distance of 5 mm between the electrodes is given. The arrangement of main and side electrodes is shown in Figure 18. Cables will be applied on the contacts of the electrodes via soldering. The cables are directly attached to the ECU.

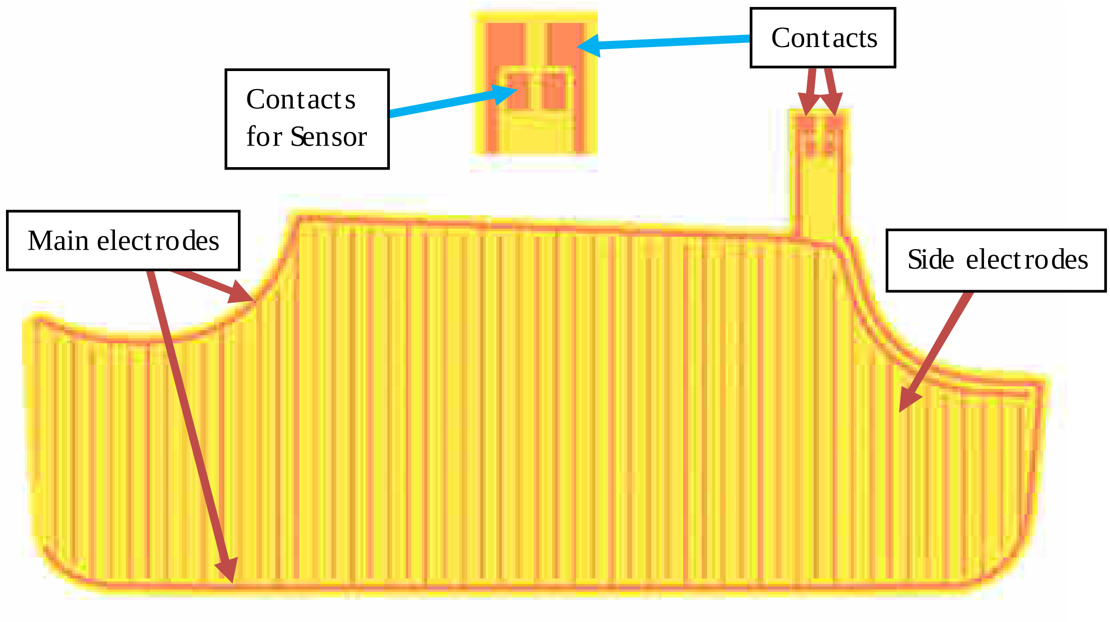

Figure 17: Types of electrodes and details of a contacting tab

The copper electrodes are produced in a subtractive etching process. The carbon ink, where the heating power is produced (shown in Figure 18), is applied by screen printing. The curing process of the carbon ink is given for 60 minutes at 140 °C in a box oven.

This project has received funding from the European Union's Horizon 2020 research and innovation programme under grant agreement No. 769826. The content of this publication is the sole responsibility of the Consortium partners listed herein and does not necessarily represent the view of the European Commission or its services.

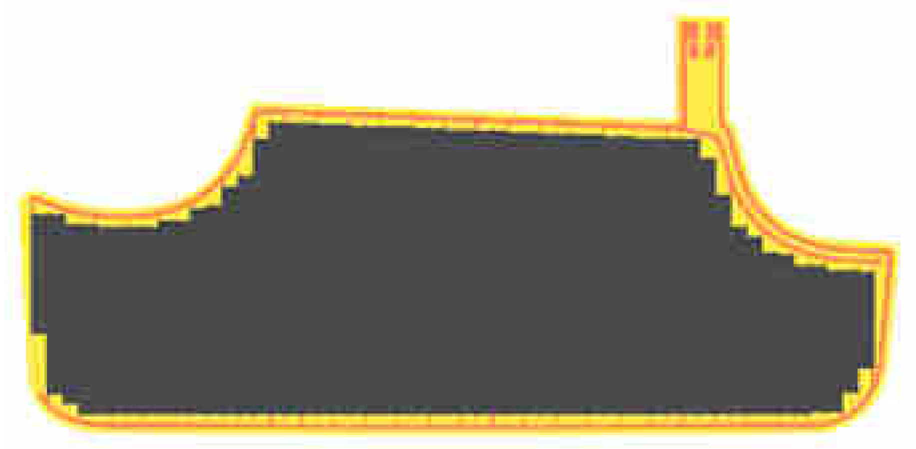

Figure 18: Carbon ink

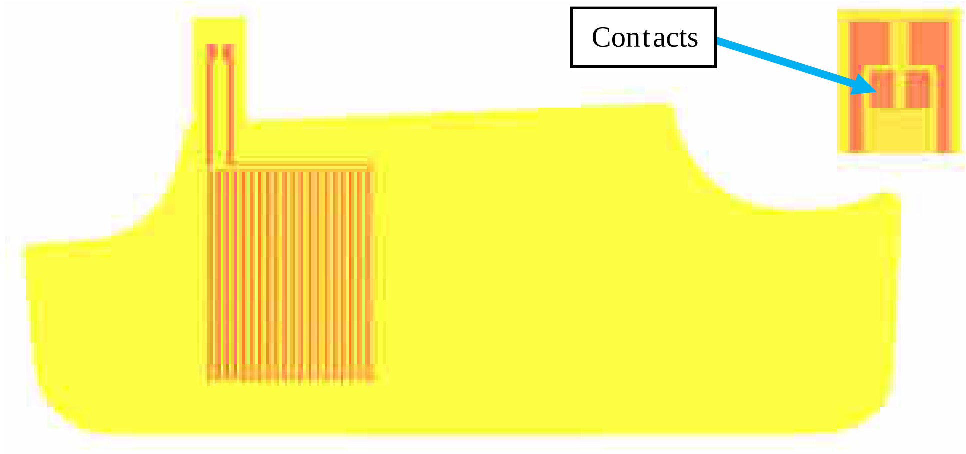

Figure 19: Sensor meander on the back side of the heating foil

A sensor meander (shown in Figure 19) is additionally etched on the back side of the heating foil. The meander of each heating foil is calibrated using a developed firmware. The temperature of the heating foil can then be calculated in real-time by the ECU through measuring the current and voltage of the meander.

The contacts of the meander are on the front and on the back side of the foil. The cables are attached through soldering on the front side. An eyelet is pressed through the contact pads and thereby gives the contact on the back side of the heating foil.

The design of each heating foil as well as the heating power can be checked by using a self-programmed simulation script. For a voltage of 48 V the heating foil of the sunvisor will have following specifications:

- Resistance: 42 Ohm
- Heating power carbon ink: ~2300 W / m²
- Heating power: 1500 W/m² à 53 W

This project has received funding from the European Union's Horizon 2020 research and innovation programme under grant agreement No. 769826. The content of this publication is the sole responsibility of the Consortium partners listed herein and does not necessarily represent the view of the European Commission or its services.

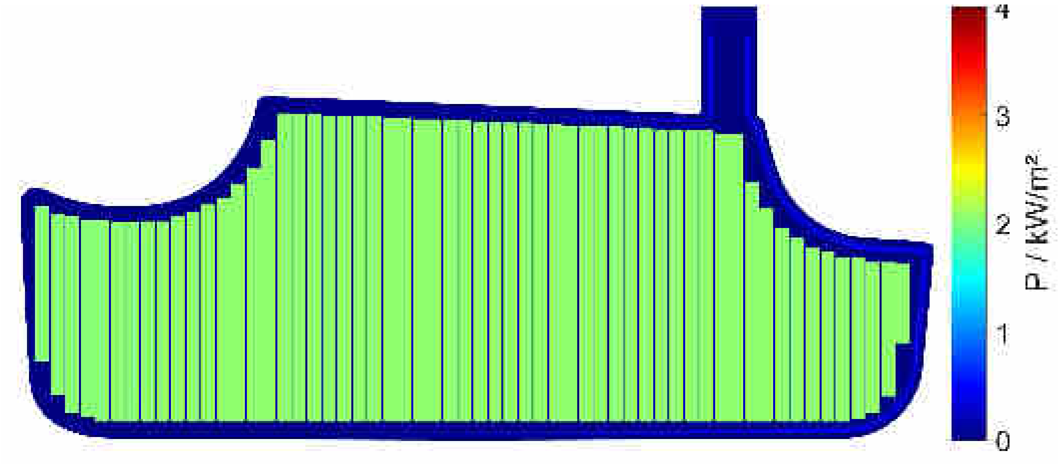

Figure 20: Simulated heating power for sunvisor

Figure 20 shows the simulated heating power for the sunvisor.
The layer structure of the heating foil is shown in Figure 21. Polyimid (PI) with a thickness of 25 µm will be used as substrate. This material is not only stable at high temperatures, with this low thickness it is also very flexible. For the protection of the carbon ink on the top side, a thermal curing protective coating is also applied through a screen-printing process. With a special adhesive, the heating foils can be attached easily on the desired interior parts. The material and thicknesses of these layers are given in Table 7.

Table 7: Layer structure with proper material and thickness

Layer	Material	Thickness [µm]
Protective Coating	Thermic curing, solvent based lacquer	10
Active Layer	Carbon ink	8
Electrodes Top	Copper (etched)	18
Substrate	Polyimid	25
Electrodes Bottom	Copper (etched)	18
Adhesive Tape	Fleece with double-sided polyacrylate adhesive	160

This project has received funding from the European Union's Horizon 2020 research and innovation programme under grant agreement No. 769826. The content of this publication is the sole responsibility of the Consortium partners listed herein and does not necessarily represent the view of the European Commission or its services.

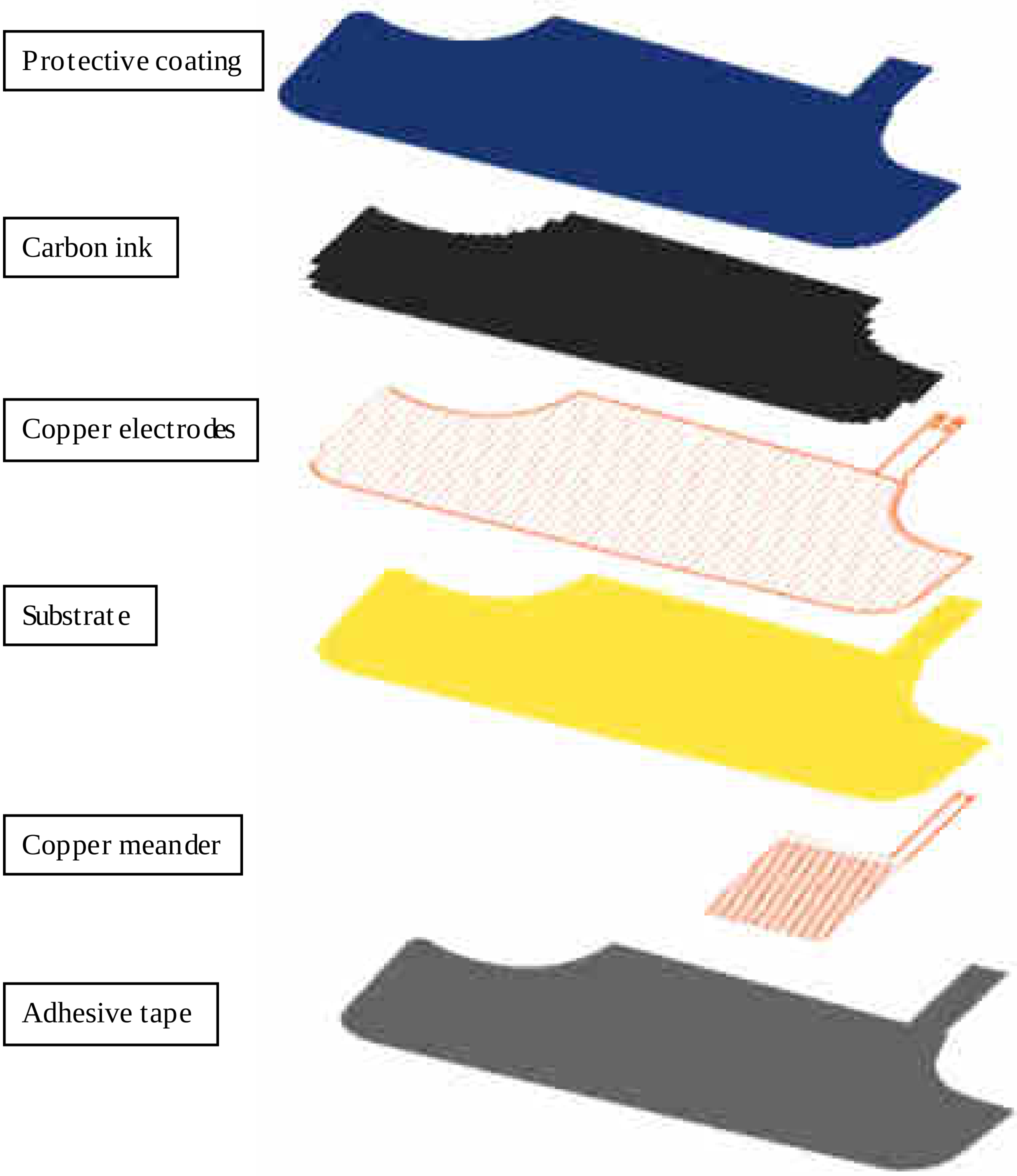

Figure 21: Layer structure of heating foil

The heating foils that will be applied to the demonstrator vehicle, together with their area, resistance and power, are listed in Table 8.

Table 8: List of heating foils with properly area, electrical resistance and power

Position	Area [cm²]	Resistance [Ω]	Power [W]
Sunvisor	353	42,25	54
Footwell Driver	485	33,56	68
Footwell Passenger	656	23,62	98
Roof Front	1045	13,25	174
Roof Back	788	17,67	130
Door Back 1	1047	13,69	168
Door Back 2	745	19,72	117
Door Front 1	1159	12,50	184
Door Front 2	600	27,13	85

This project has received funding from the European Union's Horizon 2020 research and innovation programme under grant agreement No. 769826. The content of this publication is the sole responsibility of the Consortium partners listed herein and does not necessarily represent the view of the European Commission or its services.

2.3.2.1. Sun visor

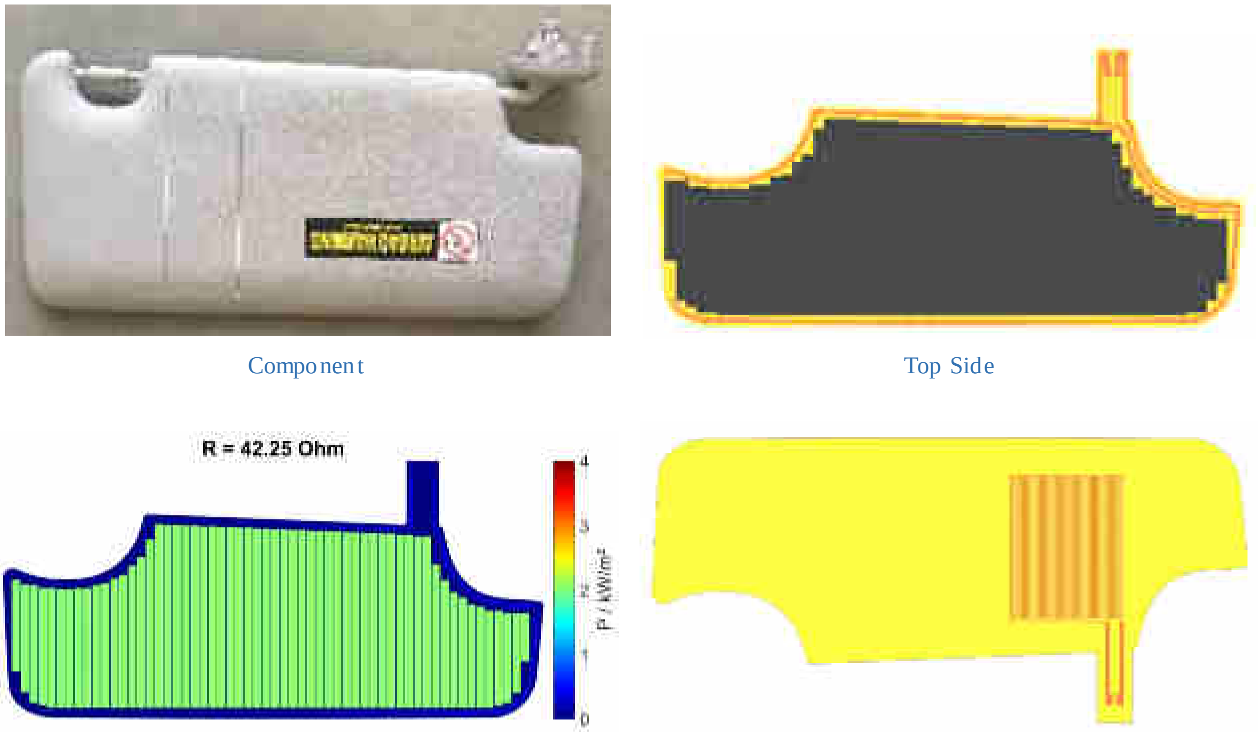

Component — Top Side — Power Density Distribution — Bottom Side (Sensor)

Figure 22: Illustrative summing up of the sun visor properties / implementation

- Area = 353 cm²
- Power = 53 W
- Resistance = 42 Ω
- Current = 1,1 A

This project has received funding from the European Union's Horizon 2020 research and innovation programme under grant agreement No. 769826. The content of this publication is the sole responsibility of the Consortium partners listed herein and does not necessarily represent the view of the European Commission or its services.

•

2.3.2.2. Footwell Driver

Component

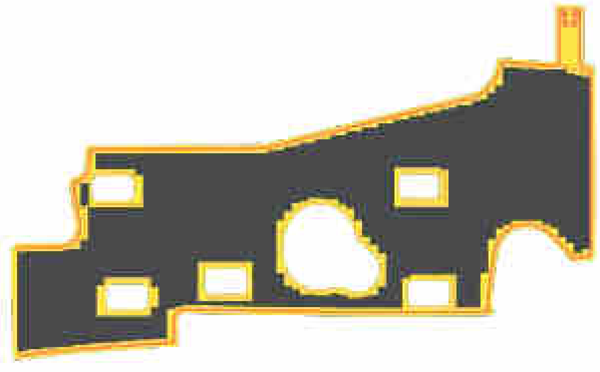

Top Side

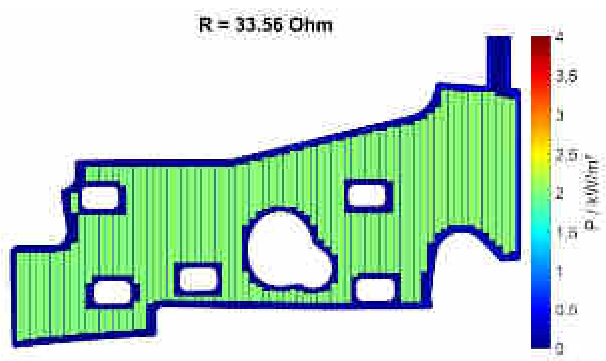

Power Density Distribution

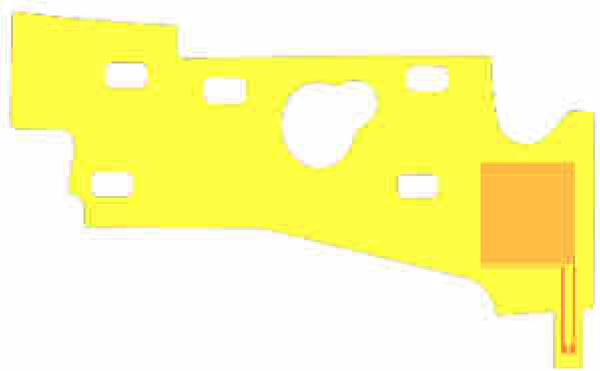

Bottom Side (Sensor)

Figure 23: Illustrative summing up of the footwell driver properties / implementation

- Area = 485 cm²
- Power = 68 W
- Resistance = 33 Ω
- Current = 1,4 A

2.3.2.3. Footwell Passenger

Component

Top Side

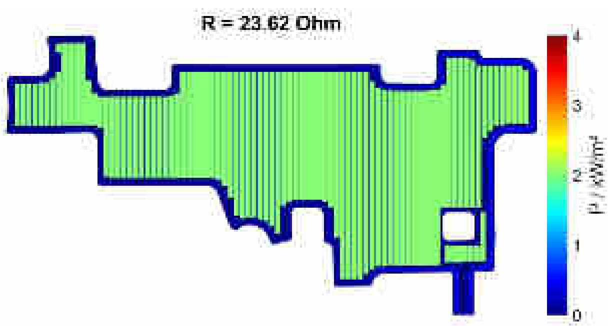

Power Density Distribution

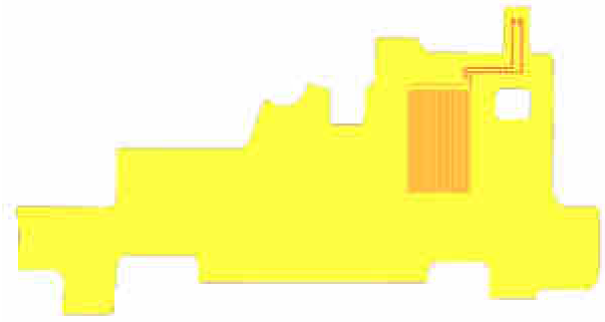

Bottom Side (Sensor)

Figure 24: Illustrative summing up of the footwell passenger properties / implementation

- Area = 656 cm²
- Power = 98 W
- Resistance = 23 Ω
- Current = 2 A

This project has received funding from the European Union's Horizon 2020 research and innovation programme under grant agreement No. 769826. The content of this publication is the sole responsibility of the Consortium partners listed herein and does not necessarily represent the view of the European Commission or its services.

2.3.2.4. Door Back 1

Component

Top Side

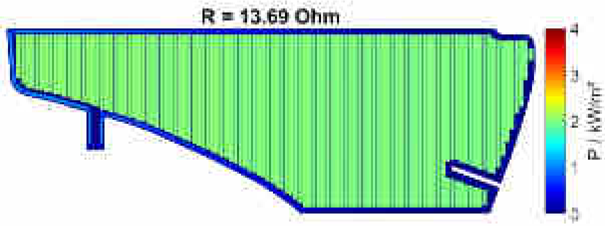

Power Density Distribution

Bottom Side (Sensor)

Figure 25: Illustrative summing up of the door back 1 properties / implementation

- Area = 1047 cm²
- Power = 168 W
- Resistance = 13 Ω
- Current = 3,5 A

This project has received funding from the European Union's Horizon 2020 research and innovation programme under grant agreement No. 769826. The content of this publication is the sole responsibility of the Consortium partners listed herein and does not necessarily represent the view of the European Commission or its services.

2.3.2.5. Door Back 2

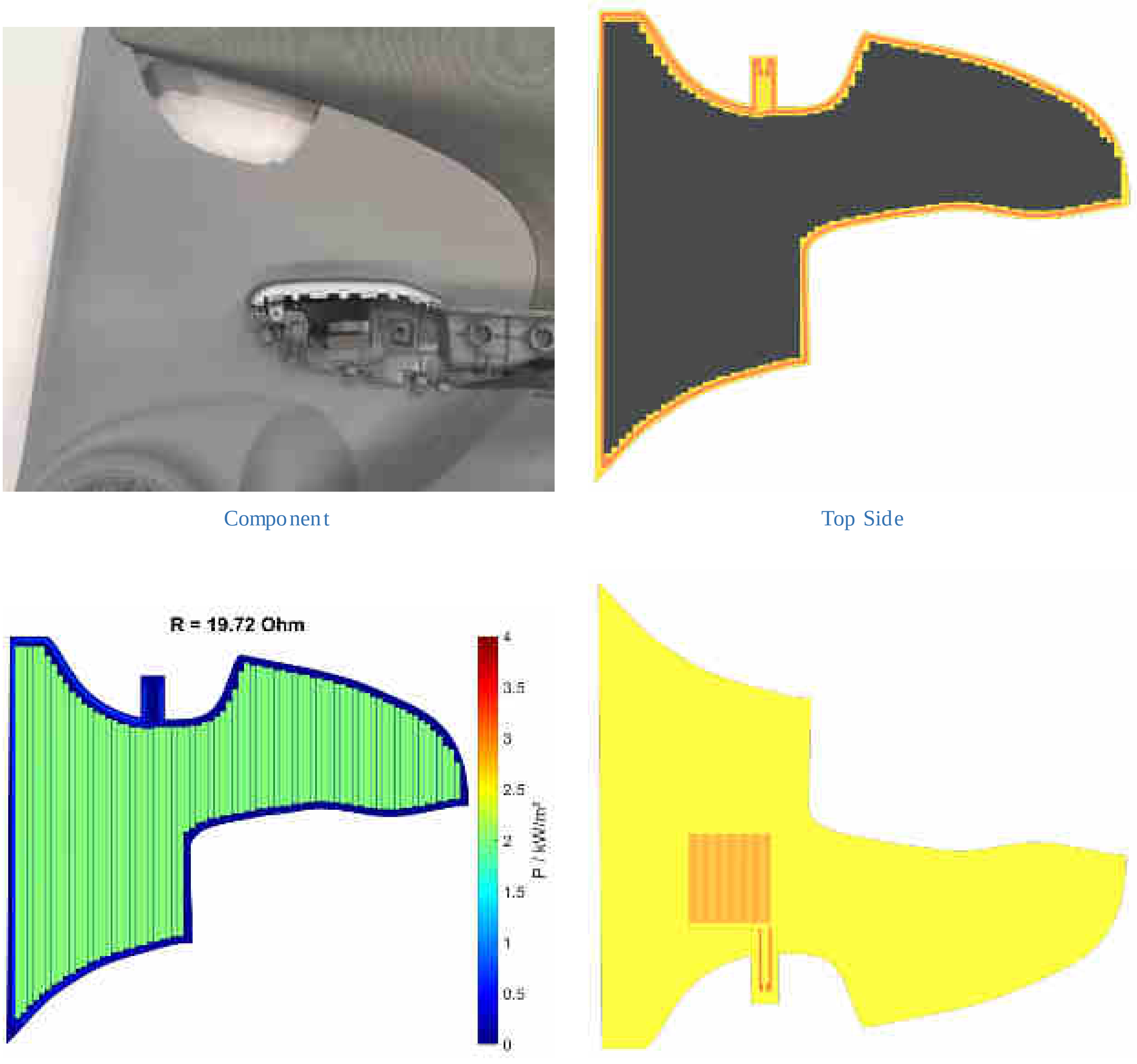

Component

Top Side

Power Density Distribution

Bottom Side (Sensor)

Figure 26: Illustrative summing up of the door back 2 properties / implementation

- Area = 745 cm²
- Power = 117 W
- Resistance = 19 Ω
- Current = 2,4 A

This project has received funding from the European Union's Horizon 2020 research and innovation programme under grant agreement No. 769826. The content of this publication is the sole responsibility of the Consortium partners listed herein and does not necessarily represent the view of the European Commission or its services.

2.3.2.6. Door Front 1

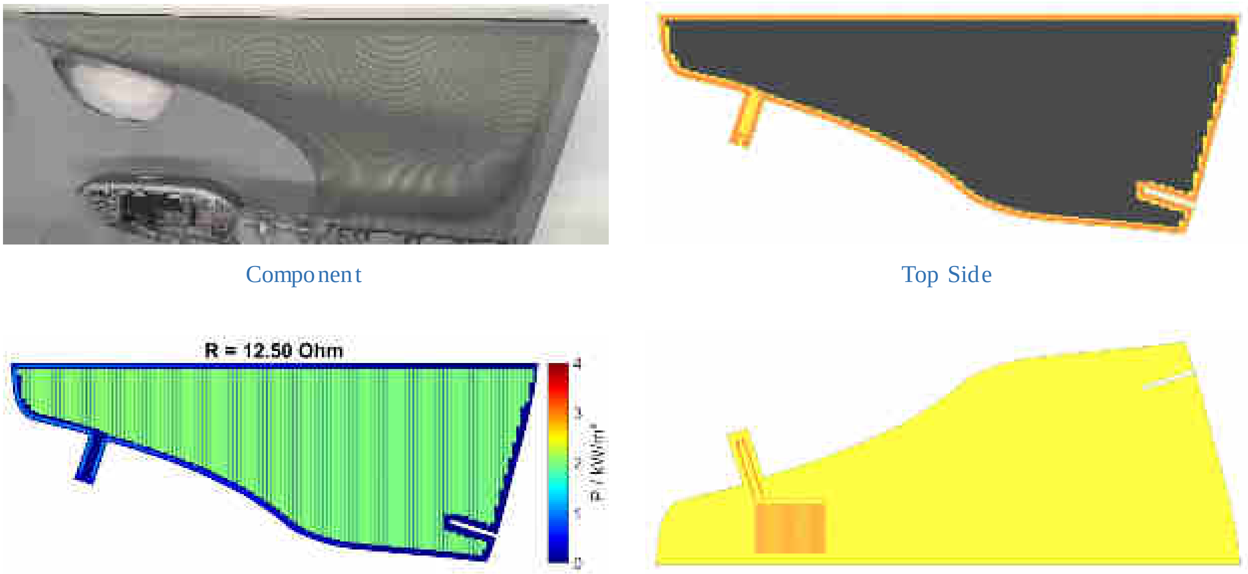

Component | Top Side | Power Density Distribution | Bottom Side (Sensor)

Figure 27: Illustrative summing up of the door front 1 properties / implementation

- Area = 1159 cm²
- Power = 184 W
- Resistance = 12 Ω
- Current = 3,8 A

This project has received funding from the European Union's Horizon 2020 research and innovation programme under grant agreement No. 769826. The content of this publication is the sole responsibility of the Consortium partners listed herein and does not necessarily represent the view of the European Commission or its services.

2.3.2.7. Door Front 2


Component

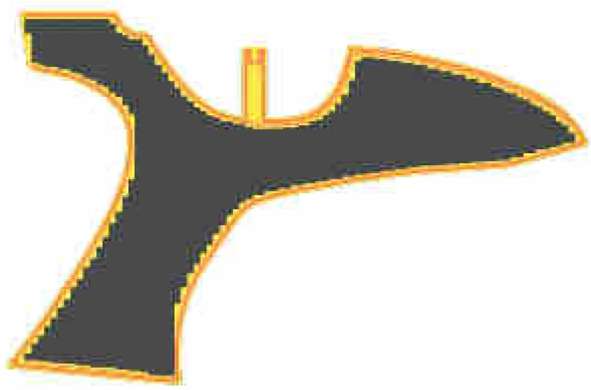
Top Side

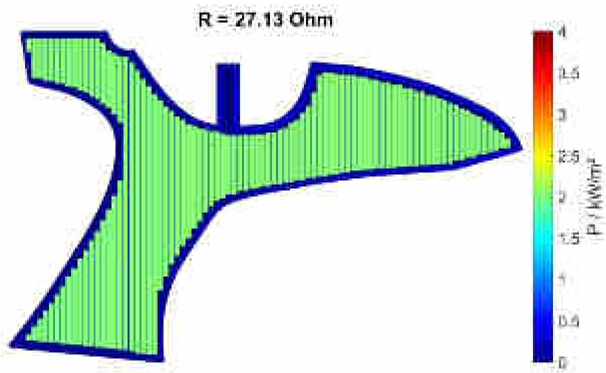

Power Density Distribution

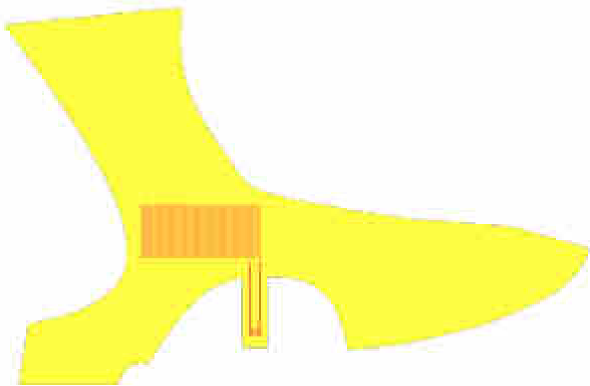
Bottom Side (Sensor)

Figure 28: Illustrative summing up of the door front 2 properties / implementation

- Area = 600 cm²
- Power = 85 W
- Resistance = 27 Ω
- Current = 1,77 A

This project has received funding from the European Union's Horizon 2020 research and innovation programme under grant agreement No. 769826. The content of this publication is the sole responsibility of the Consortium partners listed herein and does not necessarily represent the view of the European Commission or its services.

2.3.2.8. Roof Front

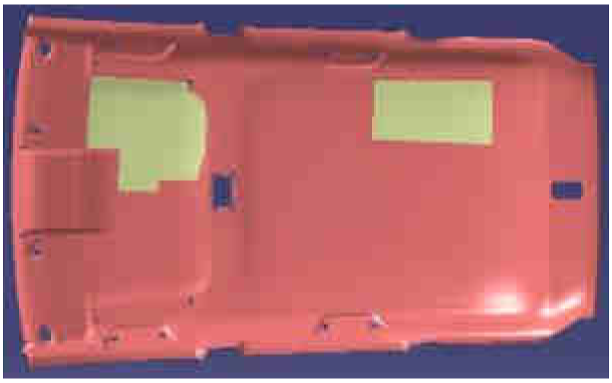

Component

Top Side

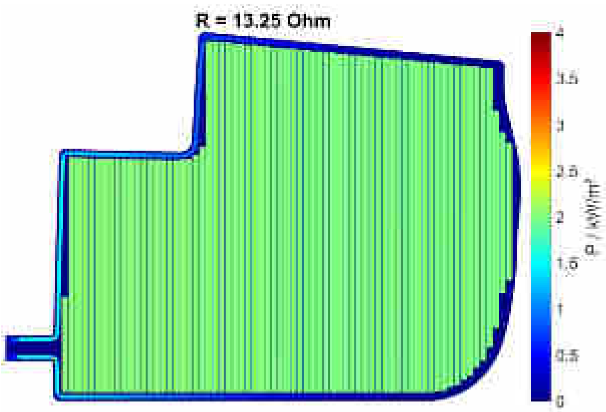

Power Density Distribution

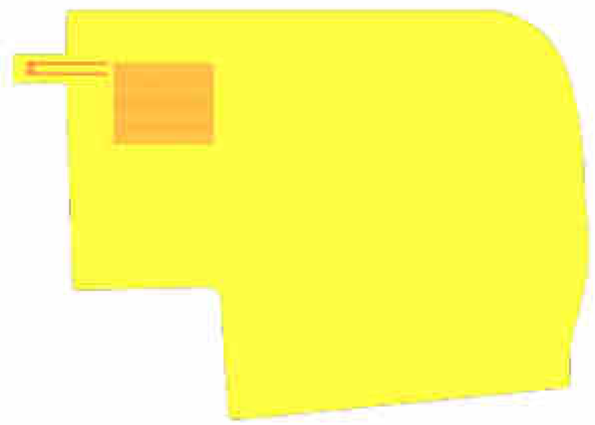

Bottom Side (Sensor)

Figure 29: Illustrative summing up of the roof front properties / implementation

- Area = 1045 cm²
- Power = 174 W
- Resistance = 13 Ω
- Current = 3,63 A

This project has received funding from the European Union's Horizon 2020 research and innovation programme under grant agreement No. 769826. The content of this publication is the sole responsibility of the Consortium partners listed herein and does not necessarily represent the view of the European Commission or its services.

2.3.2.9. Roof Rear

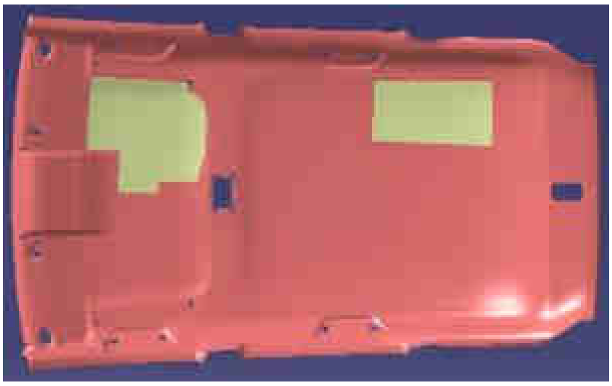

Component

Top Side

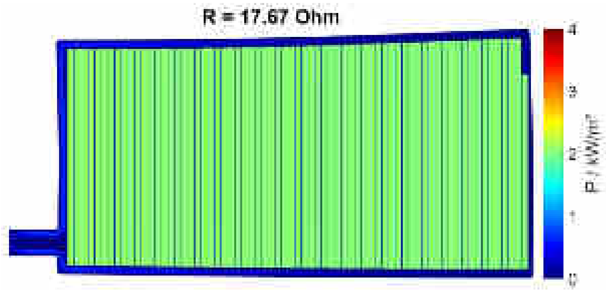

Power Density Distribution

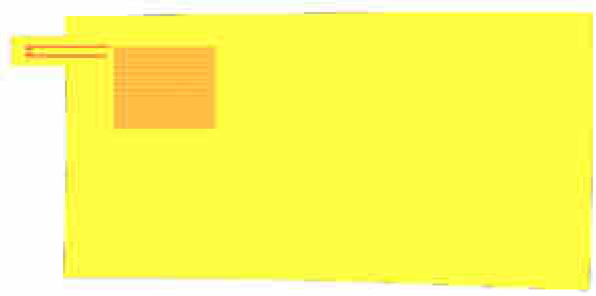

Bottom Side (Sensor)

Figure 30: Illustrative summing up of the roof rear properties / implementation

- Area = 788 cm²
- Power = 130 W
- Resistance = 17 Ω
- Current = 2,71 A

This project has received funding from the European Union's Horizon 2020 research and innovation programme under grant agreement No. 769826. The content of this publication is the sole responsibility of the Consortium partners listed herein and does not necessarily represent the view of the European Commission or its services.

3. Compressor for usage of refrigerant R290 (OBRIST)

For usage of R290 (Propane) a new compressor is necessary. Development and prototype manufacturing of this part was done by OBRIST. Based on the known specifications from OEM's the compressor envelope was elaborated and adopted for Propane (R290) in order to fulfil all current and prospective operation conditions. The envelope can be seen in Figure 31.

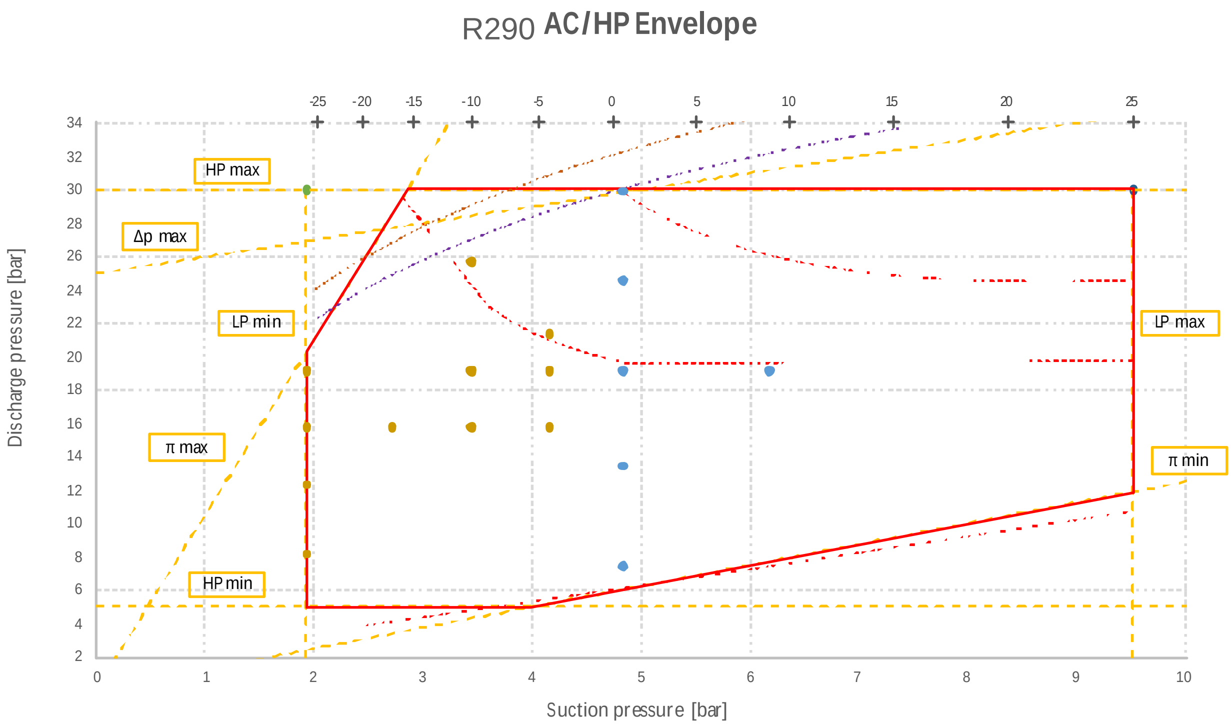

Figure 31: R290 envelope incl. all AC and HP operation conditions from several OEM's

As next step the Basic 3D concept of the compressor was worked out. The idea behind the concept is to keep the widespread VDA compliant mounting concept (3-point mounting) and dimensions. This has the advantage that the compressor is ready for mass production and usable in a wide range of applications. Moreover, a concept study of the subdivision of the individual assemblies and components was figured out. The concept of a "short rearhead" is selected as this concept has only one sealing element to the ambience and a heat transfer from the hot refrigerant on the rearhead (discharge side) is restrained by a gasket. The concept is shown in Figure 32.

This project has received funding from the European Union's Horizon 2020 research and innovation programme under grant agreement No. 769826. The content of this publication is the sole responsibility of the Consortium partners listed herein and does not necessarily represent the view of the European Commission or its services.

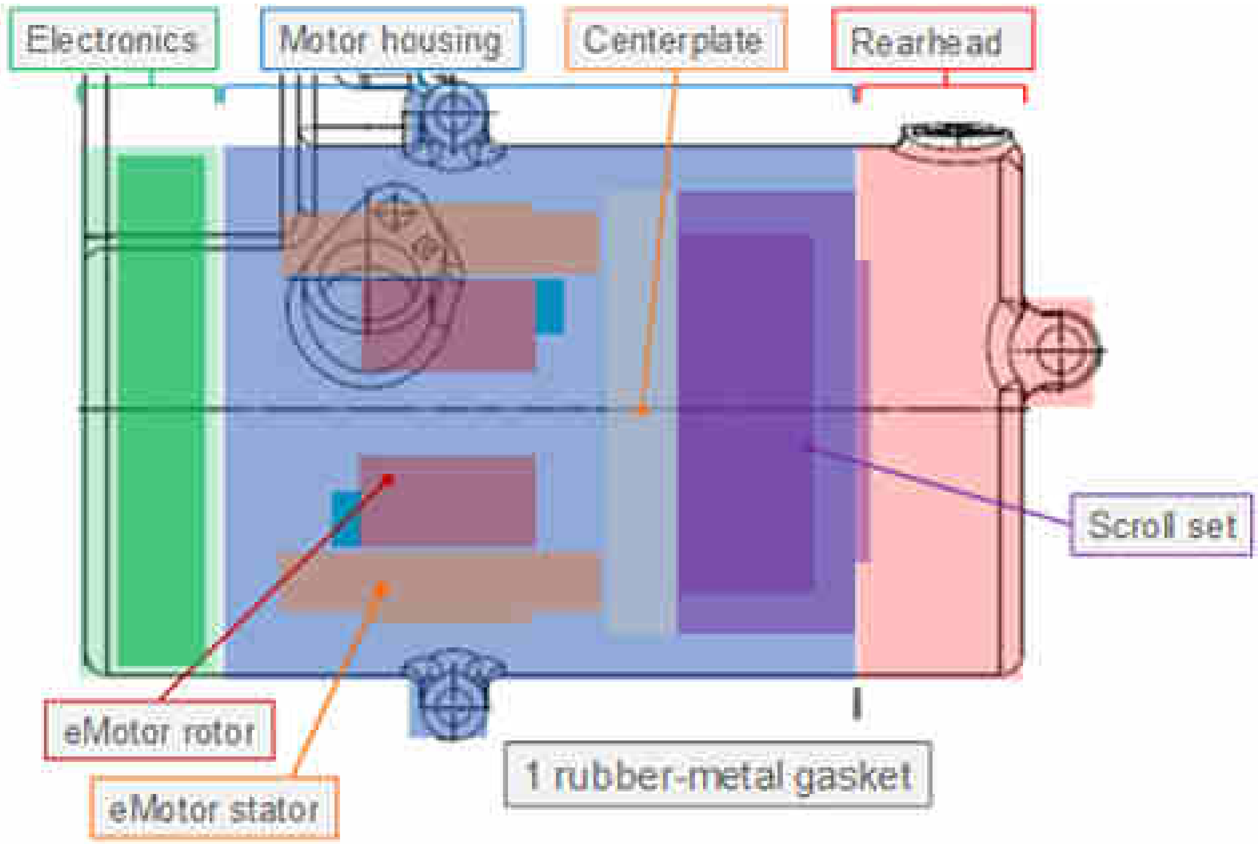

Figure 32: Compressor concept "short rearhead"

Next step of the compressor development was the design, construction and simulation. In order to fulfil requirements of standards (e.g. SAE J 639) the max. operation conditions on the high pressure and low pressure side were predefined by AVL/QPD and can be found in Table 9.

Table 9: Max. operation conditions on the high pressure and low pressure side

	Pressure in bar
High Pressure Side	45
Low Pressure Side	18,663

Based on the limits the housing of the compressor was designed. During the design process several parts were calculated and simulated:

- Scroll Geometry with OBRIST internal Scroll Tool
- Discharge valves
- Gaskets
- Bolts
- Durability of the bearings
- Sealings
- Compliance mechanism
- eMotor stator pressfit
- Balancing
- Shaft deflection
- Bending of centerplate
- Rearhead
- Compliance mechanism tolerances
- Drivepin forces

This project has received funding from the European Union's Horizon 2020 research and innovation programme under grant agreement No. 769826. The content of this publication is the sole responsibility of the Consortium partners listed herein and does not necessarily represent the view of the European Commission or its services.

In several optimization loops the components have been selected and optimized in order to fulfil strength requirements.
The 3D detailed design of the compressor can be seen in Figure 33.

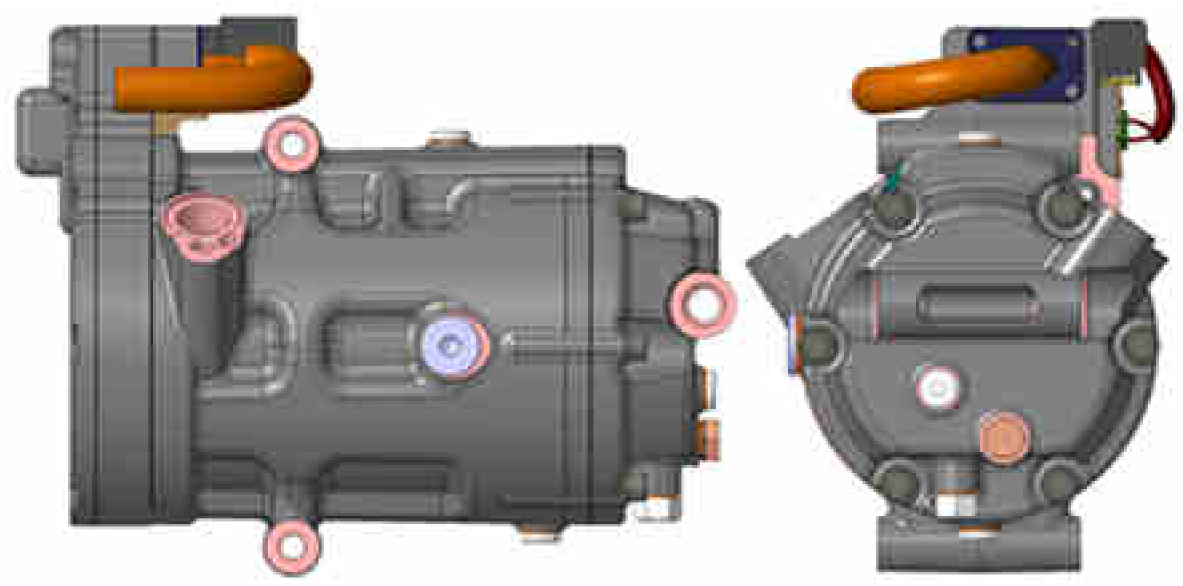

Figure 33: R290 eScroll Compressor 3D design

For illustration of the design process and optimization loop the FEA Calculation of the motorhousing is shown in Figure 34.

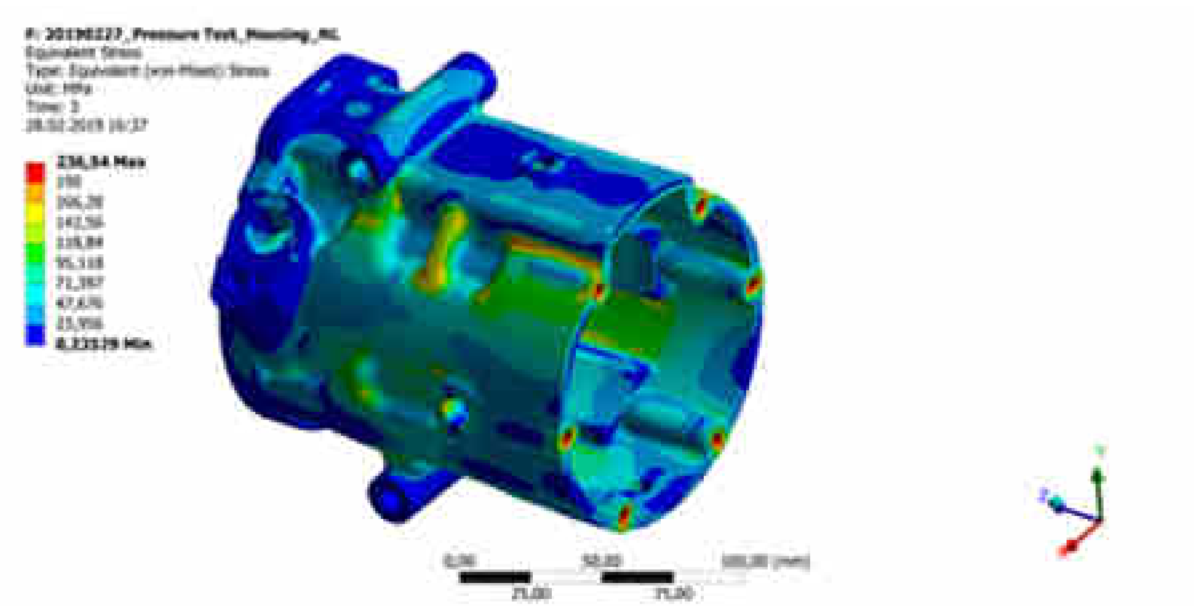

Figure 34: Equivalent Stress of motorhousing under max. design / burst pressure (38 bar)

As a next step a for the refrigerant R290 optimized contour and geometry of the scrolls was designed and simulated with the OBR internal Scroll Simulation Tool. The Swept Volume of the compressor is 27 cm³.
The Fixed and Orbiting Scroll can be found in Figure 35.

This project has received funding from the European Union's Horizon 2020 research and innovation program under grant agreement No. 769826. The content of this publication is the sole responsibility of the Consortium partners listed herein and does not necessarily represent the view of the European Commission or its services.

Figure 35: Fixed and Orbiting Scroll of the OBR R290 eScroll

As an example of the designed Scroll the pressure curve for 4,84/30 bar operation point is shown in Figure 36.

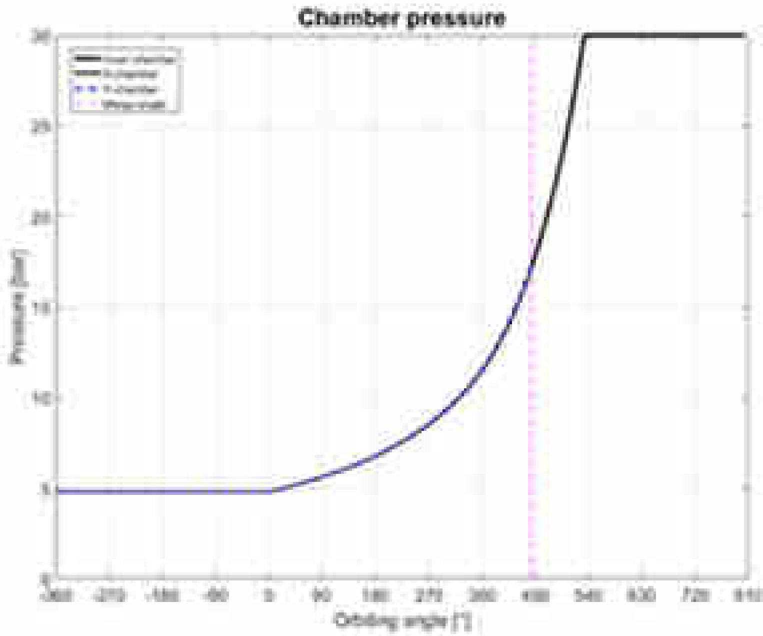

Figure 36: Pressure curve for 4,84/30 bar operation point

The results of the OBR Scroll tool are used to calculate e.g. bearing lifetime, required compliance forces and moments and shaft torque. As next step the parts and components were designed and 2D drawings were done. Based on the made drawings the parts are ordered by approved suppliers, checked and assembled.

After this initial assembly the compressor is tested on test rig. The compressor mounted on the test rig can be seen in Figure 37.

This project has received funding from the European Union's Horizon 2020 research and innovation program under grant agreement No. 769826. The content of this publication is the sole responsibility of the Consortium partners listed herein and does not necessarily represent the view of the European Commission or its services.

Figure 37: Compressor mounted at test rig for initial testing

As a next step the compressor got tested under several operation conditions and the compliance mechanism will be adjusted. After this first series of tests the compressor was disassembled, and all parts were checked in order to examine any abnormalities, wear and damage. The first results of the initial testing and comparison to the baseline Honda FIT EV (Denso ESA27C) compressor can be seen in Figure 38. In equivalent operation conditions the for R290 developed/optimized compressor runs on average about 10 % better than the baseline compressor.

Figure 38: Overall efficiency for OE eR290 01-01 (solid lines) vs. Denso ESA27C (dashed lines)

This project has received funding from the European Union's Horizon 2020 research and innovation program under grant agreement No. 769826. The content of this publication is the sole responsibility of the Consortium partners listed herein and does not necessarily represent the view of the European Commission or its services.

4. Electronic Expansion Valve for usage of refrigerant R290 (VENTREX)

4.1. Requirements

To create a high flexible valve which can be implemented at different positions at the air-condition unit, VENTREX Automotive developed a valve which can handle a big range of orifice diameters. This modularity was necessary to be able to react very fast because the system and therefore the requirements were not fixed at the beginning. Therefore, the valve is divided into three subassemblies which were developed separately:

- Actuator with a motor and a transmission,
- electronic with software and a sensor concept and a
- mechanical subassembly.

In order to find the best suited concept and to be able to deliver in time, three parallel topics were considered at the same time. First of all, many state of the art technologies and benchmarks were analyzed to define the main requirements which was the base for further actions. During that time a specification was defined and reviewed with QPD. In that document, the main requirements like burst pressure, range of orifice diameter, electrical consumption, type of control strategy, type of oil, internal and external leakage and roughly the dimension are defined. With that data, different concepts were considered, and the decision was made with a structured use-value analysis.

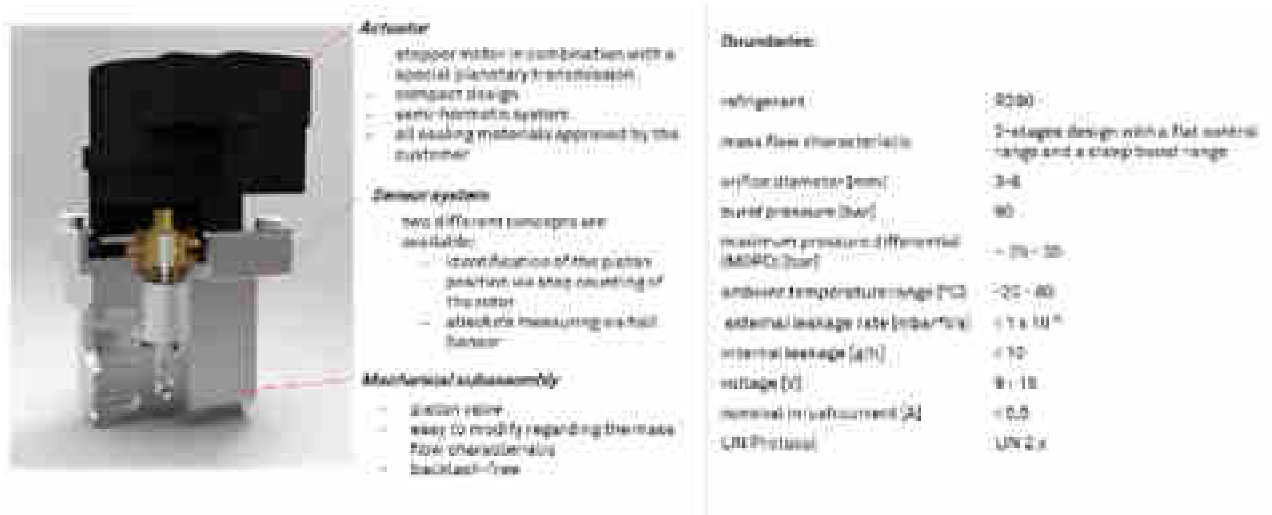

Figure 39: Final concept and boundaries

As shown in Figure 39 the mechanical subassembly consists of a plunger which regulates the mass flow and therefore the expansion. The force needed for movement is delivered by a stepper motor including a transmission. That combination of technologies delivers the flexibility which is necessary to achieve all boundary requirements on the left side the orifice diameter and to ensure that the transmission ratio can change in a wide range. To improve the accuracy, a sensor system is integrated which measures the position of the piston. Additionally, the valve can send and receive messages for controlling and sensing its status using standard automotive data transmission protocols. Therefore, a customized PCB (printed circuit board) is designed which communicates via LIN-Bus (Local Interconnect Network). It controls the motor and analyses the signal from the measuring system. Finally, to minimize the electronic consumption the valve is able to

This project has received funding from the European Union's Horizon 2020 research and innovation program under grant agreement No. 769826. The content of this publication is the sole responsibility of the Consortium partners listed herein and does not necessarily represent the view of the European Commission or its services.

remain stationary without electrical current during operation. To create such a product, it is necessary to combine simulation with real test data.

4.2. Correlation between piston geometry and product properties

To create a correlation between piston geometry and mass flow characteristics a simulation tool was developed. The program either calculates an expected mass flow characteristic according a defined piston geometry, medium and physical conditions, or the other way around. That means the mass flow characteristic acts as an input parameter and the geometry as an output parameter. Another helpful feature is to convert a mass flow characteristic in a different medium like air to propane. So, it is possible to convert the inhouse test data like mass flow into an expected propane mass flow. In Figure 40 the user interface, which provides a valve geometry according to a defined mass flow, is shown.

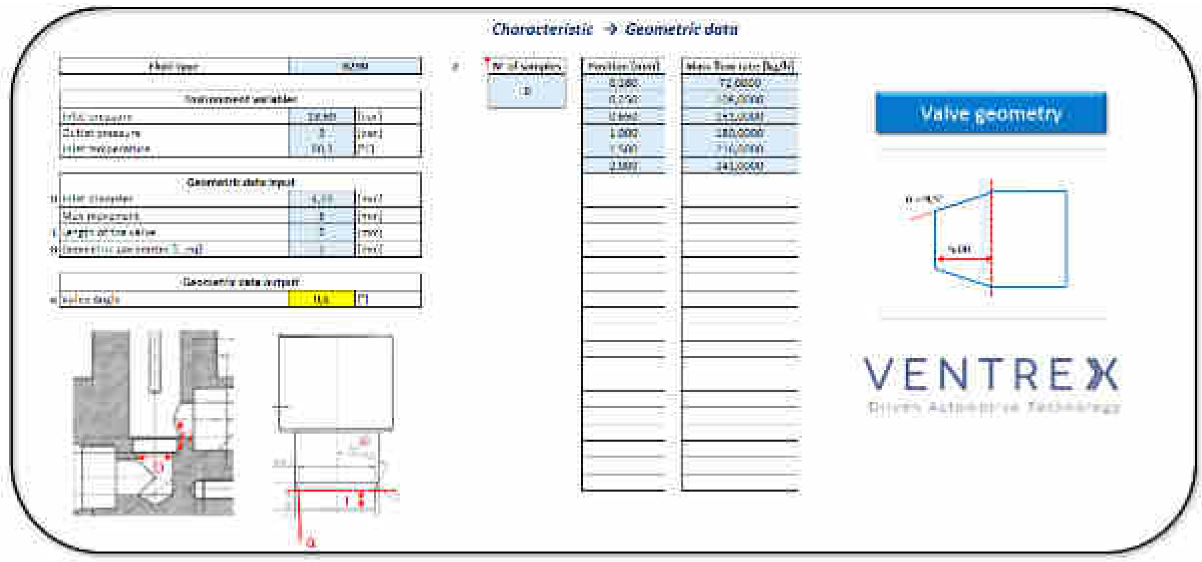

Figure 40: Simulation tool

Therefore, to provide enough data for the simulation tool and to test firsts prototypes, a test bench was designed and developed. A suitable testbed should be able to handle both subassemblies, the actuator including stepper motor, transmission and electronic and the mechanical subassembly which provide the mass flow, internal leakage, pressure drop, hysteresis etc. Only by usage of such a testbed it is possible to focus and to accelerate the development content.

This project has received funding from the European Union's Horizon 2020 research and innovation program under grant agreement No. 769826. The content of this publication is the sole responsibility of the Consortium partners listed herein and does not necessarily represent the view of the European Commission or its services.

4.3. Pneumatic test bench for expansion valves

To test the mechanical subassemblies, the test bench should be able to deliver data regarding mass flow, internal leakage, maximum operating pressure difference, travel time, hysteresis and first life cycle test. To test different development stages, it should be able to control the mechanical subassembly with an external high-performance stepper motor from National Instrument or test prototypes with direct connection to the actuator or test the prototype with integrated electronic and software via LIN Communication. Additional it is possible to operate the prototypes with different mediums like air for mass flow, pressure drop and helium to do external and internal leakage tests. Figure 33 shows on the left side the setup to test the mechanical subassembly. This setup consists of a high-performance stepper motor, a torque measurement shaft and the test object in the front. Additional different pressure levels can be set on the inlet and outlet of the test object.

Figure 41: Test bench for the mechanical subassembly

In Figure 42 the setup to test the actuator subassembly is shown. That setup is able to evaluate stepper motor with and without a transmission in different ambient temperatures. Therefore, the test object is connected to a hysteresis brake and to a load cell.

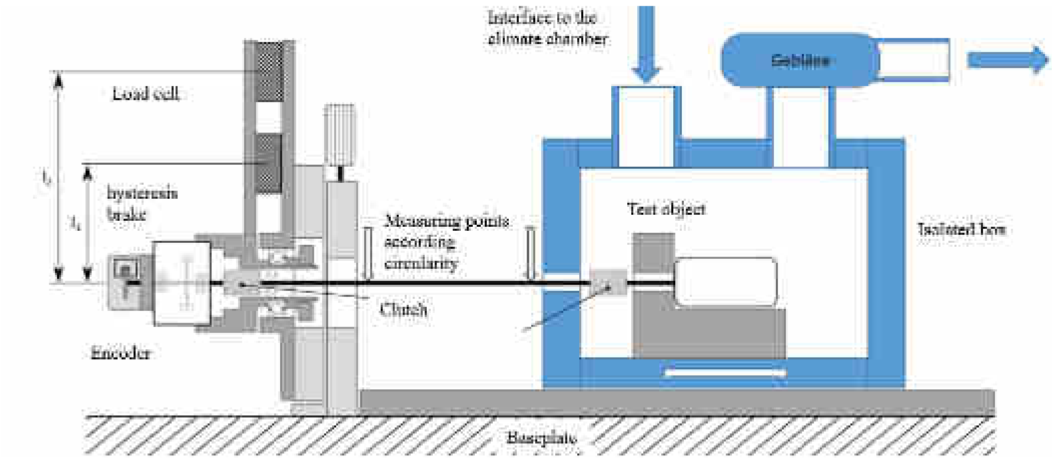

Figure 42: Schematic design of the actuator test bench

Development approach and separate consideration of subassemblies:
With that possibilities to create data with prototypes VENTREX decided to develop the subassemblies independently. The focus during development of the mechanical subassembly was on:

- two stage mass flow characteristics
- pressure drop
- internal leakage and the
- repeatability

The first two requirements were solved with a simulation test cycle. Virtual piston and valve body geometries were virtual analyzed, internal machined and tested. VENTREX repeated that procedure with different orifice diameter and different mass flow characteristics to find the most efficient geometry for the upcoming system. To fulfil the internal leakage requirements the main challenge is to reach the target by minimum required torque. To find that most efficient point, the impact of different parameter were investigated by a defined test plan by design of experience. The impact of each parameter to another one is shown in Figure 43. Parameters like different sealing angels, surface roughness and material pairings were considered. Additional, to ensure the reliable operation over the entire life time, a special low-friction axial bearing is integrated separating the mechanical subassembly from the actuator. Finally, to improve the efficiency of the system, it is important to guarantee a tight tolerance of the mass flow characteristic which means to deliver a high repeatability. That requires that the valve is be able to deliver always the same mass flow in each position of the piston. Therefore, VENTREX did a huge number of tests with different prototypes to define the needed tolerances between each part. That correlation between orifice diameter, needed piston movement, mass flow and needed torque was the basis which is necessary to define the actuator design.

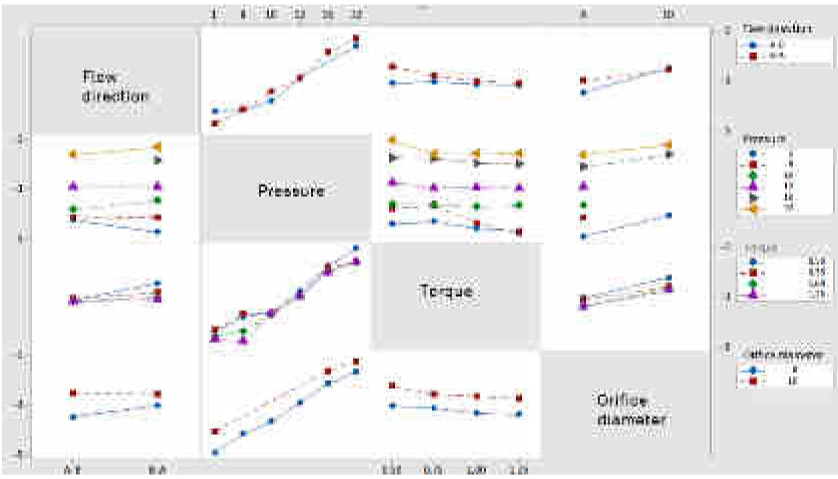

Figure 43: Interaction of parameters with DoE

To fulfil the tough external leakage requirement, a semi hermetic system was necessary. Because of that, VENTREX decided to use a stepper motor which provides the option to separate the stator from the rotor. That gives the flexibility to integrate a capsule between that two components to seal the product with a static O-ring. This principal is shown in Figure 44. The grey part illustrates the stator and blue the rotor which is separated with a capsule shown in dark grey. To have a high flexibility according transmission ratio a planetary gearbox is considered. That special gearbox, which is shown in green offers a wide range by same installation requirements.

This project has received funding from the European Union's Horizon 2020 research and innovation program under grant agreement No. 769826. The content of this publication is the sole responsibility of the Consortium partners listed herein and does not necessarily represent the view of the European Commission or its services.

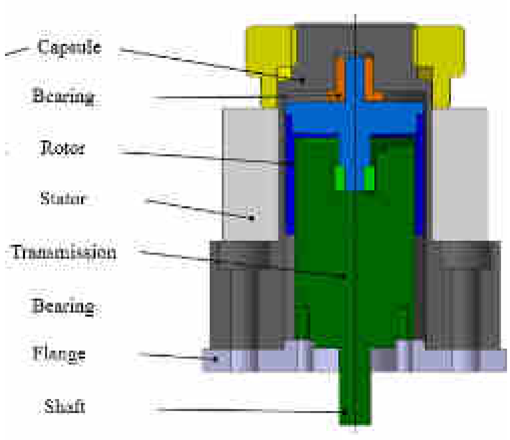

Figure 44: Actuator test object

With that test objects it was possible to combine the right components to achieve different torque requirements depending on the orifice diameter. Therefore, different windings with changed resistance and the impact of the increased airgap were investigated. The aim was to increase the torque by lower frequency which is used to close the valve and provide enough torque to move fast enough under operating conditions. Figure 45 shows a comparison of the characteristics of the two variants.

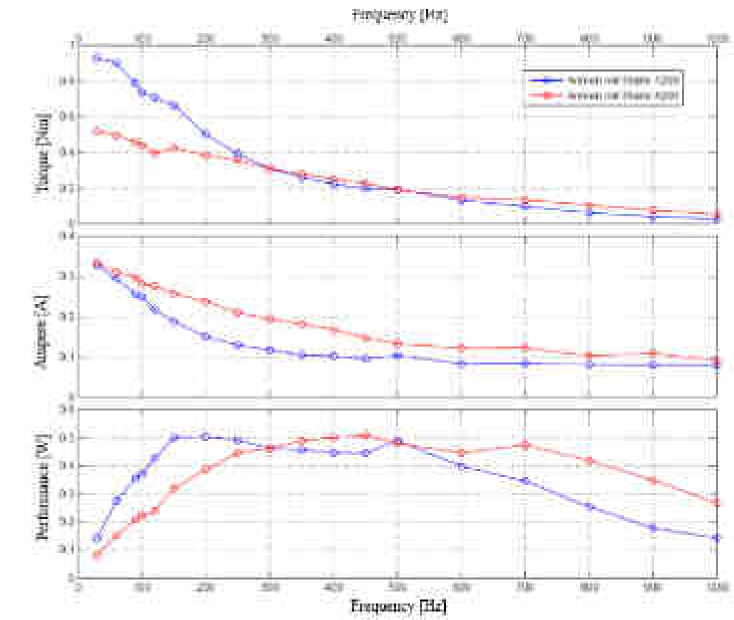

Figure 45: Influence of the winding resistance, comparison of the two variants

During intensive discussions with QPD and sharing knowledge about the system and the needed opening geometric area over time, VENTREX chose a suitable orifice diameter and correspondingly the correct transmission ratio. That kind of valve will be tested inhouse according to typical requirements and will be tested at the system under real condition. The following Figure 46 shows the requirements which VENTREX received from QPD from the system simulation. The required opening area is compared with the simulated mass flow characteristic on the right side. To increase the efficiency during system validation, VENTREX

This project has received funding from the European Union's Horizon 2020 research and innovation program under grant agreement No. 769826. The content of this publication is the sole responsibility of the Consortium partners listed herein and does not necessarily represent the view of the European Commission or its services.

provided two valves with different mass flow characteristics to AVL to find the best fitted solution for the system.

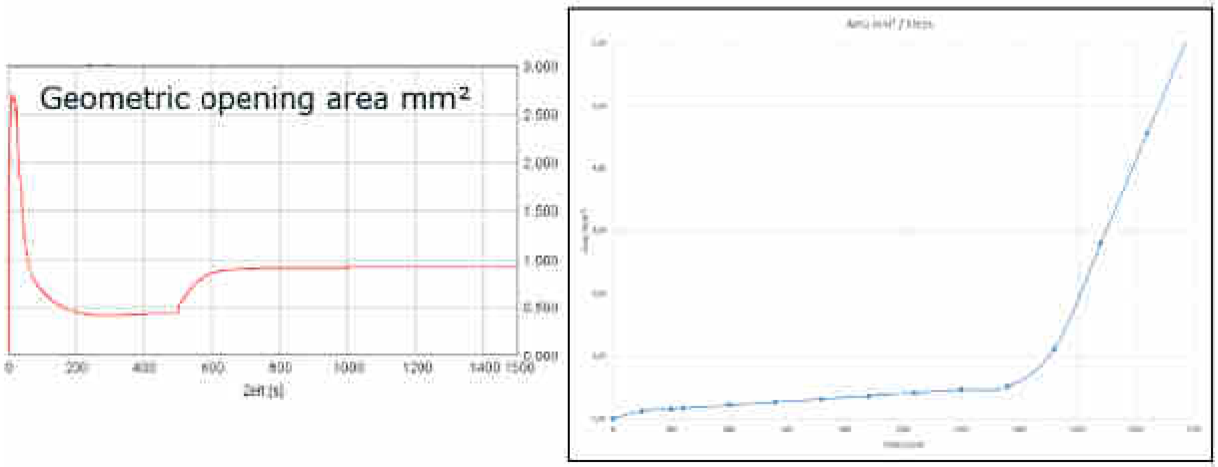

Figure 46: Comparison between needed opening area and mass flow characteristic

5. Safety Relief Valve – Pressure Relief Valve for usage of refrigerant R290 (VENTREX)

5.1. Assessment of R290 as refrigerant

As one potential source for energy savings R290 (Propane) has been chosen as refrigerant for the AC system to be developed within the present project [9], [10]. R290 meets nearly all requirements for an ideal refrigerant, which are:

- No ozone depleting potential (ODP)
- Low global warming potential (GWP)
- Chemically stable over a wide temperature range
- Compatibility with the system's materials (metals,elastomeres, oil)
- No toxicity
- No flammability
- High refrigerating capacity
- Low cost
- Availability
- Safe handling

Exception are the point of flammability and resulting out of this the point of safe handling.

Table 10 gives a good overview of thermodynamic parameters of refrigerants, comparing commonly used refrigerants with R290.

Table 10: Thermodynamic Properties of Refrigerants [11]

Refrigerant	Chemical Notation	Molar mass [kg/kmol]	Boiling Point at 1,01325 bar [°C]	Critical Temperature [°C]	Critical Pressure [bar]	Safety Class	ODP	GWP
R290	C_3H_8	44,1	-42,2	96,7	42,5	A3	0	3,3
R1234yf	$C_3H_2F_4$	114,04	-29	94,07	33,8	A2L	0	4
R134a	CH_2FCF_3	102,0	-26,0	101,1	40,6	A1	0	1430
R744	CO_2	44,01	-78,5	31,0	73,8	A1	0	1

This project has received funding from the European Union's Horizon 2020 research and innovation program under grant agreement No. 769826. The content of this publication is the sole responsibility of the Consortium partners listed herein and does not necessarily represent the view of the European Commission or its services.

It is remarkable is that R290 is classified as Safety Class A3, which means that it has a very high flammability, as can be seen in Table 11.

Table 11: Safety Groups [12], [13]

Flammability in Air @ 60 °C & 101.3 kPa	ASHRAE 34 Safety group	
Higher Flammability LFL or $ETFL_{60}$ ≤ 100 g/m³ OR HOC ≥ 19 MJ/kg	A3	B3
Lower Flammability LFL or $ETFL_{60}$ > 100 g/m³ & HOC < 19 MJ/kg	A2	B2
Lower Flammability LFL or $ETFL_{60}$ > 100 g/m³ & HOC < 19 MJ/kg with a maximum burning velocity of ≤ 10 cm/s	A2L	B2L
No flame Propagation	A1	B1
Flammability in Air @ 60 °C & 101.3 kPa	Lower Toxicity OEL ≥ 400 ppm	Higher toxicity OEL < 400 ppm

The fact that R290 is classified like that is one of the biggest issues companies face when thinking about manufacturing MACs (Mobile Air Conditions) using R290 as a refrigerant. But the issue does not come as much from its potential of being high flammable as it comes from the fact that there are no standards and/or regulations which could give guidelines when companies intend to register MACs using R290 as a refrigerant.

After talks, meetings and correspondences with numerous experts on MACs, refrigerants as well as people who work for registration institutes, a possible 'roadmap' to register MACs using R290 as a refrigerant was defined.

The central point of this roadmap is comparing R290's (flammable) properties with the ones of R1234yf, as can be seen in Table 12.

Table 12: R1234yf vs. R290 [14], [15]

	R1234yf	R290
Flash Point	Not applicable to gases and gas mixtures	-104 °C
Flammability (solid, gas)	Flammable Gas	
Flammability Limit - Upper (%)	12,3 %(V)	10,8 %(V)
Flammability Limit - Lower (%)	6,2 %(V)	1,7 %(V)
Autoignition Temperature	405 °C	472 °C
Minimum ignition energy	5 - 10 J	0,25 mJ
Hazardous Combustion Products	If involved in a fire the following toxic and/or corrosive fumes may be produced by thermal decomposition: Carbon oxides hydrogen fluoride	Incomplete Combustion may form carbon monoxide

Since R1234yf is an established and registered refrigerant for the use in MACs, the process of successful registration of a R290-MAC should be orientated on the existing process of the registration of a R1234yf-MAC.

This project has received funding from the European Union's Horizon 2020 research and innovation program under grant agreement No. 769826. The content of this publication is the sole responsibility of the Consortium partners listed herein and does not necessarily represent the view of the European Commission or its services.

Standards and regulations handling those registrations are (extract):

- ISO 13043: Road vehicles – Refrigerant systems used in mobile air conditioning systems (MAC) – Safety requirements
- DIRECTIVE 2007/46/EC OF THE EUROPEAN PARLIAMENT AND OF THE COUNCIL: establishing a framework for the approval of motor vehicles and their trailers, and of systems, components and separate technical units intended for such vehicles
- DIRECTIVE 2006/40/EC OF THE EUROPEAN PARLIAMENT AND OF THE COUNCIL: relating to emissions from air-conditioning systems in motor vehicles and amending Council Directive 70/156/EEC
- COMMISSION REGULATION (EC) No 706/2007: laying down, pursuant to Directive 2006/40/EC of the European Parliament and of the Council, administrative provisions for the EC type-approval of vehicles, and a harmonised test for measuring leakages from certain air conditioning systems
- SAE J639: Safety Standards for Motor Vehicle Refrigerant Vapor Compression Systems

Nevertheless, R290 as a refrigerant for MACs is still only used in prototypes or test benches, and a commercialization as such is – mainly due to the enormous effort – not expected to happen any time soon.

Unfortunately, Propane applications in MACs need to meet far more stringent safety requirements compared to approved ones, such as canned heat sources for gas cookers [16], [17].

5.2. Safety Concept – Pressure Relief Valve

Since for this project R290 was chosen to be the MAC's refrigerant, VENTREX' contribution is, in addition to providing the EXV as component, to ensure a sufficient level of safety when dealing with this refrigerant. To do so, two solutions have been provided which were found according to Figure 47.

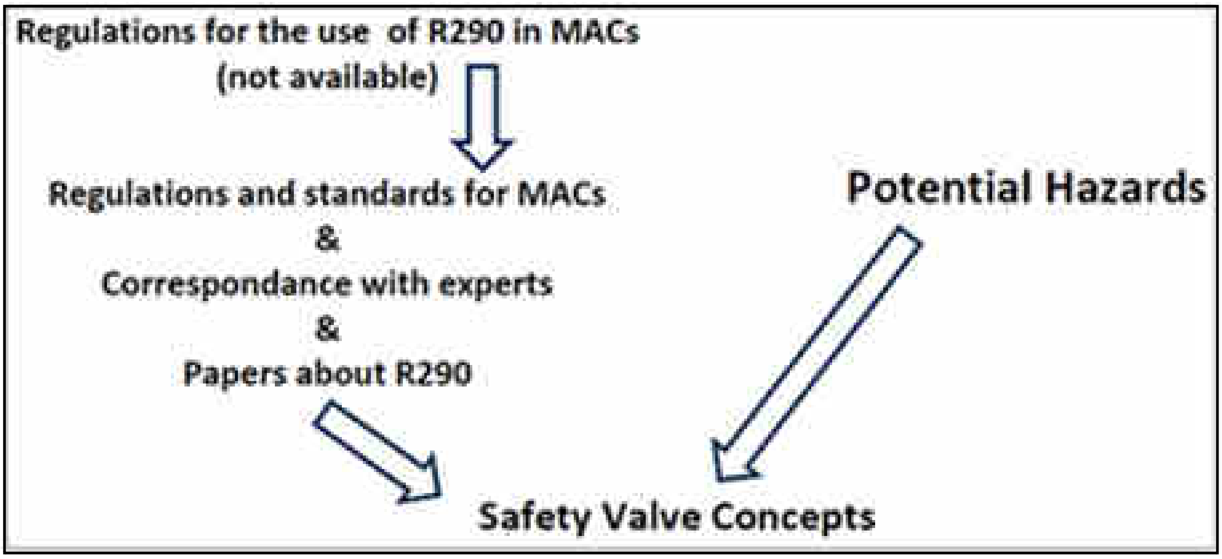

Figure 47: Process of Safety Concept Finding

The lack of data on regulations for the use of R290 led to a literature study, which evaluates the consequences of an AC's leak using R290 as a refrigerant with the help of numerical and experimental methods [16].

This project has received funding from the European Union's Horizon 2020 research and innovation program under grant agreement No. 769826. The content of this publication is the sole responsibility of the Consortium partners listed herein and does not necessarily represent the view of the European Commission or its services.

The experimental parameters were:

- Charge quantity: 200 g, 300 g and 350 g
- Leakage hole diameter: 0,5 mm, 1 mm and 4,37 mm

Main conclusions:

- Charge quantity has a major influence on the R290 concentration distribution in the room. Higher R290 charge à more extensive combustible zone and longer residence time in the room.
- A larger hole doesn't necessarily lead to a longer combustible zone's residence time
- Avoid potential ignition sources underneath the evaporator as it is the most probable zone to suffer a leakage.

Especially item 1 led to the decision to reduce the MAC's charge quantity below 150 g, which is also the limit for stationary AC's where, according to DIN EN 378 (which is no automotive regulation), no special requirements for installation need to be fulfilled if more than 4 m^3 of free volume are present [17]. The reason is that the lowest flammability concentration for R290 is 38 g/m^3. For a maximum volume of 150 g per refrigerant circuit a flammable concentration cannot develop at any time.

The second solution reacts to a sudden increase of pressure/temperature in the cooling system itself. Before the pressure in the cooling cycle gets too critical, refrigerant will be released via VENTREX' Pressure Relief Valve (PRV). A sketch can be seen in Figure 48.

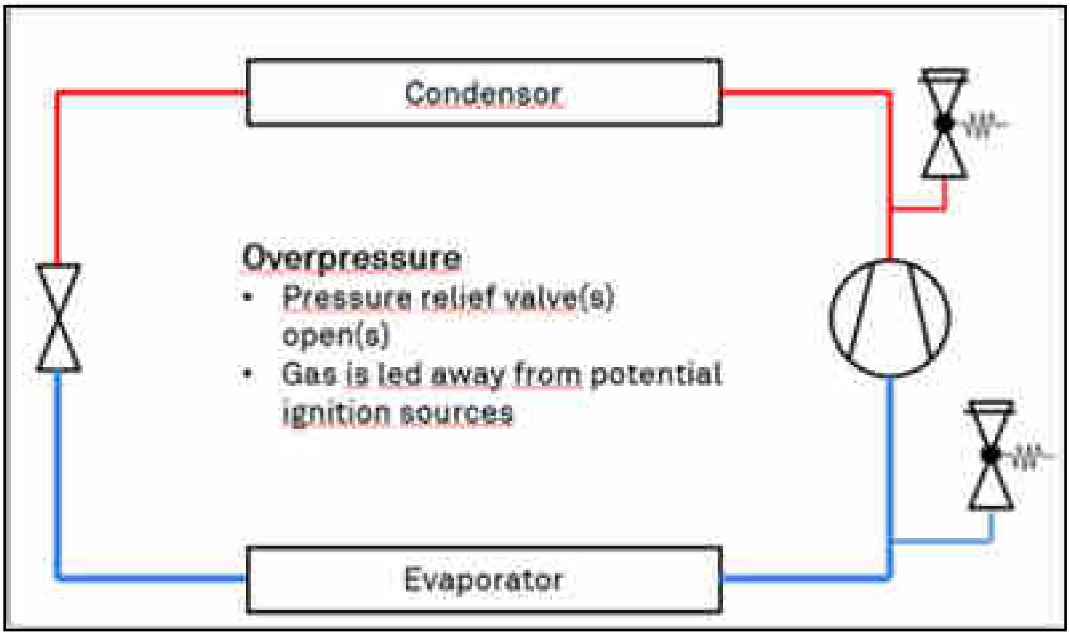

Figure 48: Sketch of Operation of Pressure Regulating Valve

The PRV can be mounted anywhere in the cycle, although it makes sense to implement it in the cooling cycle's high pressure side – after the compressor.

This project has received funding from the European Union's Horizon 2020 research and innovation program under grant agreement No. 769826. The content of this publication is the sole responsibility of the Consortium partners listed herein and does not necessarily represent the view of the European Commission or its services.

The release of refrigerant by the PRV is triggered via a spring which gets compressed at a desired pressure level and opens a path for the refrigerant. For this project, the triggering pressure is set to be at 35 +2 bar but can be easily adapted by changing the PRV's spring pre-load for small adjustments. For major triggering pressure adjustments the spring itself has to be replaced by a stronger/weaker one. Also, inside the connection geometry, a mesh is making sure that no dirt or whatever is getting in contact with the sealing which is pre-loaded by the spring. This is especially important for the sealing's tightness after the PRV has already been triggered.
When releasing refrigerant it is important to lead the discharged gas away from any potential source of ignition. For this case, a piping can be attached at the outlet side of the valve. This, together with the connection thread as well as the PRV's length is displayed in Figure 49.

Figure 49: VENTREX Pressure Regulating Valve

Before sending out the PRVs, they get internally tested at VENTREX to provide information and to be secure concerning the correct triggering pressure and the tightness, especially after the PRV has been triggered. VENTREX' test bench can be seen in Figure 50.

This project has received funding from the European Union's Horizon 2020 research and innovation program under grant agreement No. 769826. The content of this publication is the sole responsibility of the Consortium partners listed herein and does not necessarily represent the view of the European Commission or its services.

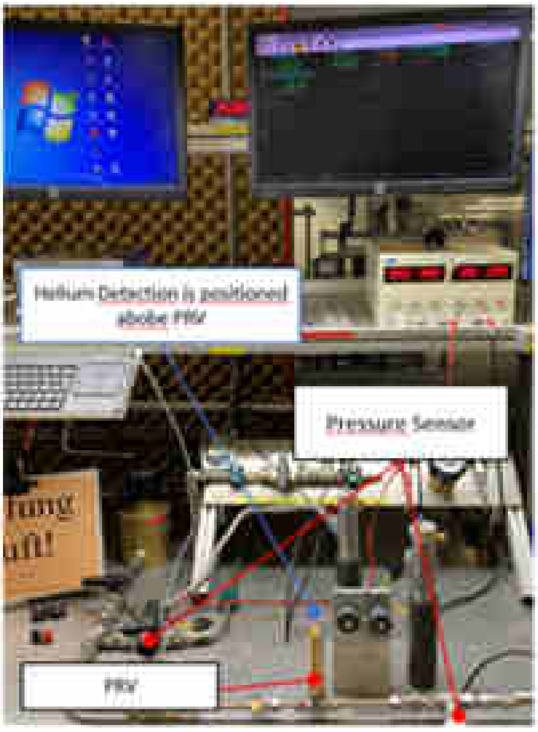

Figure 50: VENTREX Test Bench for Pressure Regulating Valves (PRVs)

Two pressure sensors detect the pressure before and after the PRV. Above the PRV, at its outlet, a Helium detection sensor is placed, as the tests are performed with a mixture of 10% Helium and Air. When testing the triggering pressure, the point of time (and the pressure) when the PRV opens up can be determined by detecting any release of Helium. The same procedure, of course, is being used for external leakage tests.

This project has received funding from the European Union's Horizon 2020 research and innovation program under grant agreement No. 769826. The content of this publication is the sole responsibility of the Consortium partners listed herein and does not necessarily represent the view of the European Commission or its services.

6. Advanced thermal storage technology based on phase change material – construction and development of a PCM heat storage (RUBITHERM)

6.1. Specifications:

Around 500W of heat should be dissipated for a period of 5 minutes (42Wh minimum capacity). The maximum storage size including insulation is: 490 x 275 x 80 mm. The usable temperature range of the storage medium needs to be between 15 °C and 20 °C.

6.2. Challenge:

The paraffin-based PCM RT18HC with a latent heat of approx. 230 kJ/kg (64 Wh/kg) and a narrow melting / solidification range around 18 °C is suitable to store 42 Wh of heat between 15 and 20 °C.

Previous applications for PCM in air- or water-guided heat exchangers allow charging and discharging times between 2h and 8h. The heat transfer rate of these systems is between 0.1 and 0.5 W output per Wh heat storage capacity. Due to the specifications of the project, the heat transfer must be increased to 12 W per Wh (factor 25-100!).

6.3. Pretests:

At the beginning of the project, different heat exchanger systems were tested: 1. a convectional water/water plate heat exchanger in which water was replaced by PCM in one part, 2. a graphite PCM mixture with integrated Cu coil and 3. Aluminium (Al) foams filled with PCM and integrated Al pipes. Only the Al foams achieved the required heat transfer rates and required power levels.

6.4. Implementation in storage size:

In order to integrate the necessary amount of PCM in the given dimensions, 4 Al foam bodies were ordered after consultation with the manufacturer (IFAM). The 8 Al-pipes (needing 16 connections) contained therein would allow a good flow of coolant and low pressure loss. As these foams could not be supplied yet, only the 26 smaller units supplied previously – each of them containing one pipe – were used so far. Combining all of them to one storage requires 52 connections leading to several design difficulties: 1. All connections have to be water tight. 2. The tightening should not influence the inner diameter of the pipes leading to pressure loss. 3. The space needed for the number of connections take up too much room in the limited space available.

6.5. Filling of Al Foam Units with PCM:

The Al foams are easy to fill with low-viscosity liquids, but have little retention capacity. For this reason, the initial tests were carried out with a sealed tank, with all pipe connections at the top and connected there to each other. The problem with this test design was that the many tight bends in the connecting hoses increased the pressure loss. Thermal measurements could be made, but the water flow had to be forced through. The pressure loss was reduced to a certain extent by connecting the pipes in parallel. However, uniform flow could not be guaranteed.

To avoid leaking on the part of the PCM the Al foams are now filled with thickened PCM using multistep vacuum infiltration. The foams filled this way are wrapped in aluminium foil and can thus be installed leak-proof. There are different degrees of PCM filling. After several filling attempts this could be traced back to slightly different porosities of the foams. On average, the weight of the empty Al foam units was 90g. After

This project has received funding from the European Union's Horizon 2020 research and innovation program under grant agreement No. 769826. The content of this publication is the sole responsibility of the Consortium partners listed herein and does not necessarily represent the view of the European Commission or its services.

filling, the weight was 150 g. The 60 g PCM consist of 90% RT18HC and 10% thickener resulting in 54 g PCM per unit. With 26 pieces this adds up to 1.4 kg RT18HC in the storage. The latent heat storage capacity is thus approx. 90 Wh. In order to achieve the required performance within the specified timeframe, overcapacity must be available. A further consequence of the many small components is the somewhat unfavourable use of space (Figure 51). As a consequence the insulation layer implemented has only a thickness of 10 mm. The melamine resin foam used has a density of about 20 kg/m³ and a thermal conductivity of about 0.02W/m*K. Despite these shortcomings a compact box could be manufactured (Figure 52) whose dimensions and connections could be adapted to the specifications (Figure 53).

Figure 51: Al Foam Units Stacked and Connected

Figure 52: Top View of the Closed Storage Unit

This project has received funding from the European Union's Horizon 2020 research and innovation program under grant agreement No. 769826. The content of this publication is the sole responsibility of the Consortium partners listed herein and does not necessarily represent the view of the European Commission or its services.

Figure 53: Connectors to the Coolant System, Possible Mounting for Installation Purposes in the Vehicle

6.6. Performance Test of the PCM Storage

Pressure loss testing:

First the pressure loss behaviour of the box was determined (Figure 54). At a 1l/minute flow the loss is 20mbar, at 1.7l/minute 200mbar. Afterwards tests were carried out with a thermostat, whereby the pump installed there does not deliver more than 1 - 1.2 l/minute. However, this was sufficient for the transfer of the desired heat quantities.

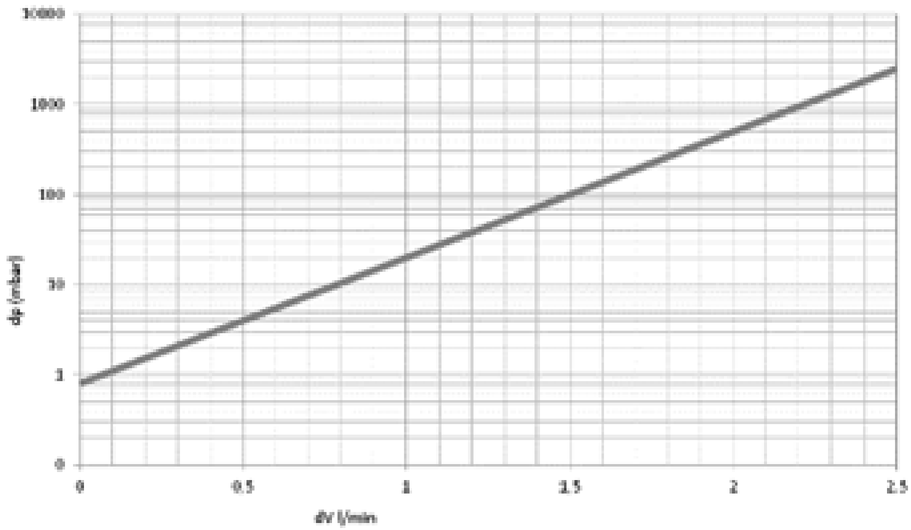

Figure 54: Pressure Loss versus Flow Rate

This project has received funding from the European Union's Horizon 2020 research and innovation program under grant agreement No. 769826. The content of this publication is the sole responsibility of the Consortium partners listed herein and does not necessarily represent the view of the European Commission or its services.

Charging with Warm Water:

The PCM in the storage was melted using a temperature reservoir of 28°C but the system temperature was still lower at the start of documentation. The flowrate used was 1.1 l/minute. The water temperature was measured at the entrance and exit of the storage (in, out in (Figure 55)). Using these data the power uptake of the storage was determined (Figure 56), and the stored heat quantity at any time during the charging process deduced (Figure 57). The experiment was repeated several times to check for cycle stability.

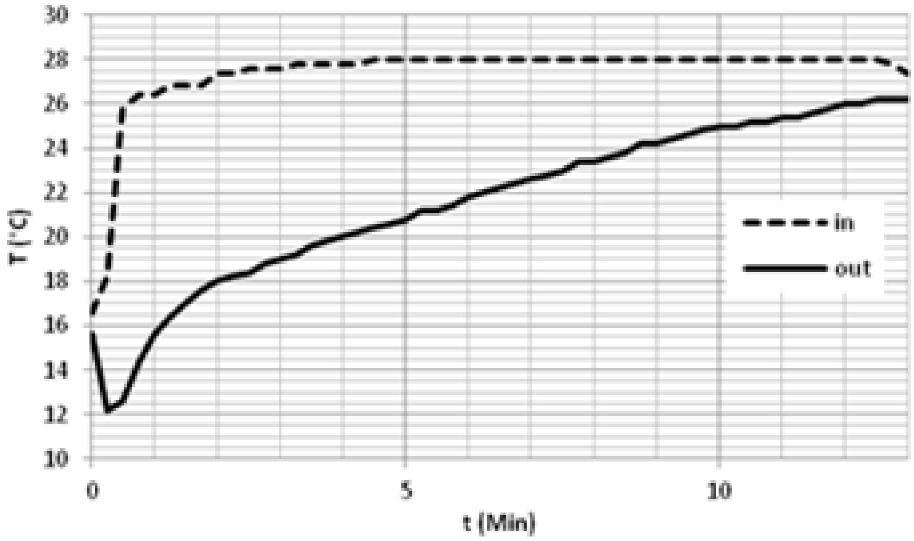

Figure 55: Charging of the Storage, in: T-Water before the Storage, out: T-Water after the Storage

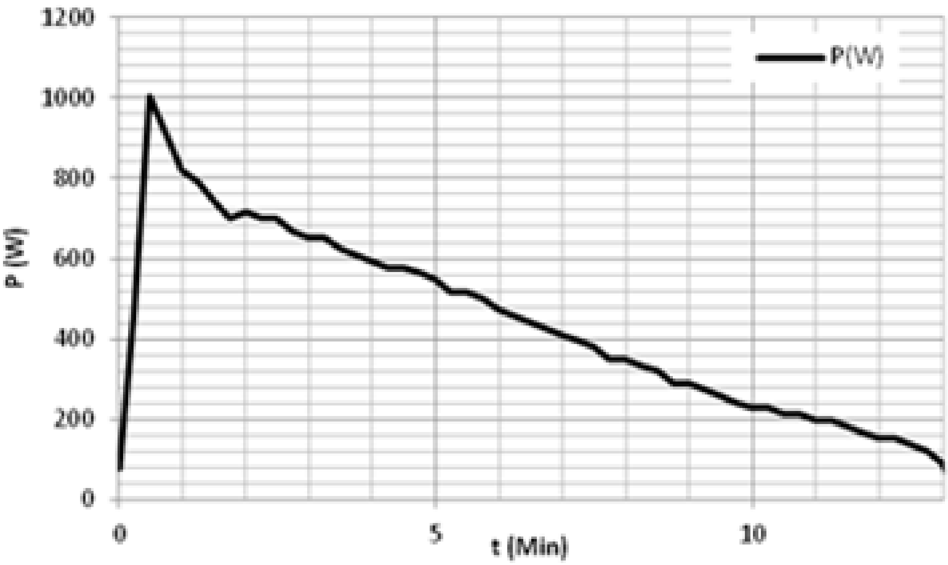

Figure 56: Power Input into the Storage

This project has received funding from the European Union's Horizon 2020 research and innovation program under grant agreement No. 769826. The content of this publication is the sole responsibility of the Consortium partners listed herein and does not necessarily represent the view of the European Commission or its services.

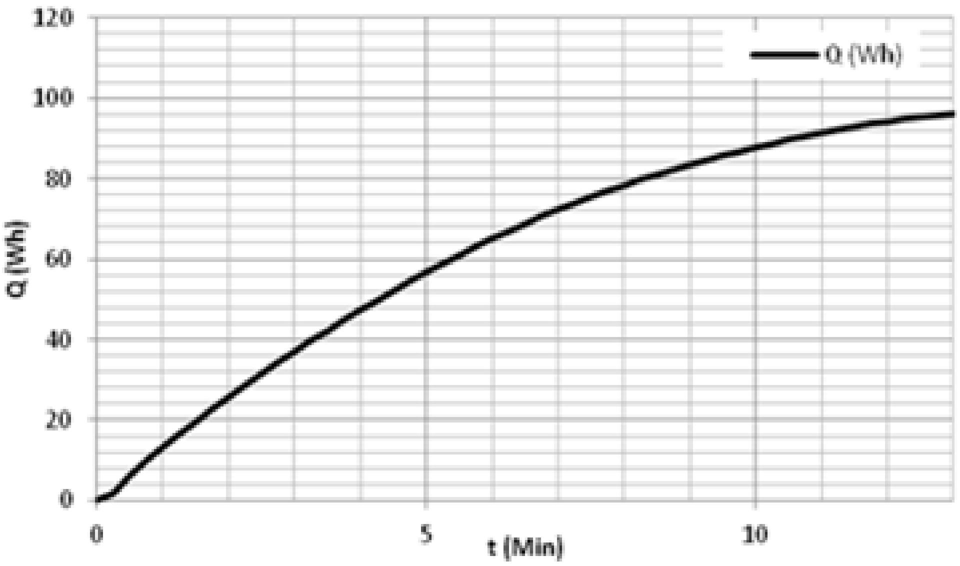

Figure 57: Stored Heat Quantity

Discharging with Cold Water:

Similar to the charging the discharging was performed using a water reservoir with a temperature of 8°C. The flow rate used was 1.0 l/minute. The experiment was repeated several times to check for cycle stability.
The water temperature was measured at the entrance and exit of the storage (see in, out in Figure 58) and the power output determined (Figure 59). In Figure 60 the heat quantity transferred to the water is shown which proves that this storage tank provides more than the required amount of heat (at least 42Wh) within the specified 5 minutes.

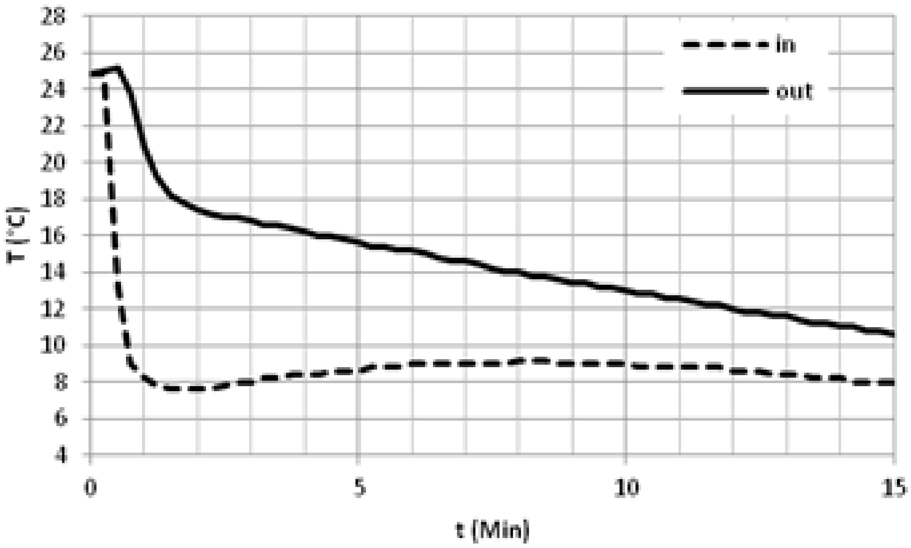

Figure 58: Discharging of the Storage, in: T-Water before the Storage, out: T-Water after the Storage

This project has received funding from the European Union's Horizon 2020 research and innovation program under grant agreement No. 769826. The content of this publication is the sole responsibility of the Consortium partners listed herein and does not necessarily represent the view of the European Commission or its services.

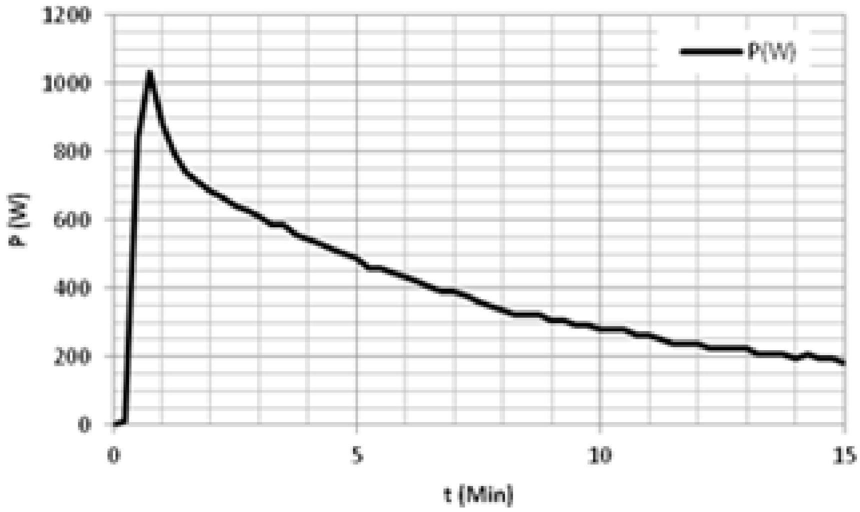

Figure 59: Power Output of the Storage

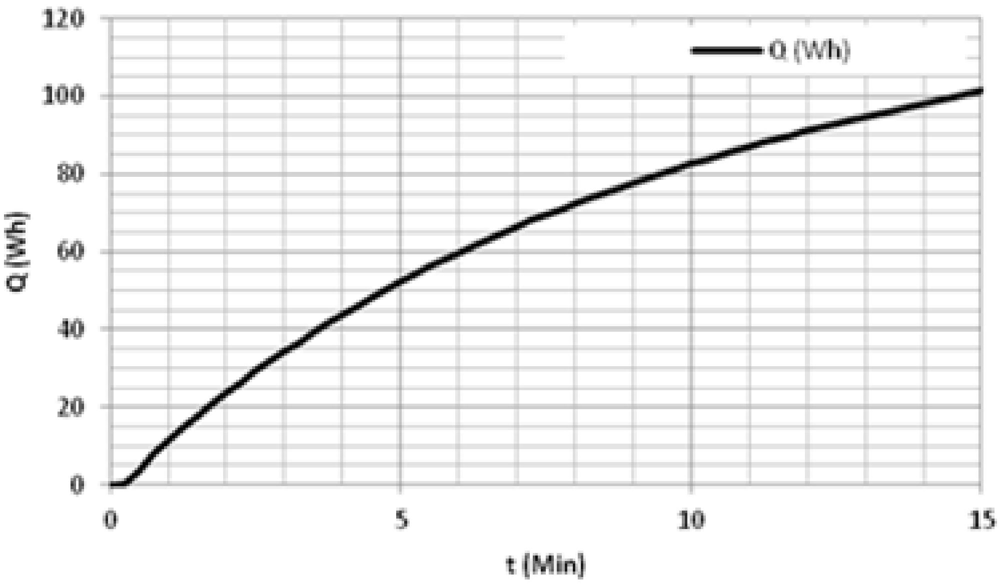

Figure 60: Delivered Heat Quantity

6.7. Conclusions

RUBITHERM succeeded to design a heat accumulator that meets the specified performance criteria regarding power, capacity and temperature range. The increased heat conduction allowing these high power levels is due to the novel Al foam supplied by IFAM. The filling with leak-proof PCM was developed at RUBITHERM to such an extent that application-safe components can be made in small numbers. The single units are combined to form a heat accumulator that reacts with unprecedented speed for PCM applications. The storage tank still needs improvement regarding use of space. The so far installed 10mm insulation layer should be replaced by a 20mm layer to reduce losses in hot and cold environments not tested yet. An improved arrangement and size of the Al foams will lead to less spatial needs and also further reduce pressure losses thus making its performance also more interesting for a broader range of applications.

This project has received funding from the European Union's Horizon 2020 research and innovation program under grant agreement No. 769826. The content of this publication is the sole responsibility of the Consortium partners listed herein and does not necessarily represent the view of the European Commission or its services.

7. System evaluation for efficient heating and cooling of passenger compartment (QPD, AVL)

To be able to assess the behaviour of the donator vehicle, and as baseline for the improvement and corresponding development of energy efficient technologies, measurement data supplied by Honda R&D Germany (HRE-G) were screened and assessed. These measurements were performed on a conditioned dyno for summer and winter cases. It was found that the HVAC system has got significant influence on driving range. The following Figure 61 shows the reduction of driving range in World Harmonized Light Vehicle Test Procedure (WLTP) caused by the HVAC system. As to see there is remarkable potential for the improvement of driving range by means of energy efficient HVAC components, incl. usage of a heat pump and corresponding smart control strategies.

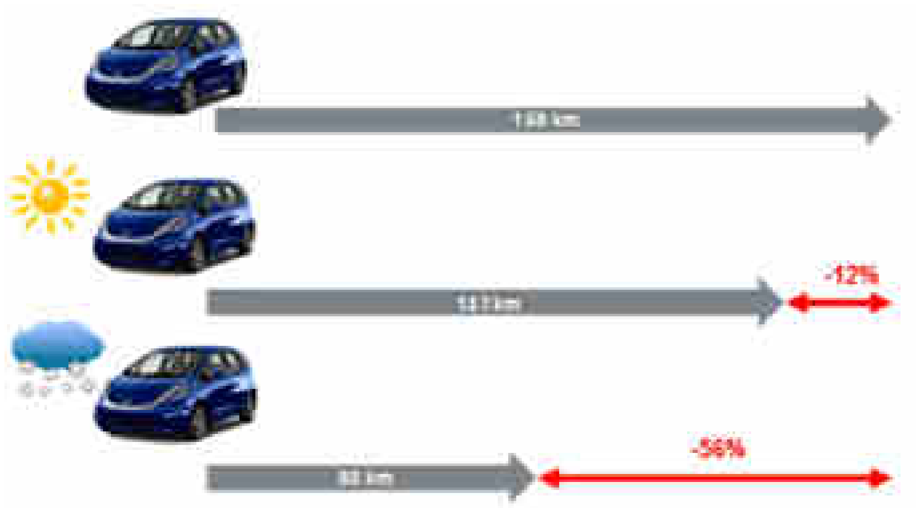

Figure 61: Reduction of driving range due to usage of HVAC system in summer / winter time

The existing VTMS of that baseline vehicle includes a simple cooling loop of the powertrain, a single-stage AC system using R134a and a heater core heated by a water PTC for the HVAC (see Figure 63). The battery is condition via air.

In terms of passenger compartment comfort these measurements contained a lot of data for the air flow out of different louvres and temporal development of local temperatures (see Table 13 and Figure 62):

Table 13: Signal list for local air temperature measurement inside passenger compartment

Category	Signal	Description
Air Outlet	T_DEF	Air temperature in DEFROST vent
Air Outlet	T_HEAT_FR	Air temperature in front HEAT vent
Air Outlet	T_HEAT_RR	Air temperature in rear HEAT vent

This project has received funding from the European Union's Horizon 2020 research and innovation program under grant agreement No. 769826. The content of this publication is the sole responsibility of the Consortium partners listed herein and does not necessarily represent the view of the European Commission or its services.

Air Outlet	T_SIDE	Air temperature in SIDE vent
Air Outlet	T_VENT	Air temperature in VENT vent
Cabin Temp	T_Chin_FR	Air temperature at Chin point of front passenger
Cabin Temp	T_Chin_RR	Air temperature at Chin point of rear passenger
Cabin Temp	T_Foot_FR_L	Air temperature at left foot point of front passenger
Cabin Temp	T_Foot_FR_R	Air temperature at right foot point of front passenger
Cabin Temp	T_Foot_RR_L	Air temperature at left foot point of rear passenger
Cabin Temp	T_Foot_RR_R	Air temperature at right foot point of rear passenger
Cabin Temp	T_Shoulder_FR_L	Air temperature at left shoulder point of front passenger
Cabin Temp	T_Shoulder_FR_R	Air temperature at right shoulder point of front passenger
Cabin Temp	T_Shoulder_RR_L	Air temperature at left shoulder point of rear passenger
Cabin Temp	T_Shoulder_RR_R	Air temperature at right shoulder point of rear passenger
Cabin Temp	T_Waist_FR_L	Air temperature at left waist point of front passenger
Cabin Temp	T_Waist_FR_R	Air temperature at right waist point of front passenger
Cabin Temp	T_Waist_RR_L	Air temperature at left waist point of rear passenger
Cabin Temp	T_Waist_RR_R	Air temperature at right waist point of rear passenger

This project has received funding from the European Union's Horizon 2020 research and innovation program under grant agreement No. 769826. The content of this publication is the sole responsibility of the Consortium partners listed herein and does not necessarily represent the view of the European Commission or its services.

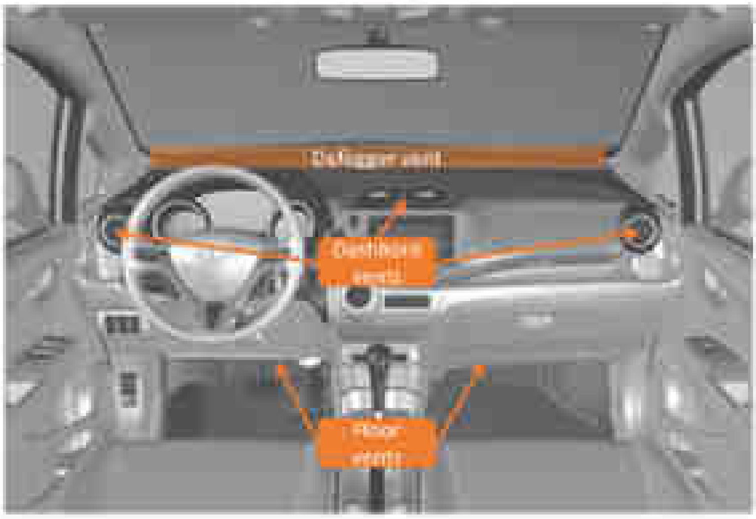

Figure 62: Outlet positions of local air temperature measurements inside passenger compartment

For a more detailed investigation of possible improvements, and for later calibrating the 1D simulation model to be set-up, additional measurement data was needed. These measurements were on a vehicle level again performed by Honda R&D Europe (Deutschland (HRE-G). Special component tests were done by AVL on the AC system testbed. The necessary additional sensors and measurements were defined by AVL, whereby the measurement matrix (see Table 14) was set-up in agreement with HRE-G.

Table 14: Measurement matrix for additional tests on road / on conditioned dyno

No	Speed [kph]	HVAC Blower	T_ambient	rh_ambient	HVAC Temp	A/C	Windows	ca Time [min]	Raditor Fan	Klappenstellung
1	vmax	7	-10	90	max	off	closed	15	max	100% Fußauströmer + 100% durch HWT
2	vmax	7	-10	90	max	off	closed	15	off	100% Fußauströmer + 100% durch HWT
3	vmax	5	-10	90	max	off	closed	15	max	100% Fußauströmer + 100% durch HWT
4	vmax	3	-10	90	max	off	closed	15	max	100% Fußauströmer + 100% durch HWT
5	vmax	0	-10	90	max	off	closed	15	max	100% Fußauströmer + 100% durch HWT
6	0	7	-10	90	max	off	closed	5	max	100% Fußauströmer + 100% durch HWT
7	0	7	-10	90	max	off	closed	5	off	100% Fußauströmer + 100% durch HWT
8	30	7	-10	90	max	off	closed	5	max	100% Fußauströmer + 100% durch HWT
9	30	7	-10	90	max	off	closed	5	off	100% Fußauströmer + 100% durch HWT
10	60	7	-10	90	max	off	closed	5	max	100% Fußauströmer + 100% durch HWT
11	60	7	-10	90	max	off	closed	5	off	100% Fußauströmer + 100% durch HWT
12	100	7	-10	90	max	off	closed	5	max	100% Fußauströmer + 100% durch HWT
13	100	7	-10	90	max	off	closed	5	off	100% Fußauströmer + 100% durch HWT
14	100	7	40	40	min	on	closed	15	max	100% Fußauströmer
15	100	7	40	40	min	on	closed	15	max	100% Personenauströmer
16	60	7	40	40	min	on	closed	15	max	VENT
17	60	7	40	40	min	on	closed	15	off	VENT
18	60	4	40	40	min	on	closed	15	max	VENT
19	60	4	40	40	min	on	closed	15	off	VENT
20	60	1	40	40	min	on	closed	15	max	VENT
21	60	1	40	40	min	on	closed	15	off	VENT
22	60	Auto	40	40	22 AUTO	on	closed	bis T_Kabine stationär	auto	VENT
23	60	Auto	40	40	22 AUTO	on	closed	bis T_Kabine stationär	off	VENT
24	60	6	40	40	22 AUTO	on	closed	bis T_Kabine stationär	max	VENT
25	60	2	40	40	22 AUTO	on	closed	bis T_Kabine stationär	off	VENT
26	WLTP	auto	-10	90	22 AUTO	of	closed	Zyklusdauer	auto	HEAT/DEF open Side Vent
27	WLTP	auto	0	60	22 AUTO	of	closed	Zyklusdauer	auto	HEAT/DEF open Side Vent
28	WLTP	7	-10	90	22 AUTO	of	closed	Zyklusdauer	auto	HEAT/DEF open Side Vent
29	WLTP	7	0	60	22 AUTO	of	closed	Zyklusdauer	auto	HEAT/DEF open Side Vent
30	WLTP	3	-10	90	22 AUTO	of	closed	Zyklusdauer	auto	HEAT/DEF open Side Vent
31	WLTP	3	0	60	22 AUTO	of	closed	Zyklusdauer	auto	HEAT/DEF open Side Vent

Especially data of the so-called under-hood flow, which is the air volume flow through vehicle front grill / main radiator, but also the air volume flow of the HVAC blower, and temperature level of the heater core in the HVAC were necessary (see Figure 63). Not every sensor that would be required was applicable. So, for

This project has received funding from the European Union's Horizon 2020 research and innovation program under grant agreement No. 769826. The content of this publication is the sole responsibility of the Consortium partners listed herein and does not necessarily represent the view of the European Commission or its services.

instance the air flow over the main radiator had to be determined by calculation of the air side and coolant side energy balance.

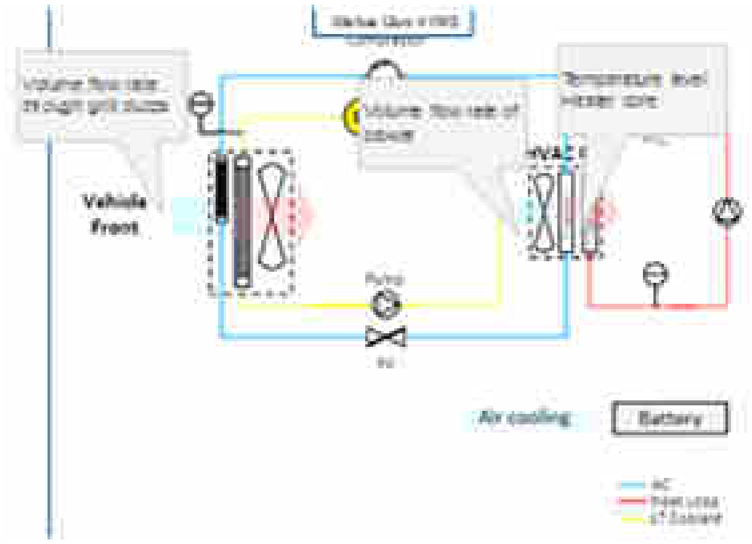

Figure 63: Additional measurements performed on vehicle level

Vehicle tests on the road were done for different ambient temperatures and driving speeds. Additionally, it was measured with and without fan operation. In Figure 64 the air flow over main radiator, derived from measurements and supported by air and coolant side energy balancing, is shown. It can be concluded that the relatively high air mass flow has a positive influence on the low pressure level of the Micro-AC circuit in the heat pump mode, when ambient air is used as heat source and further on the coefficient of performance (COP) of the system. On the other hand fan energy consumption should be as low as possible, so the interface to vehicle aerodynamics shall not be forgotten in later development.

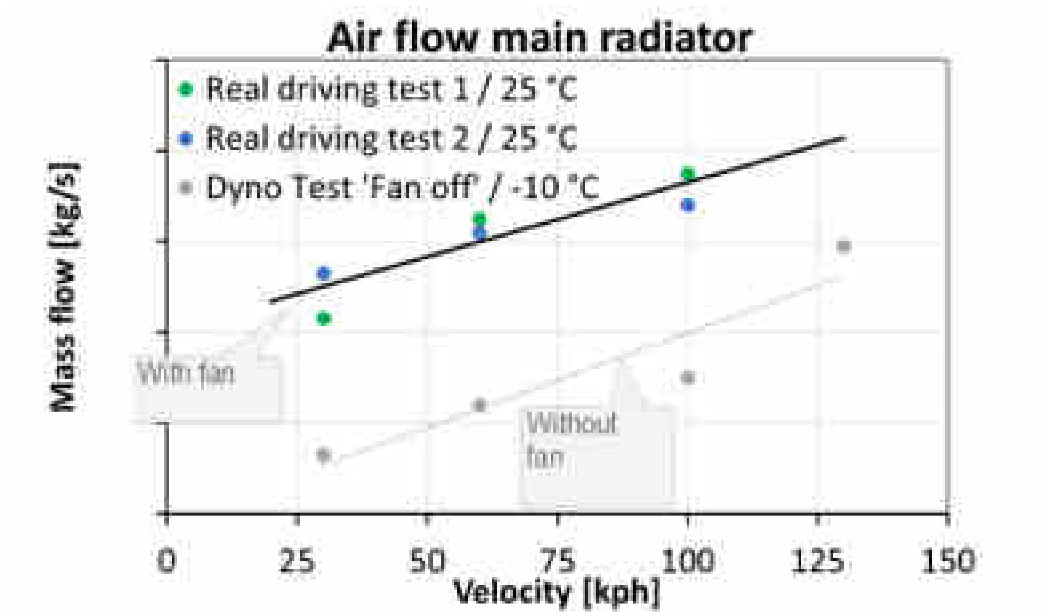

Figure 64: Air mass flow through main radiator

This project has received funding from the European Union's Horizon 2020 research and innovation program under grant agreement No. 769826. The content of this publication is the sole responsibility of the Consortium partners listed herein and does not necessarily represent the view of the European Commission or its services.

From the dyno tests data of blower air flow and behavior and resulting temperatures at ventilation duct outlets were derived (see Figure 65). It was found that e.g. for a cold start @ -10°C ambient the cabin target air temperature is reached after 24 minutes, which is an averaged value for vehicles of the same segment. The system behavior shows the close relation to HVAC systems in conventionally powered cars. The coolant temperature stays constantly at high level, which explains the high energy requirement of the PTC heater. By usage of a smart heat pump system, this energy demand will be decreased. The heat input to the cabin is controlled by varying the air mass flow of the blower. As a consequence of the high coolant temperature, the air temperatures are quite high. To keep this concept for the future demonstrator vehicle would have a negative influence onto the coefficient of performance (COP) of the planned heat pump system.

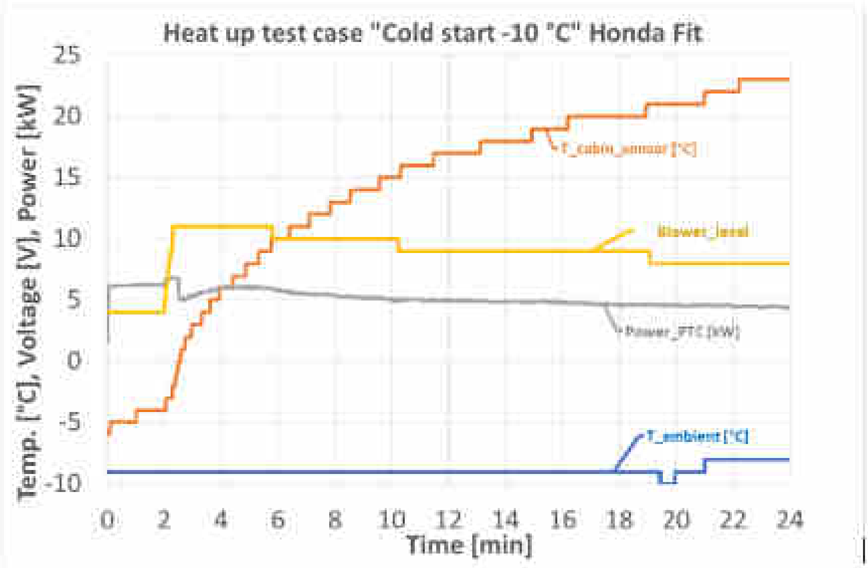

Figure 65: Measurement data of the HVAC blower and temperatures at ventilation louvres

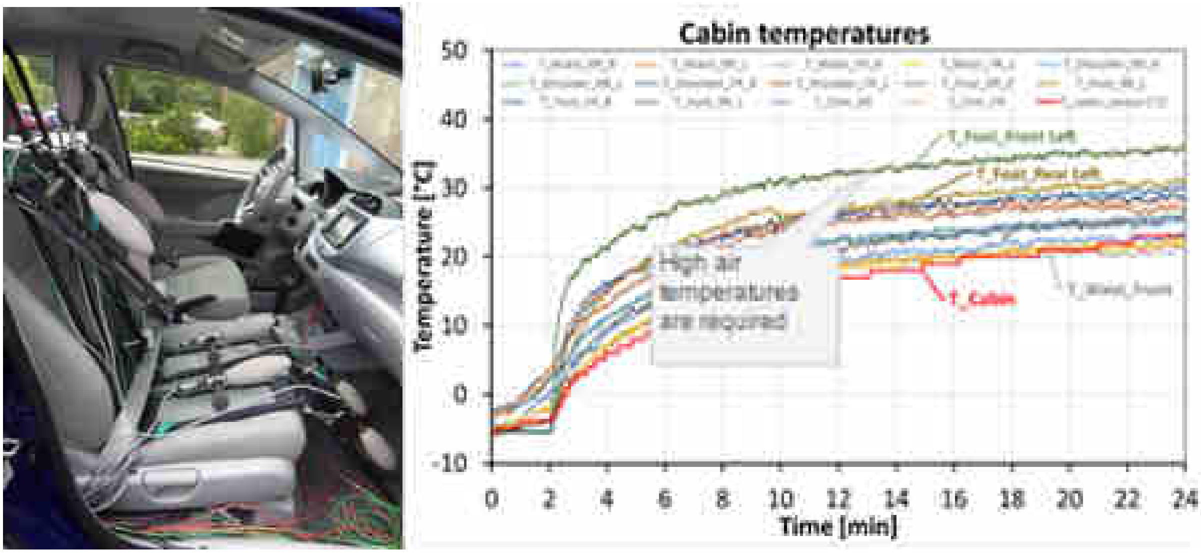

Figure 66: Local air temperatures inside passenger compartment, derived from dyno test

This project has received funding from the European Union's Horizon 2020 research and innovation program under grant agreement No. 769826. The content of this publication is the sole responsibility of the Consortium partners listed herein and does not necessarily represent the view of the European Commission or its services.

Corresponding measurements of air temperatures at different positions inside the passenger compartment (see Figure 66) show that relatively high air temperatures are required for a cabin target temperature of 22 °C. For the demonstrator vehicle it is planned to reduce these high air temperatures, and the corresponding high energy demand by application of radiation heating surfaces (infrared heating plates).

In Figure 67 results from the component tests of the heater core at the AC system testbed are shown. It can depicted, that the heater core has got a high rate of performance. For a reduction of the coolant temperature levels, which is recommended for usage of a heat pump, the air mass flow towards the cabin should be increased in order to keep heat input constant. Again, this is a sign that application of radiation heating surfaces is recommended.

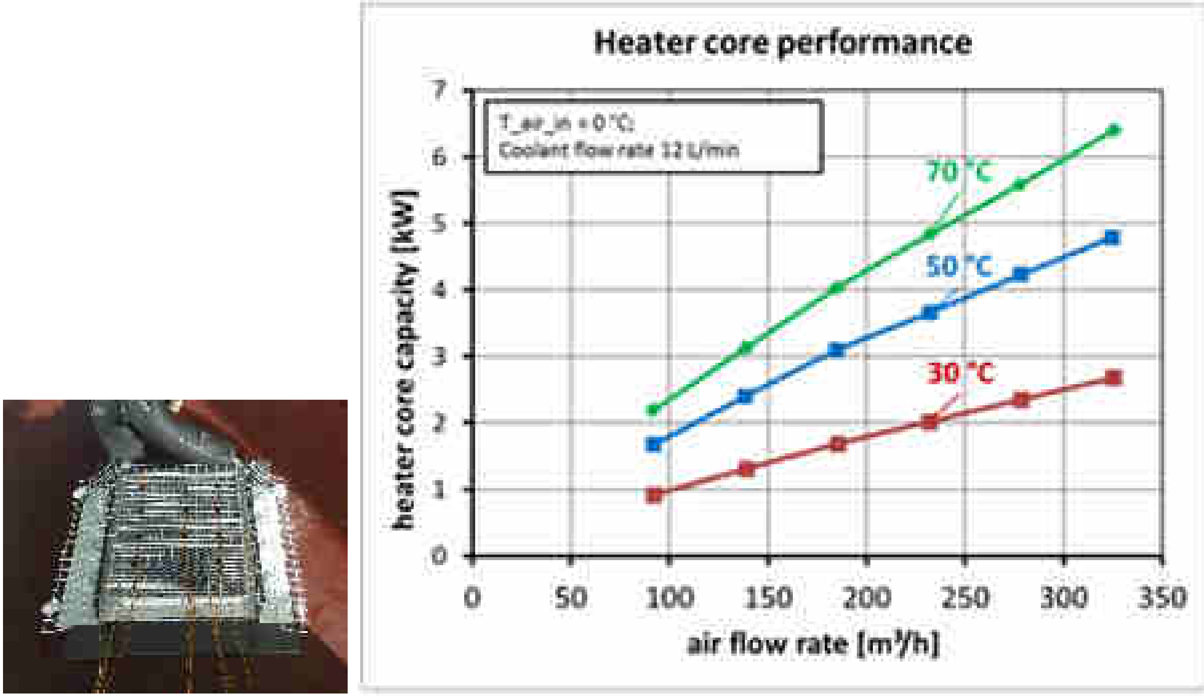

Figure 67: Heater core performance, derived from component test

This project has received funding from the European Union's Horizon 2020 research and innovation program under grant agreement No. 769826. The content of this publication is the sole responsibility of the Consortium partners listed herein and does not necessarily represent the view of the European Commission or its services.

8. First-level assessment of technologies for enhanced energy efficiency and comfort (AVL)

8.1. Choice of refrigerant and basic circuit layout:

Based on the findings from the measurements of the donator vehicle a concept assessment of options for the future VTMS of the demonstrator vehicle was done. The smart VTMS will include a reversible AC circuit, which can also be used in heat pump mode. It was decided to use an AC circuit is considered as an indirect AC system, which means externally switchable instead of an internally switchable system. The major advantages are low amount of refrigerant, which is especially important for the usage of R290 (Propane), and less safety issues.

As refrigerant the standard medium R134a and R290 (Propane) were compared. Figure 68 shows the decision matrix used to determine which refrigerant is better for future application in the demonstrator vehicle.

Parameter	R134a	R290
GWP	1430	3
AC-Power	J	J
HP-Power	K	J
Efficiency (COP/EER)	K	J
Flameable	J	L

Figure 68: Decision matrix for usage of refrigerant

Compared to R134a the natural refrigerant R290 has a much lower Global Warming Potential (GWP). Due to its thermo dynamical properties propane suited much better for high heat pump operational mode shows better COP (see (3)) compared to R134a or the new R1234yf, particular for cold ambient conditions, as shown in Figure 69. For the same conditions and the same swept volume of the compressor Propane gives the possibility to use a higher heat power based on the fact that R290 has a higher volumetrically heat power. The operation of a heat pump using R1234yf, is mostly limited by ambient temperatures below – 5 or - 10°C (depends on system design) based on the low pressure level. Propane offers the possibility to heat the cabin with the more efficient heat pump mode instead of a PTC heater also for ambient temperatures below – 10°C.

$$= \frac{\dot{}}{} = \frac{}{} \quad (3)$$

$$= \frac{\dot{}}{} = \frac{}{} \quad (4)$$

This project has received funding from the European Union's Horizon 2020 research and innovation program under grant agreement No. 769826. The content of this publication is the sole responsibility of the Consortium partners listed herein and does not necessarily represent the view of the European Commission or its services.

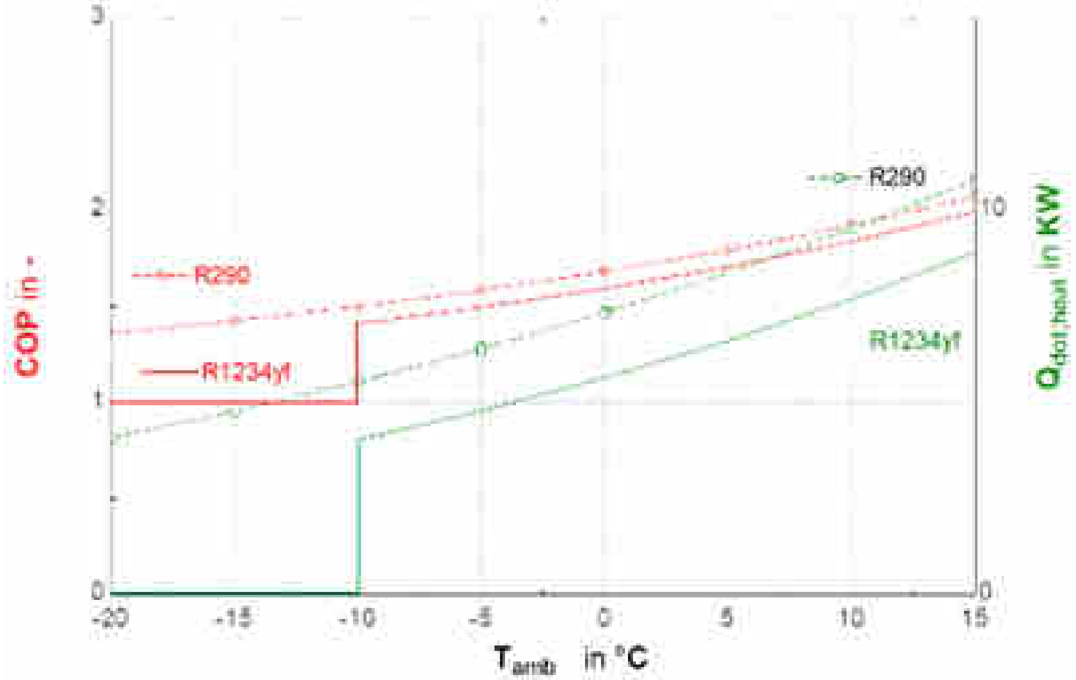

Figure 69: COP and heat power for different ambient conditions using R1234yf or Propane at the same heat sink temperature (equal swept volume)

This is based on the lower boiling temperature of R290, as shown in Figure 70. For AC mode operation it is similar to R134a in terms of efficiency (Energy Efficiency Ratio: EER, as given in (4)). Only in terms of flammability R290 shows disadvantages. By only using a small amount of Propane and a smart safety concept, it is not expected to lead to a problem for the vehicle or human beings. Based on these facts it was decided to use Propane (R290) as refrigerant for the AC system of the VTMS to be developed.

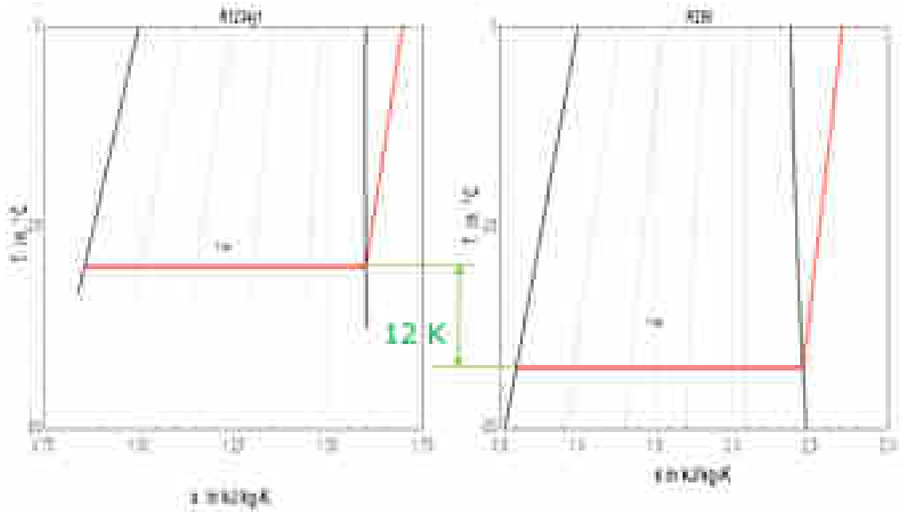

Figure 70: The difference of boiling temperature of R290 and R1234yf shown in the T,s –diagrams

Furthermore R290 can be useful to overcome the risk with Trifluoroacetic Acid (TFA) which is given by using R1234yf [18]. According to this article, for R1234yf an atmospheric lifetime of about 2 weeks is assumed. In the atmosphere R1234yf transforms itself mainly into TFA . This extremely water-soluble and algae-toxic acid

This project has received funding from the European Union's Horizon 2020 research and innovation program under grant agreement No. 769826. The content of this publication is the sole responsibility of the Consortium partners listed herein and does not necessarily represent the view of the European Commission or its services.

is registered with the precipitation in the waters, it is considered persistent and extremely difficult to decompose. General refrigerant circuit and heat pump functionality layout.

In terms of heat sources to be used also a decision matrix was set up (see Figure 71). It turned out that, in addition to usage of ambient air, the usage of component waste heat, i.e. the waste heat of e-motor and power electronics, shows most advantages. It is on sufficient temperature level, is able to deliver enough power, and is easy to integrate. Only in in the temporal availability it shows a medium value. It was decided to use ambient air as major heat source for heat pump mode, and waste heat of the electrical powertrain components as support when the availability is given.

Heat Source	Temperature Level	Power	temporal Availability	Ease of Integration
Ambient heat	L	J	J	J
Component waste heat	J	J	K	J
BATTERY	K	K	L	K
Cabine exhaust air	J	J	K	L

Figure 71: Decision matrix for heat source to be used

As a first step for the choice of the future VTMS the present system of the donator vehicle was investigated. It contains no heat pump functionality in the AC circuit, the waste heat of the e-powertrain is cooled away to ambient and a water PTC is used to heat up the cabin heater circuit.

Two possible new concepts were found (see Figure 72), both allowing waste heat usage from e-powertrain and applying a coolant-refrigerant heat exchanger in the refrigerant circuit and an coolant-air tube fin heat exchanger in the HVAC box instead of an refrigerant-air heat exchanger for safety reasons. They were evaluated using the following criteria:

- Fitting to components, especially e-motor
- Packaging
- Costs
- Efficiency
- Transient behaviour
- Control behaviour

This project has received funding from the European Union's Horizon 2020 research and innovation program under grant agreement No. 769826. The content of this publication is the sole responsibility of the Consortium partners listed herein and does not necessarily represent the view of the European Commission or its services.

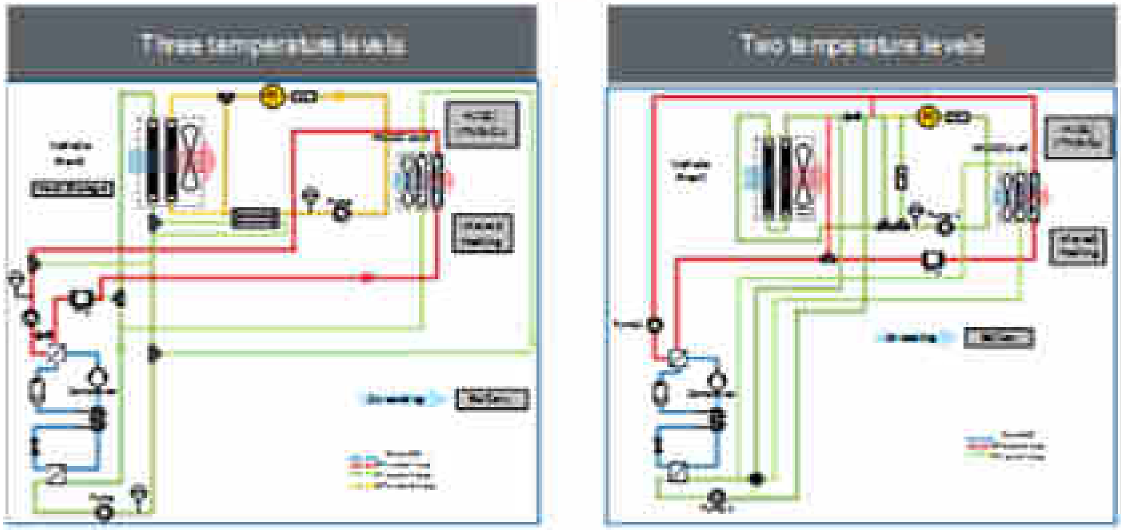

Figure 72: Two different possibilities for future VTMS

The system with three different temperature levels in the coolant circuits is easier / better to control and additionally has got the advantage of split in temperature levels between e-powertrain components and heat pump. Based on this assessment it was decided to use it for the present development and for later integration into the future demonstrator vehicle.

The new system (see Figure 73) consists of following coolant loops:

- Powertrain coolant loop (orange)
- Heating coolant loop (red)
- Cooling c coolant loop (light blue)
- Refrigerant circuit (dark blue)
- Radiator coolant loop (can use the ambience as heat sink or heat source) (green)

Whereby the particular loops cover following functions:

The powertrain coolant loop contains the EM and PCU, a controllable electrical coolant pump, a smart thermo valve, an accumulator and frontal radiator as well as a plate heat exchanger for the waste heat use. With that coolant loop the waste heat can be reject to the ambience or even allow to use the waste heat as a heat source for the heat pump. With a smart control strategy, the cold start behaviour can be improved for the powertrain.

The so-called heating coolant loop contains also a controllable electrical coolant pump, a wet PTC, an iCond and a heater core in the HVAC box, as well as an accumulator and frontal radiator. This coolant loop can be connected to the radiator coolant loop over a smart control valve for rejecting waste heat of the AC circuit in the cooling mode to the ambience.

The so-called cooling coolant loop contains also a controllable electrical coolant pump, a chiller and a tube fine heat exchanger in the HVAC box, which is used as "evaporator". This coolant loop can be connected to the radiator coolant loop over a smart control valve for absorbing waste heat of the powertrain circuit or from the ambience for heating applications.

This project has received funding from the European Union's Horizon 2020 research and innovation program under grant agreement No. 769826. The content of this publication is the sole responsibility of the Consortium partners listed herein and does not necessarily represent the view of the European Commission or its services.

The refrigerant circuit is self uses a controllable scroll compressor an iCond, a chiller, an internal heat exchanger (IHX), a Receiver and an EXV. No refrigerant switching valve is needed to change between cooling or heating mode.

Via the so-called radiator coolant loop the system can reject or absorb heat to or for the ambience, via two coolant-air tube fin heat exchangers in an efficient way.

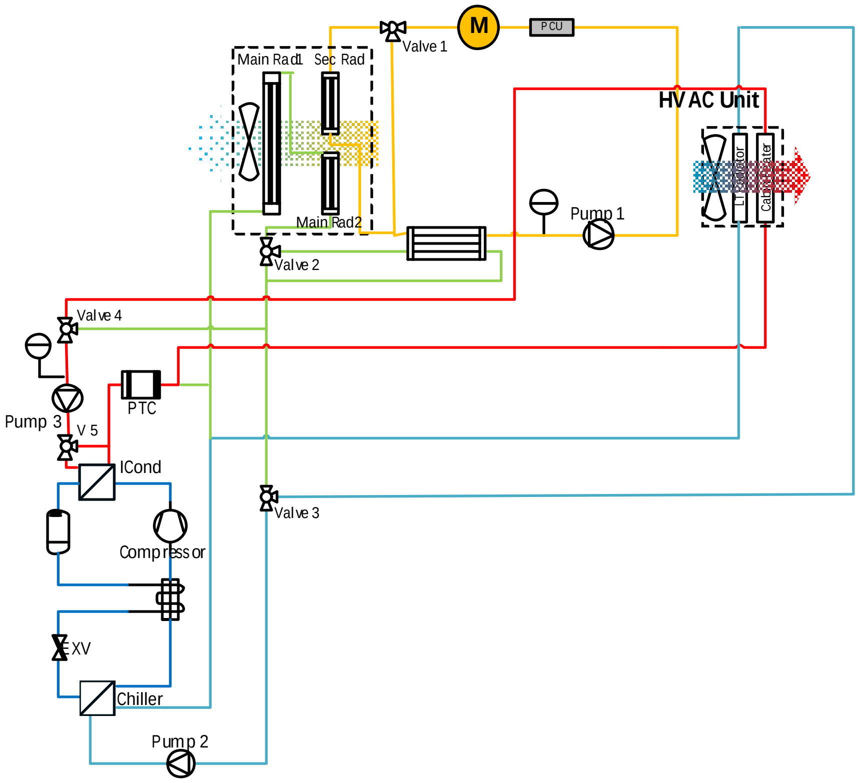

Figure 73: Schematics of the entire VTMS system

Figure 74 shows the circuit logic for all different required operational modes that are necessary for a such smart VTMS and that will be possible for the final system (bold lines mark the schematic and flow directions of each particular mode). The corresponding control strategy is developed in parallel and will be implemented in WP5, Task 5.2.

This project has received funding from the European Union's Horizon 2020 research and innovation program under grant agreement No. 769826. The content of this publication is the sole responsibility of the Consortium partners listed herein and does not necessarily represent the view of the European Commission or its services.

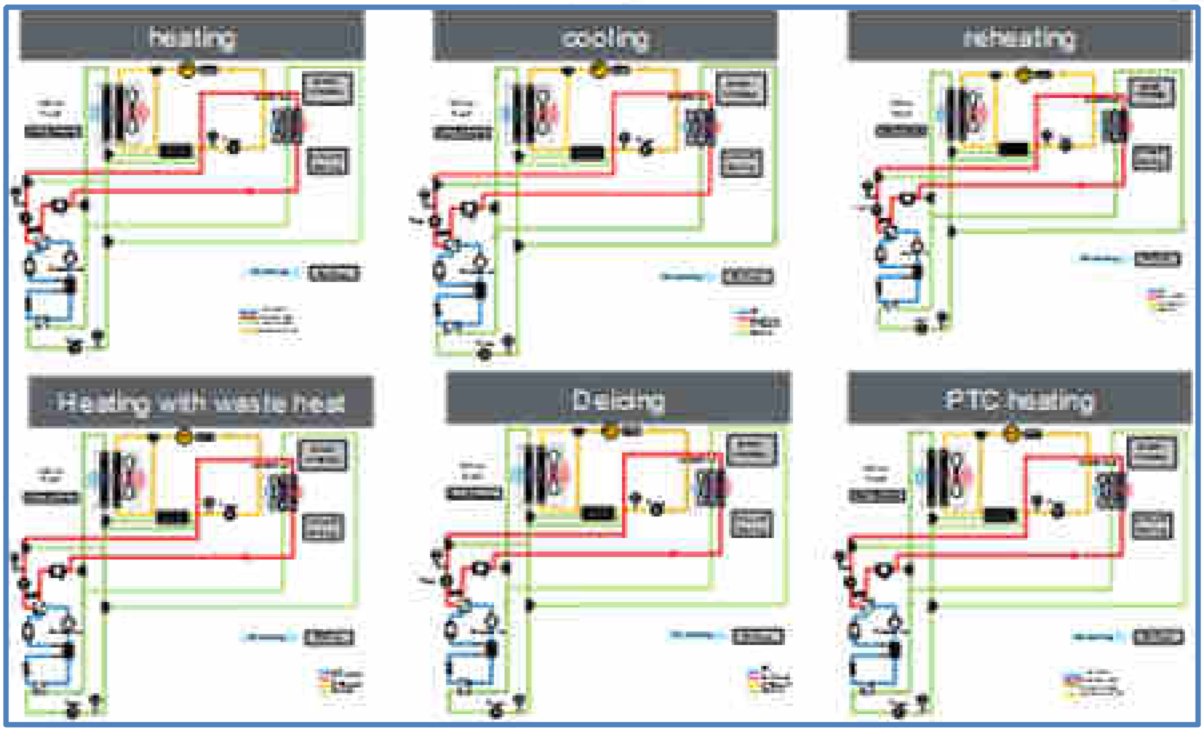

Figure 74: Control logic for all different operational modes of the chosen smart VTMS

8.2. 1D Simulations for circuits and components layout

For development of subsystems and component specification a detailed 1D simulation model was set up in 1D simulation tool (see). It contains all coolant circuits incl. the Micro-AC and uses air temperatures and flow rates as input. In a later stage the VTMS control will be implemented as sub-model as well. In the Micro-AC subsystem isentropic and volumetric efficiencies of the compressor are currently assumed, if later particular data will be available this will be implemented as well.

Using the 1D simulation model first an investigation of COP and EER of the AC circuit in heat pump or AC mode under different boundary conditions was done. For the present situation a COP of approx. 1.8 seems to be achievable.

- Besides other components the condenser and chiller were dimensioned by means of 1D simulation (heat pump mode @ -10°C ambient / 4.5 kW cabin heating). The following findings and technology data were taken into account (see Figure 75):High COP
- Packaging
- Avoiding oil separation

This project has received funding from the European Union's Horizon 2020 research and innovation program under grant agreement No. 769826. The content of this publication is the sole responsibility of the Consortium partners listed herein and does not necessarily represent the view of the European Commission or its services.

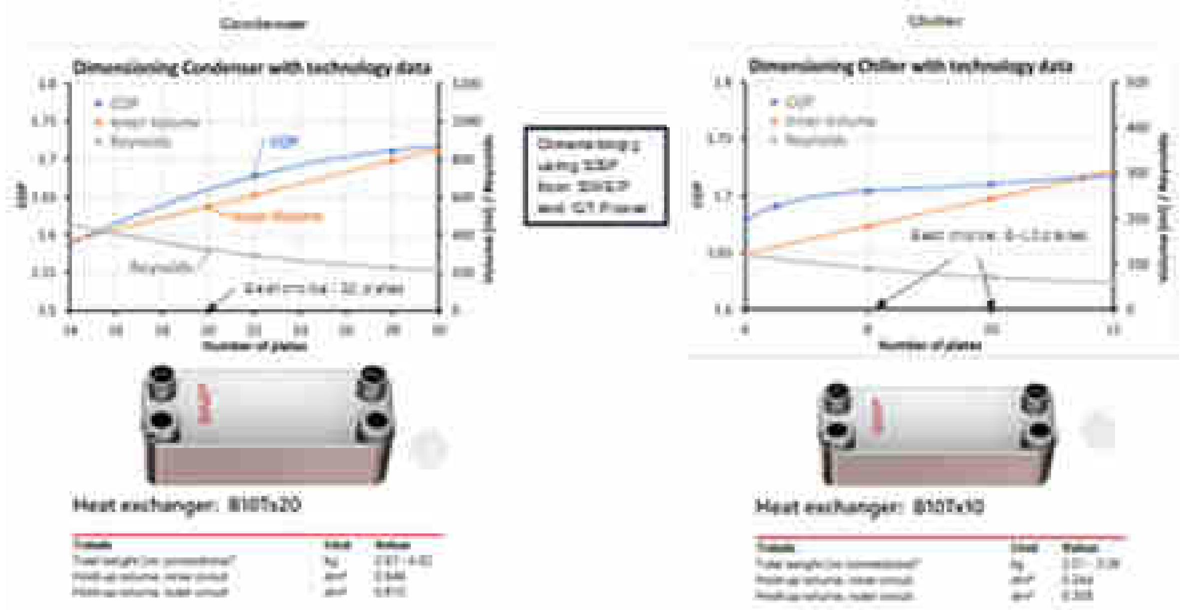

Figure 75: Dimensioning of condenser and chiller

After the specification and the dimensioning was done the purchasing of the iCond and chiller were started. Both were delivered by June 2019 and will be used for build-up of the AC circuit on the AC system testbed.

Based on the envelop of the compressor, supplied by OBRIST, the ability of the AC system for usage of heat pump mode under different boundary conditions was investigated (Figure 76). It was found that it most likely will not be possible to operate the heat pump at low ambient temperatures without additional support from the electric PTC. Below -10 °C such an operation without PTC would lead to too low values in the high pressure part of the system. Since this assessment is done by means of simulation and available data, a final statement can only be made after the AC system measurements on the AC system testbed.

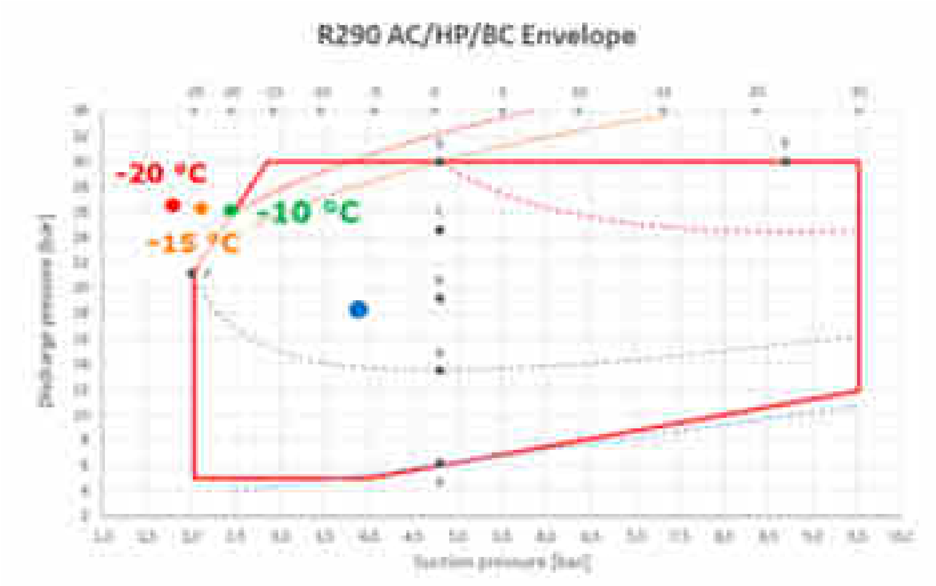

Figure 76: Operation of heat pump under different boundary conditions

This project has received funding from the European Union's Horizon 2020 research and innovation program under grant agreement No. 769826. The content of this publication is the sole responsibility of the Consortium partners listed herein and does not necessarily represent the view of the European Commission or its services.

An investigation of the transient behavior of the VTMS system was done by 1D simulation as well. Figure 77 shows that for heating @ -10°C ambient, as well as for cooling @ 40°C ambient, it will take approx. 6 to 10 minutes to reach the target temperatures in the HVAC box. As a conclusion it can be said that the control needs to be optimized to be able to shorten these durations.

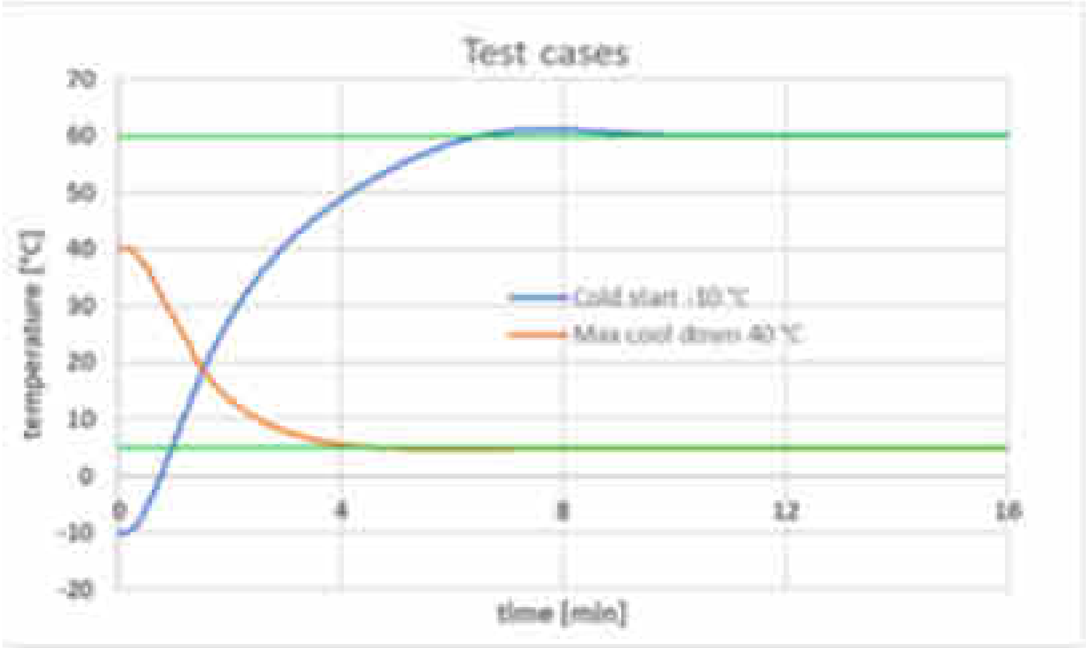

Figure 77: Temporal development of HVAC target temperatures.
Heating mode @ -10°C ambient, max. Cooling mode @ 40°C ambient

This project has received funding from the European Union's Horizon 2020 research and innovation program under grant agreement No. 769826. The content of this publication is the sole responsibility of the Consortium partners listed herein and does not necessarily represent the view of the European Commission or its services.

8.3. Components selected for future FIT-EV thermal management system (AVL)

Based on the above described development and layout procurement was started for all components necessary for the build-up of the thermal management system. Except the hoses for the coolant side and the coolant pumps, all parts of the set-up were delivered up to now. For the missing hoses purchasing takes very long. There are all together 36 hoses necessary to connect all parts, each of them of different shape. Manufacturing of the cores necessary for hoses production is a labour and time extensive process. All missing hoses are expected to be delivered in September 2019.
The following describes and shows these components.

8.3.1. Compressor

The compressor was developed by OBRIST (cp. Figure 78) and provided for usage at the testbed. For more detailed information on this part please see chapter 3. Additionally, the corresponding .dbc-file was provided for control of the compressor via CAN protocol.

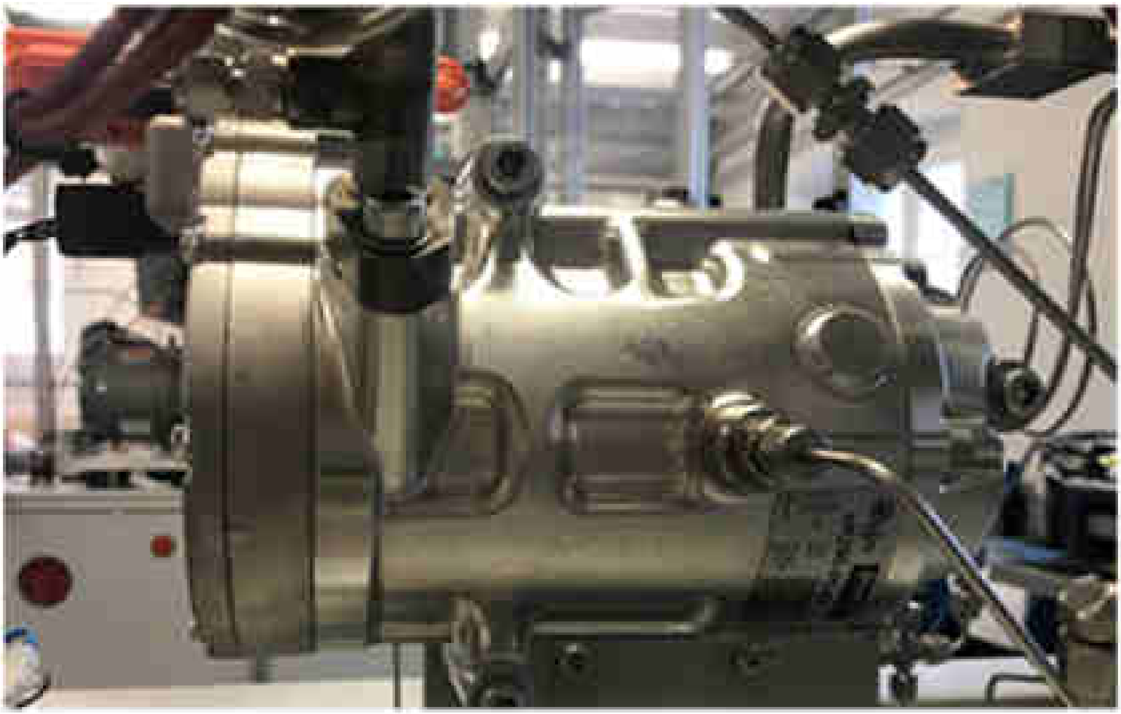

Figure 78: Compressor for usage with R290, provided by OBRIST

This project has received funding from the European Union's Horizon 2020 research and innovation program under grant agreement No. 769826. The content of this publication is the sole responsibility of the Consortium partners listed herein and does not necessarily represent the view of the European Commission or its services.

8.3.2. Electronic Expansion Valve (EXV)

The electronic expansions valve was developed by VENTREX (cp. Figure 79) and provided for usage at the testbed. For more detailed information on this part please see chapter 4. Additionally, the corresponding .ldf-file was provided for control of the compressor via LIN protocol.

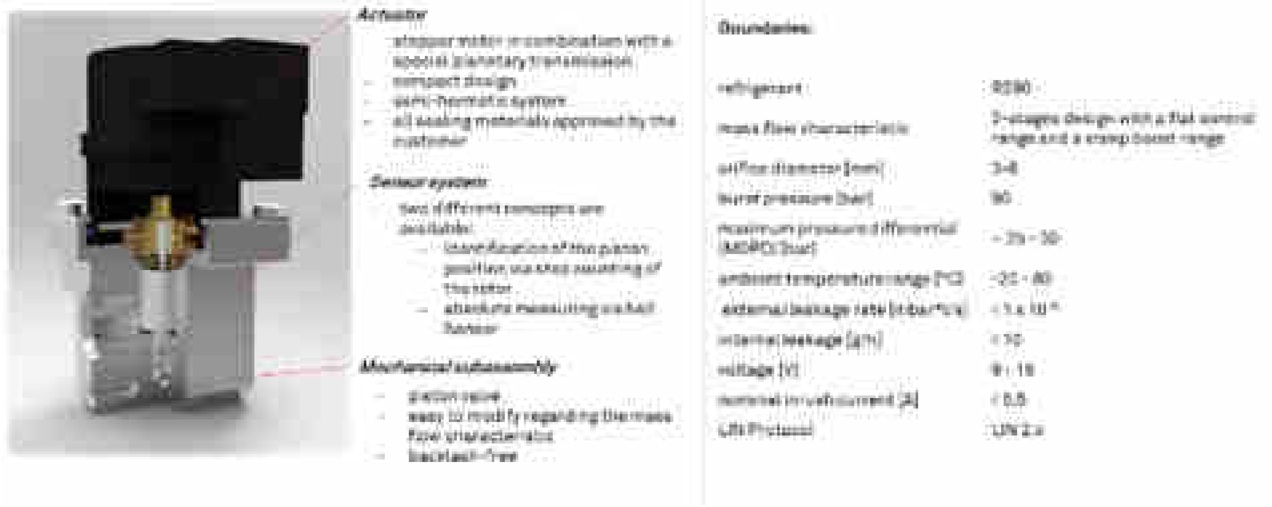

Figure 79: EXV for usage with R290, provided by VENTREX

8.3.3. Pressure Relief Valve

The pressure relief valve (PRV) was developed by VENTREX (cp. Figure 80) and provided for usage at the testbed. For more detailed information on this part please see chapter 5.

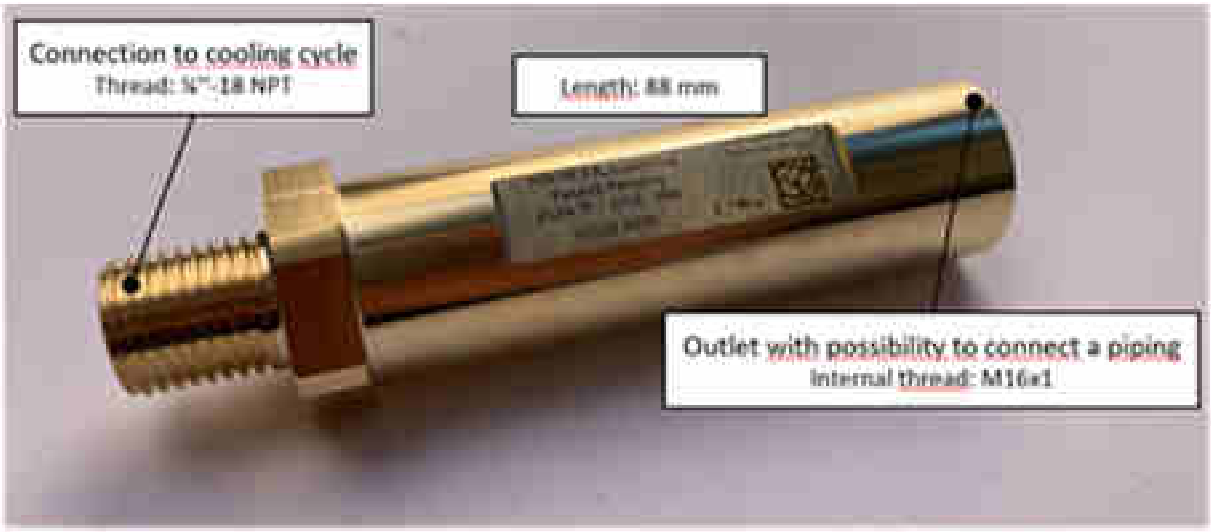

Figure 80: PRV for usage with R290, provided by VENTREX

This project has received funding from the European Union's Horizon 2020 research and innovation program under grant agreement No. 769826. The content of this publication is the sole responsibility of the Consortium partners listed herein and does not necessarily represent the view of the European Commission or its services.

8.3.4.Chiller

The layout of the chiller was done based on the simulations performed by QPD. For usage on the testbed, and later in the demonstrator vehicle, a sufficient type was chosen from SWEP (brand, cp. Figure 81). It was delivered in June 2019 and implemented into the testbed build-up.

Figure 81: Chiller for usage in QUIET micro AC system set-up

8.3.5.ICond

The layout of the condenser (ICond) was done based on the simulations performed by QPD. Finally, a sufficient type was chosen from SWEP (cp. Figure 82). It was delivered in June 2019 and implemented into the testbed build-up.

Figure 82: Condenser for usage in QUIET micro AC system set-up

8.3.6.Receiver

The receiver (cp. Figure 83) was designed and manufactured according to the 1D layout simulation done by QPD. It was delivered in July 2019 and implemented into the testbed build-up.

Figure 83: Receiver for usage in QUIET micro AC system set-up

This project has received funding from the European Union's Horizon 2020 research and innovation program under grant agreement No. 769826. The content of this publication is the sole responsibility of the Consortium partners listed herein and does not necessarily represent the view of the European Commission or its services.

8.3.7. Internal heat exchanger (IWT)

The internal heat exchanger was developed and manufactured according to the layout simulations done by QPD (cp. Figure 84). It is included in the piping of the high pressure side of the micro AC circuit and delivered in July 2019. After receipt it was implemented into the testbed set-up.

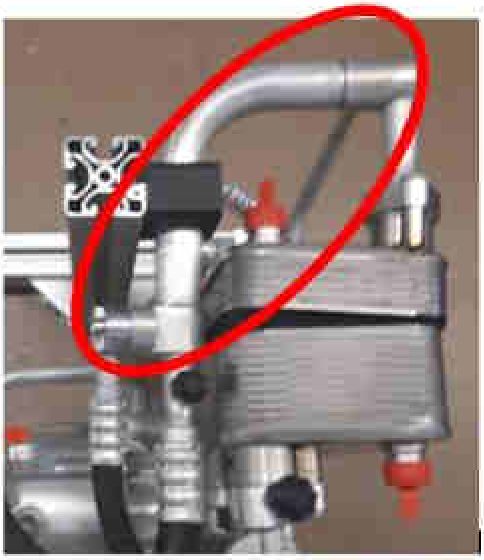

Figure 84: Internal heat exchanger (IWT) for usage in QUIET micro AC system set-up

8.3.8. Hoses and pipes:

The hoses and pipes were designed according to 1D simulations performed at QPD. The aluminium pipes of the micro AC circuit were procured as an assembly in connection with condenser, chiller, IWT and collector. For this purpose the mentioned chiller and condenser were, after their delivery from the heat exchanger manufacturer, sent to the company which manufactured the piping. There connections were adapted, they were welded / soldered together and supplied as two separate assemblies.
Since the delivery times are very long for coolant hoses, these parts are actually in procurement and are expected to be delivered in September 2019. The following table (included in Figure 85) describes the inner diameter and length of all the hoses.

This project has received funding from the European Union's Horizon 2020 research and innovation program under grant agreement No. 769826. The content of this publication is the sole responsibility of the Consortium partners listed herein and does not necessarily represent the view of the European Commission or its services.

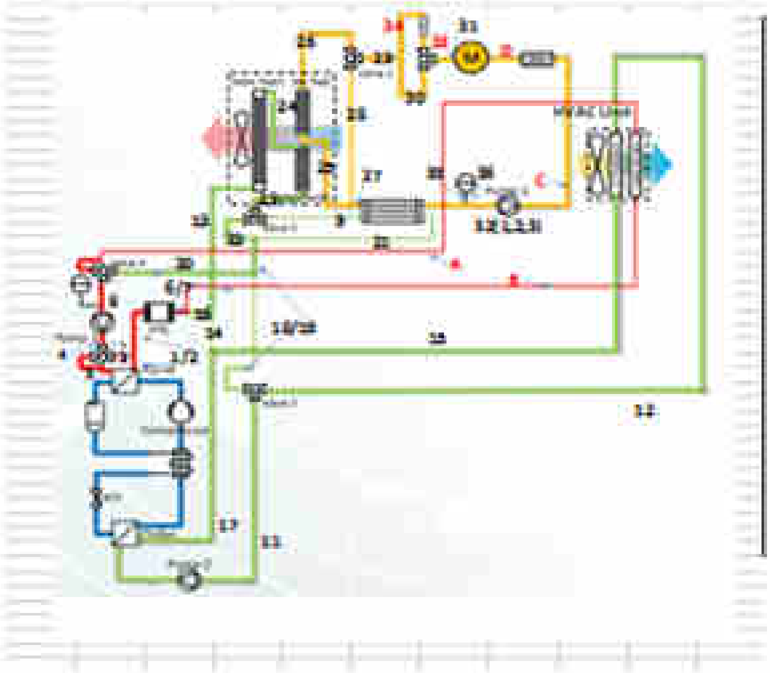

Hose No.	Length [mm]	Inner diameter	Material:
1	376	20mm	EPDM
2	539	20mm	EPDM
3	351	20mm	EPDM
4	114	20mm	EPDM
5	136	20mm	EPDM
6	117	20mm	EPDM
7	107	20mm	EPDM
8	249	20mm	EPDM
9	311	20mm	EPDM
10	574	20mm	EPDM
11	242	20mm	EPDM
12	1034	20mm	EPDM
13	134	20mm	EPDM
14	126	20mm	EPDM
15	1008	20mm	EPDM
16	228	20mm	EPDM
17	335	20mm	EPDM
18	104	20mm	EPDM
19	289	20mm	EPDM
20	500	20mm	EPDM
21	175	20mm	EPDM
22	276	20mm	EPDM
23	880	20mm	EPDM
24	439	20mm	EPDM
25	831	20mm	EPDM
26	719	20mm	EPDM
27	178	20mm	EPDM
28	67	20mm	EPDM
29	156	20mm	EPDM
30	191	20mm	EPDM
31	502	20mm	EPDM
32	479	20mm	EPDM
33	360	20mm	EPDM
34	304	20mm	EPDM
35	362	20mm	EPDM
36	304	20mm	EPDM

Figure 85: Dimensions of coolant hoses of QUIET thermal management system set-up

8.3.9. Switching Valves:

The layout of the switching valves was done based on the simulations performed by QPD. Finally, a sufficient type (cp. Figure 86) was chosen and procured. These parts were received in late June 2019.

Figure 86: Switching valves to be used in QUIET thermal management system set-up

This project has received funding from the European Union's Horizon 2020 research and innovation program under grant agreement No. 769826. The content of this publication is the sole responsibility of the Consortium partners listed herein and does not necessarily represent the view of the European Commission or its services.

8.3.10. Coolant Pumps:

The layout of the coolant pumps was done based on the simulations performed by QPD. Finally, a sufficient type was chosen and is currently in procurement. The chosen type is Pierburg-CWA150 (cp. Figure 87), which is able to provide the necessary pressure increase / mass flow and also is capable of being controlled the necessary way. The necessary number of pumps was procured from MS Motorservice International GmbH. The parts were delivered end of July 2019.

Figure 87: Coolant pump to be used in QUIET thermal management system set-up

This project has received funding from the European Union's Horizon 2020 research and innovation program under grant agreement No. 769826. The content of this publication is the sole responsibility of the Consortium partners listed herein and does not necessarily represent the view of the European Commission or its services.

8.3.11. Coolant-coolant heat exchanger:

The coolant-coolant heat exchanger was developed according to the 1D layout simulations done by QPD. In agreement with the derived specifications it was chosen as B10THx20/1P-SN-S3x Hose 20 and procured from SWEP (cp. Figure 88). The part was delivered in June 2019, it will be implemented into the testbed set-up as soon as the coolant hoses will be delivered.

Figure 88: Coolant–coolant heat exchanger for QUIET thermal management system set-up

8.3.12. Main Radiator 1:

The main radiator 1 used for the testbed build-up and the demonstrator vehicle will be carried over from the baseline vehicle. It was already provided by HRE-G (cp. Figure 89).

Figure 89: Main radiator 1 for usage in QUIET thermal management system set-up

This project has received funding from the European Union's Horizon 2020 research and innovation program under grant agreement No. 769826. The content of this publication is the sole responsibility of the Consortium partners listed herein and does not necessarily represent the view of the European Commission or its services.

8.3.13. Main Radiator 2:

As main radiator 2, used for the testbed build-up and the demonstrator vehicle, a component of a different HONDA model was selected out of the range of HONDA spare parts. It was already provided by HRE-G (cp. Figure 90).

Figure 90: Main radiator 2 for usage in QUIET thermal management system set-up

8.3.14. Secondary Radiator:

For the secondary radiator the same part as for main radiator 2 will be used for the testbed build-up and the demonstrator vehicle. It is therefore also taken from the range of available original HRE-G parts.

8.3.15. HV-PTC:

The same HV-PTC as in the baseline / donator vehicle will be used. It currently is in procurement and will be supplied by HRE-G.

8.3.16. New Heat Exchanger in HVAC unit:

For the new heat exchanger inside the HVAC unit (instead of the former evaporator) used for the testbed build-up and the demonstrator vehicle, a component of a different HONDA model was selected out of the range of HONDA spare parts. It was already provided by HRE-G.

8.3.17. Cabin Heater in HVAC unit:

The cabin heater inside the HVAC unit used for the testbed build-up and the demonstrator vehicle will be carried over from the baseline vehicle. It is included in the HVAC unit already provided by HRE-G.

8.3.18. Thermal Storage tank:

The thermal storage tank will be provided by RUBITHERM, it is expected to be delivered in September 2019. For more detailed information on this part please see chapter 6.

This project has received funding from the European Union's Horizon 2020 research and innovation program under grant agreement No. 769826. The content of this publication is the sole responsibility of the Consortium partners listed herein and does not necessarily represent the view of the European Commission or its services.

8.3.19. Equalizing Tank:

This part was layouted according to the needs of the system, currently this part is in procurement. Delivery is expected for September 2019.

8.3.20. HVAC unit and blower unit:

The HVAC unit and the corresponding blower unit (cp. Figure 91) used for the testbed build-up and the demonstrator vehicle will be carried over from the baseline vehicle, some regions will be modified / reworked. These parts were already provided by HRE-G.

Figure 91: HVAC and Blower units for QUIET thermal management system set-up

8.4. Packaging Investigation and CAD design of components, hoses, etc. (QPD / AVL-D)

The packaging of the existing Honda FIT EV vehicle was analysed in CAD. Based on geometrical information from OBRIST and VENTREX the placement of the Micro-AC circuit in the vehicle was defined as shown in Figure 92.

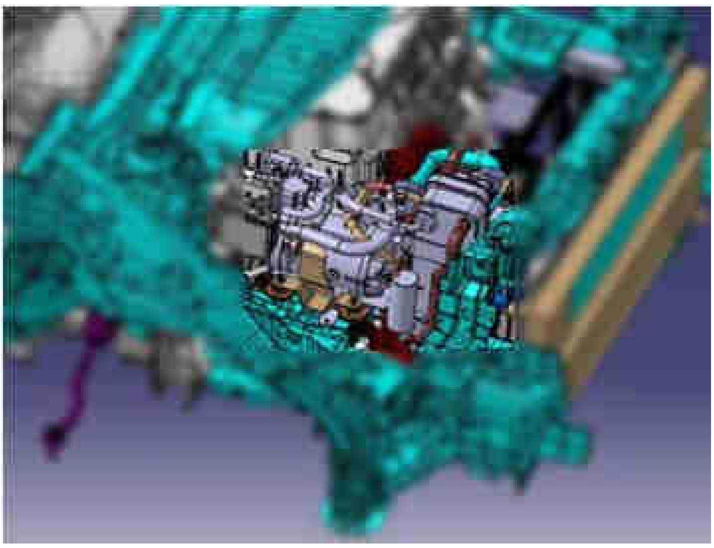

Figure 92: Placement of Micro-AC circuit in the demonstrator vehicle

This project has received funding from the European Union's Horizon 2020 research and innovation program under grant agreement No. 769826. The content of this publication is the sole responsibility of the Consortium partners listed herein and does not necessarily represent the view of the European Commission or its services.

Considering the geometrical demand of RUBITHERM the position of the thermal storage tank was derived (see Figure 93).

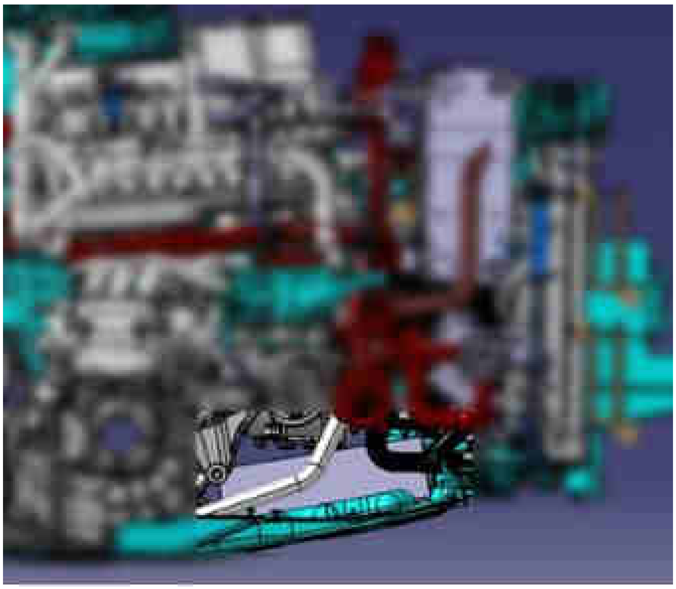

Figure 93: Placement of Thermal Storage Tank in the demonstrator vehicle

Based on the given packaging, the already known dimensions of particular components, the geometrical and thermodynamical demands of the system, the hoses, aluminium lines etc. of the Micro-AC circuit were designed. Figure 94 shows the Micro-AC circuit as it will be implemented into the demonstrator vehicle. Here the initial layout is shown, modifications of the orientation of the heat exchangers might be necessary to enable the de-airation of the water circuits and the AC-oil return to the compressor.

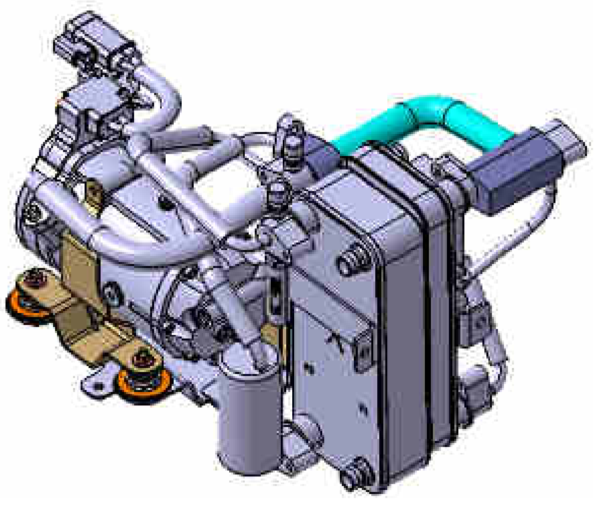

Figure 94: Micro-AC circuit for testbed and demonstrator vehicle

Similar to the AC circuit, components for the coolant circuits, incl. heat exchangers, pumps, valves etc. were either designed or chosen from existing hardware by AVL.

This project has received funding from the European Union's Horizon 2020 research and innovation program under grant agreement No. 769826. The content of this publication is the sole responsibility of the Consortium partners listed herein and does not necessarily represent the view of the European Commission or its services.

8.5. Procurement of parts, necessary sensors, testbed build-up and measurement planning:

Most of the parts and components necessary for testbed build-up have already been delivered, only coolant hoses and coolant pumps are missing. Additionally, the condenser of the micro AC circuit needed to be procured again because the part delivered first did not fulfil the specifications. The missing parts shall be delivered in late August or in September 2019 to be used for the build-up of the system on the AC system testbed.

Measurements on the AC system testbed will be done in two steps. As step 1 only the AC circuit will be built up, the two coolant circuits connected via refrigerant-coolant plate heat exchanger will be represented by two separate conditioning units. As step 2 the entire VTMS system, including all coolant circuits, coolant fan, etc., will be build-up. Here the waste heat of e-powertrain will be represented by conditioning unit as well.
The instrumentation will be done by a high number of pressure and temperature sensors / devices implemented into the refrigerant and coolant circuits (see Figure 95 and Figure 96). This will be done to be able to derive all measurement data necessary for assessment of the system performance and control development. In the AC circuit a Coriolis device will be used for measurement of refrigerant mass flow. The oil concentration present in the system will be measured by means of an OCR device (supplier Anton Paar). In order to deliver correct data the OCR needs to be calibrated to the present combination of Propane and a particular compressor oil. The type of oil to be used was defined by OBRIST based on their compressor tests. According to this definition provision of necessary calibration curve was done. This calibration curve was delivered in late June 2019 and has already been implemented into the OCR device of the testbed system.

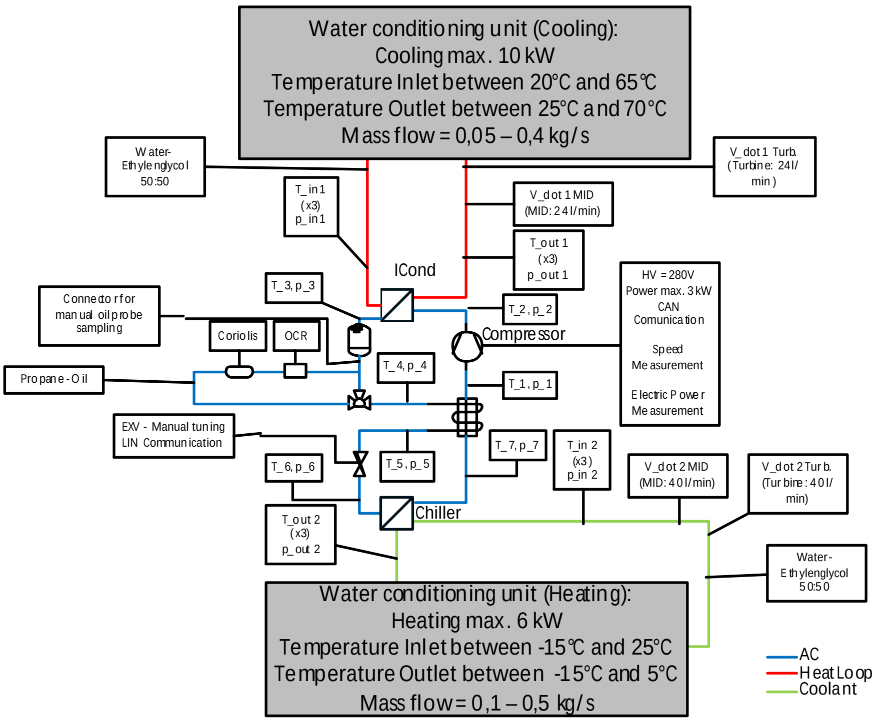

Figure 95: Instrumentation of testbed build-up step 1 (Micro-AC circuit)

This project has received funding from the European Union's Horizon 2020 research and innovation program under grant agreement No. 769826. The content of this publication is the sole responsibility of the Consortium partners listed herein and does not necessarily represent the view of the European Commission or its services.

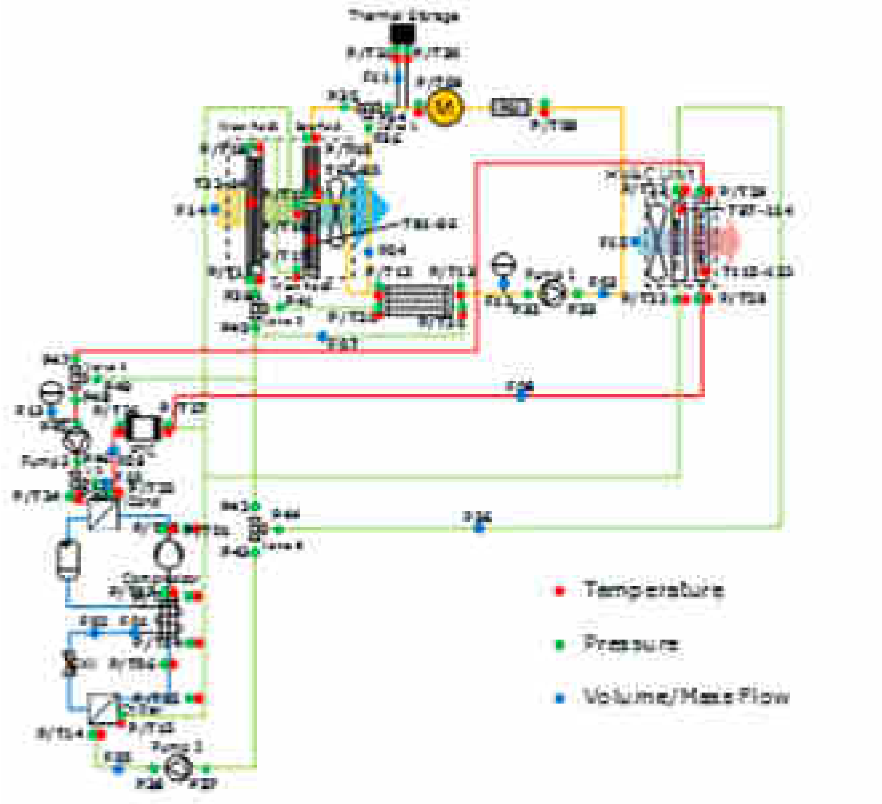

Figure 96: Instrumentation of testbed build-up step 2 (entire VTMS)

The provision of all necessary measurement equipment is finished. Delivery of all sensors, CAN cases, etc. for step 1 and for step 2 the measurement equipment took place in July 2019.

The build-up of the system step 1 (only AC system, coolant circuits represented by two conditioning units) is done (cp. Figure 97). It was realized that one of the refrigerant-coolant heat exchangers does not fulfil the required specification. Accordingly, it was necessary to procure it again. The delivery is now scheduled for late August 2019. Since commissioning of the set-up cannot be done without this component, commissioning is planned to be finished in CW36-2019. Corresponding measurements shall be done from CW37-2019 to CW38-2019.

This project has received funding from the European Union's Horizon 2020 research and innovation program under grant agreement No. 769826. The content of this publication is the sole responsibility of the Consortium partners listed herein and does not necessarily represent the view of the European Commission or its services.

Figure 97: Build-up of QUIET micro AC incl. measurement devices

For system measurement step 2 (entire VTMS, incl. all circuits) the build-up and commissioning is currently planned for CW40-2019 to CW41/42-2019, of course depending on the delivery schedule of the necessary coolant hoses. If manufacturing and delivery of these hoses would take even longer, it is currently seen as an option to substitute the original hoses by handcrafted ones. This is of course only fallback solution and shall be avoided. Associated commissioning and measurements are planned to be performed from 43-2019 to CW45/CW46-2019. As mentioned above the build-up and testing schedule is of course dependent on delivery of all necessary parts.

8.6. Control strategy for the vehicle thermal management system (VTMS):

In parallel to the provision of parts a control strategy for the vehicle thermal management system was developed. It contains all the necessary sensors and valves to be controlled for proper and smart operation of the VTMS. All operational modes possible are included, to guarantee desired passenger comfort and energy efficient operation of the entire VTMS, which covers all required functions like cooling, re-heating, heating the cabin with or without waste heat, de-icing the front radiator as well as take care of the windscreen defrost mode. Furthermore, also a strategy improving the cold start behaviour of the powertrain was also developed as well as the possibility that we can use as much waste heat from the powertrain in winter as possible. Figure 98 gives an impression of the complexity of the system. The I/Os and the communication with the different control units in the vehicle have been clarified. The existing HVAC box will be used and for that reason the same sensors in the cabin which influence the HVAC control for the blower speed or the air mixing flaps will be re-used. However, the control strategy as well as the control parameters for all the electrical actuators will be parametrised by the use of simulation, which will reduce in vehicle parametrisation effort. Therefore, using the already existing 1D simulation plant model a model based control will be developed and evaluated, like e.g. multiple input multiple output (MiMo). This will significantly increase efficiency and enhance improve the useable driving range of the vehicle. To avoid a oscillation of the entire system the necessary hysteresis curves need to be adapted. The final development and optimization of the control strategy will be done in cooperation by the project partner University of Zagreb (UOZ).

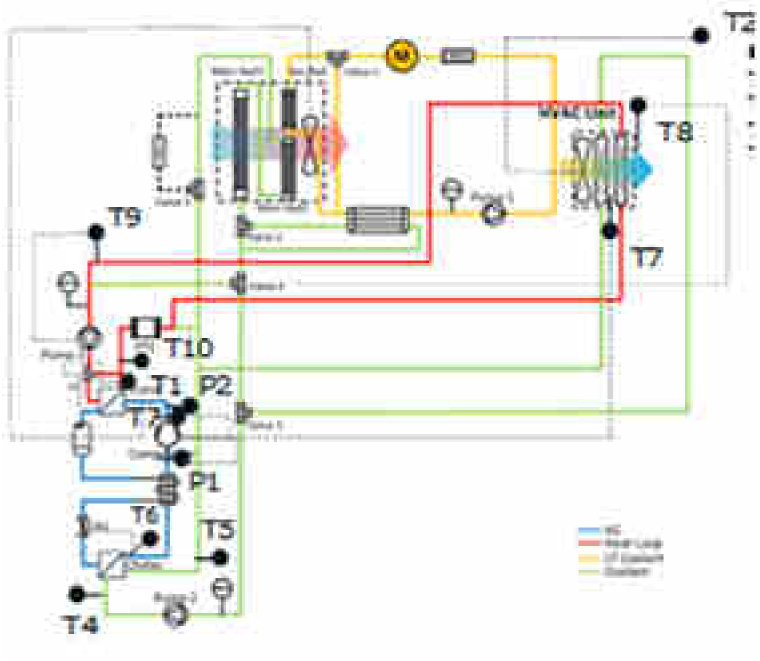

Figure 98: VTMS control strategy (Cabin Cooling incl. Re-Heat)

This project has received funding from the European Union's Horizon 2020 research and innovation program under grant agreement No. 769826. The content of this publication is the sole responsibility of the Consortium partners listed herein and does not necessarily represent the view of the European Commission or its services.

9. Conclusions

For all the components of the innovative thermal management system layout / definition and development was done. The parts have been manufactured and pre-tested. Where parts existing on the market have been chosen they were procured. Unfortunately, currently the hoses for the coolant circuits are still not delivered due to long manufacturing and delivery time schedules. The delivery is scheduled for late September 2019.

ATT layout the radiation heat surfaces and did corresponding comfort and efficiency simulations. OBRIST developed and delivered the new compressor for usage with R290. VENTREX developed and delivered the new electronic expansion valve (EXV) for R290 and the pressure relief valve (PRV) for safe usage of this refrigerant. RUBITHERM did the development of the thermal storage based on PCM. Here still work is going on due to spatial problems inside the thermal storage tank. An improved arrangement and size of the Al foams will lead to less spatial needs and also further reduce pressure losses thus making its performance also more interesting for a broader range of applications.

QPD and AVL (former QPA) have done layout of the entire thermal management system, incl. procurement of parts and build-up of the first stage of the system for testbed measurements. Additionally, a first layout of the control strategy was developed. It was handed over to the project partner University of Zagreb (UOZ) for further optimization.

Accordingly, the micro AC circuit incl. conditioning units at the two heat exchangers (iCond and Chiller), which are in connection with the coolant circuits, was build-up. It has been equipped with measurement devices and will be commissioned in early September 2019. Afterwards the measurements will be done. As soon as the missing hoses will be available also the full system including the two coolant circuits will be build-up, commissioned and measured.

This project has received funding from the European Union's Horizon 2020 research and innovation program under grant agreement No. 769826. The content of this publication is the sole responsibility of the Consortium partners listed herein and does not necessarily represent the view of the European Commission or its services.

10. Bibliography

[1] THESEUS. THESEUS FE Database.

[2] THESEUS-FE 5.0.03 Theory Manual.

[3] Davis, S C, Diegel, S W and Boundy, R G. Transportation Energy Data Book. 2014.

[4] Facanha, C, Blumberg, K and J, Miller. Global transportation energy and climate roadmap. s.l. : International Council on Clean Transportation.

[5] Verschuren, Olaf. [Online] https://www.researchgate.net/figure/definitions-of-the-activity-continuum-MET-the-metabolic-equivalent-of-task-MET_tbl1_265609419.

[6] technologies, ATT advanced thermal. Fahrzeugvermessung intern. 2016.

[7] DIN EN ISO 7730. 2003. "Analytische Bestimmung und Interpretation der thermischen Behaglichkeit durch Berechnung des PMV- und des PPDIndexes und der lokalen thermischen Behaglichkeit".

[8] H., Zhang. Human Thermal Sensation and Comfort in Transient and Non-Uniform Thermal. Berkley: University of California, 2003.

[9] Heubes J., Papst I., König H., Usinger J., Gschrey B., Kimmel T., Schwarz W., 2014: Kohlenwasserstoffe sicher als Kältemittel einsetzen - Entwicklung einer Strategie zum vermehrten Einsatz von Kohlenwasserstoff-Kältemitteln als Beitrag zum deutschen Klimaschutzziel unter Berücksichtigung des Energieziels 2050, CLIMATE CHANGE 30/2014

[10] October 2018: https://www.engineeringtoolbox.com/fluids-evaporation-latent-heat-d_147.html

[11] Choudharia C. S., Sapalib S.N., 2016: Performance Investigation of Natural Refrigerant R290 as a Substitute to R22 in Refrigeration Systems, Energy Procedia 109, 346 – 352

[12] Prof. Jignesh K. Vaghela, 2016: Comparative evaluation of an automobile air - conditioning system using R134a and its alternative refrigerants, Energy Procedia 109, 346 – 352

[13] October 2018: https://en.wikipedia.org/wiki/List_of_refrigerants

[14] LINDE, 2016: SAFETY DATA SHEET Propane

[15] LINDE, 2016: SAFETY DATA SHEET 2,3,3,3-Tetrafluoropropene

[16] Assessment of leakage and risk reduction of R290 in a split type household air conditioner Weier T., Guogeng H., Wei S., Sai Z., Dehua C., Yihao Z., 2017, International Journal of Refrigeration 89 (2018) 70–82

[17] Oktober 2018: https://www.haustec.de/klima-lueftung/kaeltetechnik/wie-sie-propan-als-kaeltemittel-fuer-gewerbliche-anwendungen-einsetzen

[18] July 2019: https://www.umweltbundesamt.de/themen/auf-umweltfreundliche-kaeltemittel-umsteigen

This project has received funding from the European Union's Horizon 2020 research and innovation program under grant agreement No. 769826. The content of this publication is the sole responsibility of the Consortium partners listed herein and does not necessarily represent the view of the European Commission or its services.

11. Acknowledgment

European Union's Horizon 2020 research and innovation program

This project has received funding from the European Union's Horizon 2020 research and innovation program under grant agreement No. 769826. The content of this publication is the sole responsibility of the Consortium partners listed herein and does not necessarily represent the view of the European Commission or its services.

Project Partners:

The author(s) would like to thank the partners in the project for their valuable comments on previous drafts and for performing the review.

Participant No	Participant short name	Participant organisation name	Country
1 Coordinator	AIT	AIT Austrian Institute of Technology GmbH	Austria
2	HRE	Honda R&D Europe (Deutschland) GmbH	Germany
3	AVL	AVL List GmbH	Austria
4	QPD	qpunkt Deutschland GmbH	Germany
5	VEN	VENTREX Automotive GmbH	Austria
6	UOZ	University of Zagreb	Croatia
7	IFAM	Fraunhofer Institute for Manufacturing Technologies and Advanced Materials IFAM	Germany
8	ATT	ATT advanced thermal technologies GmbH	Austria
9	ECON	eCon Engineering Kft.	Hungary
10	RUB	RUBITHERM Technologies GmbH	Germany
11	STS	SeatTec Sitztechnik GmbH	Germany
12	OBR	OBRIST Engineering GmbH	Austria
13	JRC	Joint Research Centre - European Commission	Italy